1

Crystal Structures of Natural Zeolites

Thomas Armbruster

Laboratorium für chemische und mineralogische Kristallographie
University of Bern
CH-3012 Bern, Switzerland

Mickey E. Gunter

Department of Geological Sciences
University of Idaho
Moscow, Idaho 83844

INTRODUCTION

General aspects

According to the recommended nomenclature for zeolite minerals (Coombs et al. 1998), there are more than eighty distinct zeolite species. Table 1 (see Appendix below) is a listing of the zeolite minerals discussed in this chapter. Although zeolites are not as geologically abundant or widespread as many other silicate mineral groups, there is perhaps more interest in the crystal structures of zeolites than in any other mineral group, as evidenced by the number of reported crystal structure refinements (Table 2).

Table 2. Number of crystal structures reported in ICSD (1995) for selected mineral groups.

Zeolites	273
Cation-exchanged zeolites	409
Feldspars	136
Amphiboles	99
SiO_2 polymorphs	76
Micas	75
Pyroxenes	51

Oxygen and silicon are the two most abundant elements in the Earth's crust, followed by Al, Fe, Ca, Na, Mg, K. Along with H, Ba, and Sr, these are also the major elements found in most zeolite minerals. In fact, many similarities can be drawn between the feldspars, the most abundant mineral group in the Earth's crust, and zeolites. The two most important principles in understanding zeolites (or any mineral group) are that charge balance must be maintained (i.e. the sum of the formal valence charges of the ions in the chemical formula must equal zero) and that the atoms must fit together to form a stable structure under the conditions of formation. Zeolites form at low pressures and temperatures in the presence of H_2O and possess channels and voids in their structures. Their frameworks are thus more open (i.e. they have lower densities) than other silicates. Much of the information about the crystal structure of a zeolite, or any mineral, can be gained from a correct interpretation of its chemical formula. With this in mind, it seems worthwhile to develop systematically the chemical formulas of zeolites based upon a progression from quartz to feldspars and finally to zeolites.

Quartz, feldspars, and zeolites are all classified as tetrahedral framework structures; they have a 1:2 ratio of tetrahedra cations to oxygen. This means that every TO_4 tetrahedron (where T is most commonly Si or Al) shares every O with an adjacent tetrahedron. Quartz (or any SiO_2 polymorph) exists because of the charge balance between one Si^{4+} and two O^{2-} and the fact that Si^{4+} and O^{2-} can be assembled to form a framework. Feldspars, in turn, can be viewed as four SiO_2 or Si_4O_8 groups, with Al substituting for Si. This substitution causes a charge imbalance in the framework. For

1529-6466/01/0045-0001$10.00 DOI: 10.2138/rmg.2001.45.1

instance, when one Al replaces one Si in Si_4O_8, $[AlSi_3O_8]^{1-}$ results. Thus, a monovalent cation, such as Na^+ or K^+ is needed for charge balance. This would result in $Na[AlSi_3O_8]$ or $K[AlSi_3O_8]$, or in general $(Na,K)[AlSi_3O_8]$. Enclosing Na and K in parentheses, separated by a comma, indicates that they can substitute for each another in the same structural site in feldspar. Although Si and Al are tetrahedrally coordinated by O, the relatively large Na and K ions occupy structural "voids" surrounded by six to eight oxygen atoms. With continued Al substitution, $[Al_2Si_2O_8]^{2-}$ arises. This composition is often considered the maximum Al substitution which is possible without direct contact of two AlO_4 tetrahedra, named Loewenstein's rule or the aluminum avoidance rule (Loewenstein 1954). This rule also requires that Si and Al must be well ordered in a framework with an Si to Al ratio of 1:1.

There are various methods to determine (Si,Al) ordering in framework silicates. The simplest approach uses the T-O distance calculated from atomic coordinates of an X-ray crystal-structure refinement. In feldspars a SiO_4 tetrahedron has a mean T-O distance of ~1.61 Å whereas an AlO_4 tetrahedron has a mean T-O distance of ~1.75 Å (e.g. Kunz and Armbruster 1990). Intermediate values are characteristic of a mixed (Si,Al) occupancy. In reality, however, Si-O and Al-O mean distances are not constant values but vary with the distortion of an individual tetrahedron or of the whole framework and depend on additional bonds from extraframework cations (e.g. Alberti et al. 1990, Alberti 1991). For neutron diffraction experiments, Si and Al exhibit different scattering powers and their respective populations can directly be refined. Magic-Angle-Spinning Nuclear Magnetic Resonance (MAS NMR) spectroscopy is a useful powder method to study the (Si,Al) distribution in a mineral, for example for the nuclei ^{29}Si or ^{27}Al (e.g. Kirkpatrick 1988). The MAS NMR spectrum provides information on the local environment of a tetrahedron (i.e. the type and number of neighboring T sites). A typical result could be that an SiO_4 tetrahedron is connected to one Al and three Si tetrahedra.

The (Si,Al) distribution within a tetrahedral framework has a strong bearing on the position of the extraframework cations. According to Pauling's (1939) electrostatic valence rule not only must charge neutrality of a chemical formula be maintained, but each ion must approach an electrostatically balanced structural environment. The strength of an electro-static bond may be defined as a cation's valence charge divided by its coordination number. In an (Si,Al) framework, an SiO_4 tetrahedron may be bonded to three Si and to one Al tetrahedra. Each of the Si-O bonds contributes an electrostatic bond strength of $4/4 = 1$ and each of the Al-O bonds contributes a bond strength of $3/4 = 0.75$. An oxygen atom sharing two Si tetrahedra has a bond strength sum of two which agrees with its formal charge (-2) though with opposite sign. In contrast, an oxygen atom sharing an Si and an Al tetrahedron has a bond strength sum of $1 + 0.75 = 1.75$. Such an oxygen is termed underbonded and is capable of accepting a bond from an extraframework cation. If this oxygen additionally bonds to eight-coordinated extraframework Ca^{2+}, the bond strength sum is increased by $2/8 = 0.25$ and oxygen becomes electrostatically neutral. There are other ways that an ion can achieve an electrostatically balanced environment (e.g. underbonding may lead to shortening and overbonding to lengthening of a bond). An electrostatically balanced structural environment, including the bond length variation, can be evaluated using the bond valence concept of Brown (1992). However, even Pauling's (1939) simple bond strength approach indicates that framework structures with a disordered (Si,Al) distribution prefer a rather disordered extraframework distribution, whereas (Si,Al) ordered structures commonly have an ordered extraframework arrangement.

The chemical formulas for the zeolites are similar to the feldspars with the addition of H_2O. The 1:2 ratio of T to O must be maintained (exceptions are interrupted

frameworks). The greater the substitution of Al for Si, the larger the charge deficiency which must be compensated by cations entering the structure. An aluminosilicate framework has the general formula $[Al_{nx}Si_{n(4-x)}O_{n8}]^{nx-}$, where n is some multiple of this basic building unit needed to fill the unit cell. These frameworks contain voids or cages (Fig. 1) and channels into which cations, commonly referred to as channel or extraframework cations, enter for charge balance. As an example, starting with $[AlSi_3O_8]^{1-}$ and letting n = 9 and x = 1, the framework composition $[Al_9Si_{27}O_{72}]^{9-}$ would be created. Thus, this particular framework would need nine positive charges.

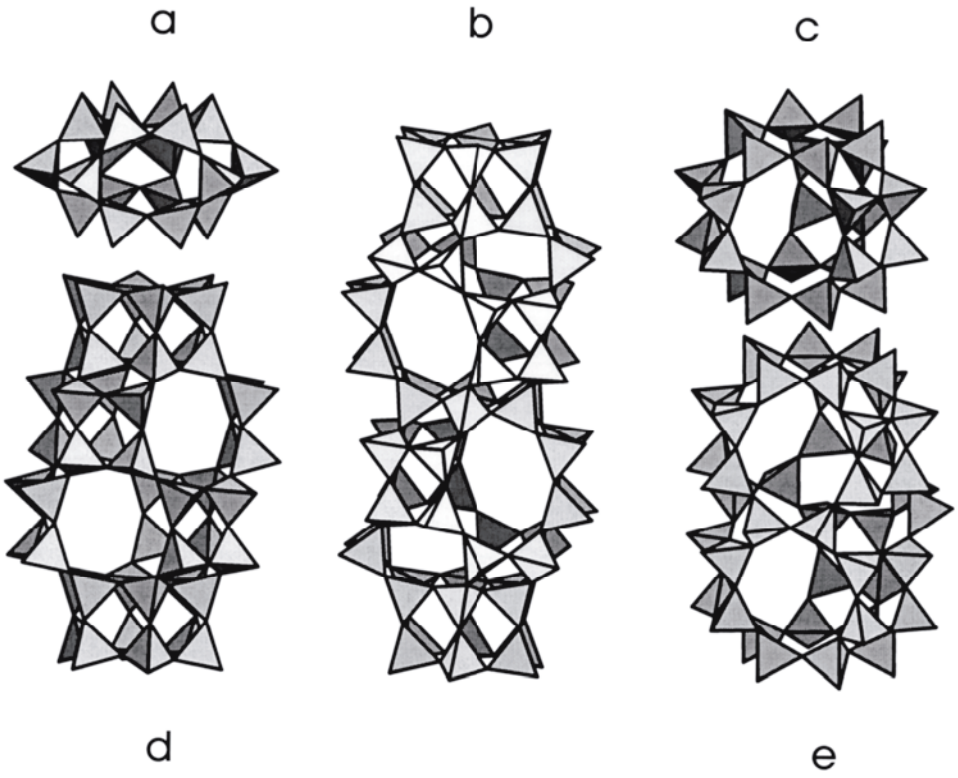

Figure 1. Some characteristic cages found in natural zeolites: (a) cancrinite cage, (b) gmelinite cage, (c) chabazite cage, (d) levyne cage, and (e) erionite cage. The sodalite cage (β-cage) and the α-cage are shown in Figure 13 (below).

One possible way to obtain this would be $(Na,K)Ca_4[Al_9Si_{27}O_{72}]$. The channel cations bond into the frameworks but commonly have one or more sides "exposed" in the channel. These exposed sides lack local charge satisfaction. H_2O can enter the structure to form partial hydration spheres around the channel cations, with the negative dipole of the H_2O molecule pointing toward the exposed positive portion of the channel cation. To complete the above zeolite formula, one could write $(Na,K)Ca_4[Al_9Si_{27}O_{72}]\cdot 24H_2O$. This is the general formula for the zeolite heulandite. Clinoptilolite has a similar framework $[Al_6Si_{30}O_{72}]^{6-}$ but with less Al, thereby requiring a lower channel cation charge (-6 vs -9). Clinoptilolite's general formula can be written as $(Na,K)_6[Al_6Si_{30}O_{72}]\cdot 20H_2O$. Note that clinoptilolite has fewer H_2O molecules than heulandite. Divalent cations, like Ca^{2+} and Mg^{2+}, will in general have larger hydration spheres than monovalent cations, like Na^+ and K^+. Thus, zeolites with divalent channel cations will have more channel H_2O than monovalent cations. There is also more room in the channels for H_2O because one Ca^{2+} occupies less space than two Na^+.

The tetrahedral framework of any zeolite is structurally and chemically much more

rigid and stable than the channel cations and H_2O molecules. The extraframework content in zeolites can be exchanged and dehydrated, which is why zeolites have found so many important industrial applications. Heulandite, $(Na,K)Ca_4[Al_9Si_{27}O_{72}]\cdot 24H_2O$, and clinoptilolite, $(Na,K)_6[Al_6Si_{30}O_{72}]\cdot 20H_2O$, can be used as examples. Their framework structures are identical and a solid solution exists between these two idealized members. The main difference in the above formulas is the ratio of Si to Al. Gunter et al. (1994) and Yang and Armbruster (1996a) performed single-crystal structure refinements on completely exchanged Na, Pb, K, Rb, and Cs heulandites. For these samples the framework remained essentially unchanged. In a similar manner, Armbruster and Gunter (1991) performed crystal structure refinements on a fully hydrated and four partially hydrated phases of a clinoptilolite, yielding a different cation arrangement, but the cation content remained unchanged. Thus the channel occupants can be altered both artificially and in nature.

However, other zeolites exist which have identical framework structures but do not exhibit a continuous solid solution series with respect to the channel cations. An example of this is natrolite $Na_{16}[Al_{16}Si_{24}O_{80}]\cdot 16H_2O$, mesolite $Na_{16}Ca_{16}[Al_{48}Si_{72}O_{240}]\cdot 64H_2O$, and scolecite $Ca_8[Al_{16}Si_{24}O_{80}]\cdot 24H_2O$. From a first glance at the chemical formulas, it might appear there is a solid solution, with two Na cations substituting for one Ca. However, very little variation exists from these ideal formulas found in nature or synthesized in the lab (Ross et al. 1992).

Extended definition of a zeolite mineral

Hey (1930) recognized that zeolites in general have aluminosilicate frameworks with loosely bonded alkali and/or alkali-earth cations and H_2O molecules occupying extraframework positions. More recently, synthetic zeolites have been produced which have tetrahedral sites occupied by elements other than Si and Al. Such examples also exist in the mineral kingdom (e.g. weinebeneite, $Ca[Be_3P_2O_8(OH)_2]\cdot 4H_2O$). Furthermore, certain minerals exist where the tetrahedral framework is interrupted by an OH group (e.g. parthéite). On the other hand, some structures exist with tetrahedral frameworks, large cavities and/or channels with a charge-balanced framework, and extraframework ions are not necessary (e.g. clathrasils, ALPOs, SAPOs). A natural representative of clathrasils is melanophlogite with a pure SiO_2 framework (Gies 1985). Because these "zeolite-like" materials occur, the subcommittee on zeolites of IMA CNMMN (Coombs et al. 1998) proposed a revised definition of a zeolite mineral:

A zeolite mineral is a crystalline substance with a structure characterized by a framework of linked tetrahedra, each consisting of four O atoms surrounding a cation. This framework contains open cavities in the form of channels and cages. These are usually occupied by H_2O molecules and extra-framework cations that are commonly exchangeable. The channels are large enough to allow passage of guest species. In the hydrated phases, dehydration occurs at temperatures mostly below 400°C and is largely reversible. The framework may be interrupted by (OH,F) groups; these occupy a tetrahedron apex that is not shared with adjacent tetrahedra.

This more general view of zeolites, without any constraint in chemical composition, has also been adopted in the following review of zeolite structures. Excluded are frameworks in which any channels are too restricted to allow typical zeolitic behavior, such as reversible dehydration, molecular sieving, or cation exchange (e.g. feldspars, feldspathoids, scapolites, and melanophlogite). In addition, cancrinites are not considered because they represent an independent mineral group.

Zeolitic behavior is not limited to tetrahedral framework structures. The mineral

cavansite $Ca(VO)(Si_4O_{10})\cdot 4H_2O$ (Evans 1973, Rinaldi et al. 1975a) has a tetrahedral framework similar to the zeolite gismondine but with intercalated square pyramidal VO_5 groups. A review of additional minerals not regarded as zeolites but with zeolitic properties is given by Zemann (1991). Two of his prominent examples are: pharmakosiderite with a porous framework $[(Fe_4(OH)_4(AsO_4)_3]^-$ formed by $FeO_3(OH)_3$ octahedra and AsO_4 tetrahedra with H_2O and cations like Na, K, Ba, and Ag occupying the structural voids; and zemannite, $Na_2[Zn_2(TeO_3)_3]\cdot H_2O$, which has wide channels confined by ZnO_6 octahedra and TeO_3 pyramids. Even carbonates like defernite, $Ca_6(CO_3)_{1.58}(Si_2O_7)_{0.21}(OH)_7[Cl_{0.5}(OH)_{0.08}(H_2O)_{0.42}]$, (Armbruster et al. 1996) and holdawayite $(Mn_6(CO_3)_2(OH)_7[Cl,OH]$ (Peacor and Rouse 1988) have wide channels confined by eight $(Ca,Mn)O_{6\text{-}7}$ polyhedra. The channels are lined by OH^- groups with Cl^-, OH^-, or H_2O sitting at the center.

Classification

Currently, three classification schemes are used widely for zeolites. Two of these are based upon specifically defined aspects of the crystal structure, whereas the third has a more historical basis, placing zeolites with similar properties (e.g. morphology) into the same group. Because the physical properties of a mineral (e.g. morphology) are related to its crystal structure, this third method is also indirectly based upon the zeolite's crystal structure.

The first structural classification of zeolites is based upon the framework topology, with distinct frameworks receiving a three-letter code (Table 3; Meier et al. 1996). For instance, the framework for heulandite and clinoptilolite are identical. A framework code of HEU has been assigned to these two zeolites. Heulandite was named before clinoptilolite and was thus given priority in the naming. The frameworks of natrolite, mesolite, scolecite, and gonnardite are all identical, and the code NAT is used to describe these four zeolites. Again, natrolite was the first discovered of the group. Because the channel occupants can be exchanged, a classification based upon framework topology is logical, and this classification scheme works well for those zeolite researchers whose major interests are in cation exchange and synthetic zeolites. Because these codes "should not be confused or related to actual minerals" (Meier et al. 1996), this classification scheme does not work for geologists attempting to name zeolite minerals.

Another structural aspect associated with structure codes is the framework density (FD), which is the number of T-atoms per 1,000 $Å^3$. At a glance, this value reflects the porous nature of a zeolite (i.e. the lower the FD, the larger proportion of the structure is occupied by voids and channels). One criterion Meier et al. (1996) used for inclusion in their Atlas of Zeolite Structure Types is an FD smaller than 21. Other silicates such as scapolite and quartz have FDs of about 22 and 27, respectively. For a complete discussion of framework codes, see Meier et al. (1996).

A second structural method for the classification of zeolites is based upon a concept termed "secondary building units" (SBU). The primary building unit for zeolites is the tetrahedron. SBUs are geometric arrangements of tetrahedra. Here an analogy with general silicate mineralogy will be helpful. In silicate minerals, the tetrahedra can be arranged into groups such as rings, chains, sheets, or frameworks. Thus, in silicate mineralogy we could consider each of these an SBU. (This simplification is not exactly correct, because silicate minerals are mostly composed of additional polyhedral units which are neglected in this SBU model.) In zeolites, groupings of tetrahedra also exist within the framework structure. Quite often, these SBUs tend to control the morphology of the zeolite.

Table 3. Framework codes (Meier et al. 1996) and associated mineral names for zeolites.

ANA (ammonioleucite, analcime, hsianghualite, leucite, pollucite, wairakite)
BEA (tschernichite)
BIK (bikitaite)
BOG (boggsite)
BRE (brewsterite)
CHA (chabazite, willhendersonite)
-CHI (chiavennite)
DAC (dachiardite)
EAB (bellbergite)
EDI (edingtonite, kalborsite)
EPI (epistilbite)
ERI (erionite)
FAU (faujasite)
FER (ferrierite)
GIS (amicite, garronite, gismondine, gobbinsite)
GME (gmelinite)
GOO (goosecreekite)
HEU (clinoptilolite, heulandite)
LAU (laumontite)
LEV (levyne)
LOV (lovdarite)
LTL (perlialite)
MAZ (mazzite)
MER (merlinoite)
MFI (mutinaite)
MON (montesommaite)
MOR (mordenite)
-MOR (maricopaite)
NAT (gonnardite, mesolite, natrolite, paranatrolite, scolecite)
NES (gottardiite)
OFF (offretite)
-PAR (parthéite)
PAU (paulingite)
PHI (harmotome, phillipsite)
RHO (pahasapaite)
-RON (roggianite)
STI (barrerite, stellerite, stilbite)
TSC (tschörtnerite)
TER (terranovaite)
THO (thomsonite)
VSV (gaultite)
WEI (weinebeneite)
YUG (yugawaralite)
no framework code (cowlesite, tvedalite)

Breck (1974) lists seven major groups of zeolites based upon the geometry of the SBU (Table 4). For instance, he classifies NAT structures into his Group 5 with a T_5O_{10} SBU. The predominant crystallographic component of this group is linked chains of tetrahedra parallel to the **c**-axis, which in turn causes minerals of this group to be morphologically elongated parallel to the **c**-axis (Fig. 2), sometimes to the point of appearing fibrous. Group 7 zeolites ($T_{10}O_{20}$), which include heulandite (HEU), clinoptilolite (HEU), stilbite (STI), and brewsterite (BRE), tend to be platy in nature. Their form can be explained by the orientation of their SBUs and, in turn, their channels.

Table 4. Zeolite classification scheme developed by Breck (1974) based on SBUs. This is Breck's table; it has not been updated.

Group 1 (S4R - single 4-ring)
- analcime
- harmotome
- phillipsite
- gismondine
- paulingite
- laumontite
- yugawaralite
- (P)

Group 2 (S6R - single 6-ring)
- erionite
- offretite
- levynite
- sodalite hydrate
- (T, omega, losod)

Group 3 (D4R - double 4-ring)
- (A, N-A, ZK-4)

Group 4 (D6R - double 6-ring)
- faujasite
- chabazite
- gmelinite
- (X, Y, ZK-5, L)

Group 5 (T_5O_{10})
- natrolite
- scolecite
- mesolite
- thomsonite
- gonnardite
- edingtonite

Group 6 (T_8O_{16})
- mordenite
- dachiardite
- ferrierite
- epistilbite
- bikitaite

Group 7 ($T_{10}O_{20}$)
- heulandite
- clinoptilolite
- stilbite
- brewsterite

For instance, the channels in heulandite parallel to the **c**-axis (Fig. 16, below) allow the mineral to break easily along (010), thus yielding perfect (010) platy cleavage. Thus, SBUs aid in understanding of the external morphology of the mineral as well as the crystal structure. See Gottardi and Galli (1985) and Meier et al. (1996) for a more complete discussion of SBUs.

The third broad classification scheme is similar to the SBU classification of Breck (1974), except that it includes some historical context of how the zeolites were discovered and named. This scheme uses a combination of zeolite group names which have specific SBUs and is the most widely used by geologists. This is the classification scheme used by Gottardi and Galli (1985), shown in Table 5.

Newcomers to zeolite research may find these multiple classification schemes very confusing, yet they are necessary. Each scheme is used by certain scientists; the structure codes and SBUs are used more by zeolite researchers (both crystallographers and mineralogists), whereas the group names of Gottardi and Galli (1985) are more useful to geologists and descriptive mineralogists. We had originally thought to propose yet a fourth classification scheme based upon the number of channels, their size and orientation, but we chose not to add more confusion to zeolite classification schemes. Instead, we have adopted a slightly modified classification of Gottardi and Galli (1985).

ZEOLITES WITH T_5O_{10} UNITS — THE FIBROUS ZEOLITES

The basic building block for the zeolites in this subgroup is T_5O_{10} chains of $(Al,Si)O_4$ tetrahedra running parallel to the **c**-axis (Figs. 2a-c) with a periodicity along the

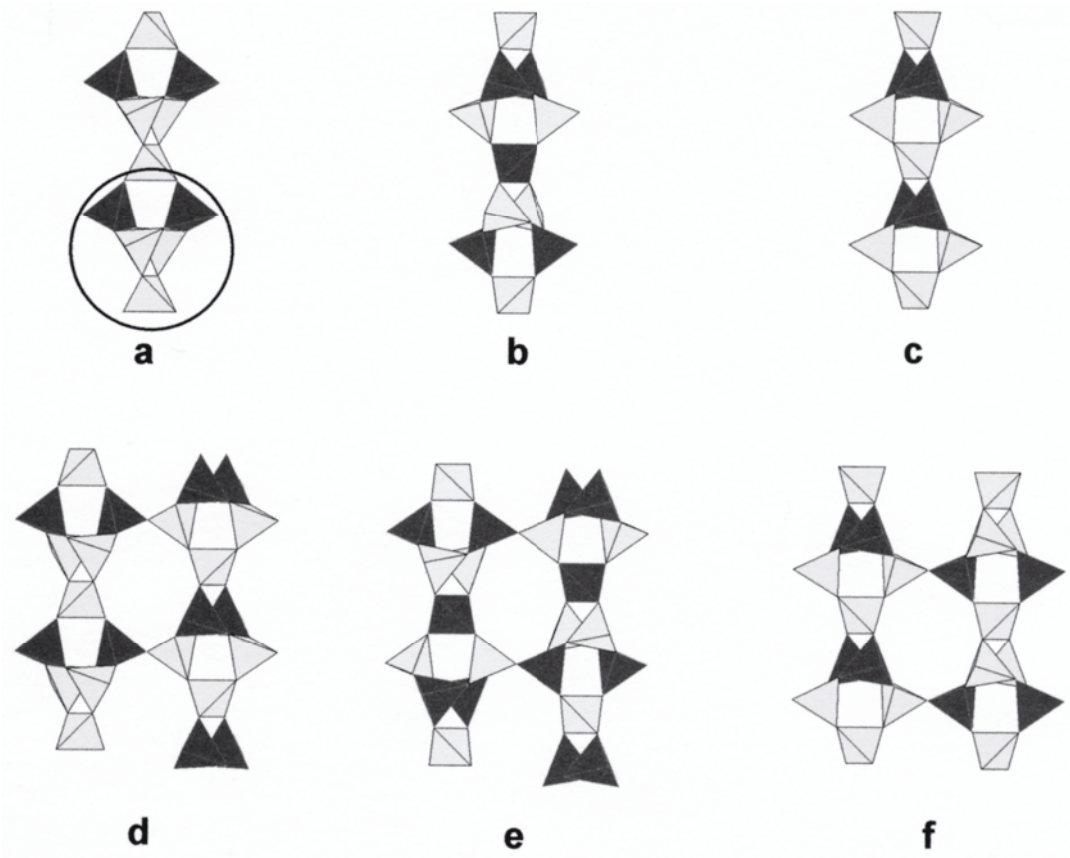

Figure 2. Tetrahedra linking and different types of T_5O_{10} tetrahedra chains for the fibrous zeolites and differing types of cross-linking of tetrahedra chains creating the different framework topologies. The shading of an individual tetrahedron represents its Si (lighter shading) or Al (darker shading) content. The **c**-axis is vertical for all projections. (a) The chain from natrolite viewed down the **a**-axis with an Si/Al ratio of 1.5. The circle outlines a single T_5O_{10} SBU. (b) The chain from thomsonite viewed down the **a**-axis with an ordered Si/Al ratio of 1.0 (i.e. largest amount of Al for any zeolite in this group). (c) A (110) projection of a T_5O_{10} tetrahedra chain from edingtonite viewed down [110] with an Si/Al ratio of 1.5. (d) A $(1\bar{1}0)$ projection showing cross-linking of the T_5O_{10} chains in natrolite. One chain is translated about 1.65 Å in relation to the next. This translation also occurs in (110) (i.e. the plane perpendicular to $(1\bar{1}0)$). (e) A (010) projection showing cross-linking of the T_5O_{10} chains in thomsonite. This translation does not occur in the (100) plane (i.e. the plane perpendicular to (010)). (f) A (110) projection showing cross-linking of the T_5O_{10} chains in edingtonite. No translation occurs in this plane, or in any other plane, in the edingtonite framework.

c-axis of approximately 6.6 Å, or some multiple of 6.6 Å. This 6.6-Å repeat, circled in Figure 2a, contains five tetrahedral sites and ten oxygens, thus the distinction of the T_5O_{10} unit for this group (Breck 1974). Morphologically, this subgroup often appears as needle-like and fibrous crystals extended parallel to the tetrahedral chains. Because of this dominant morphology, this subgroup of zeolites is often referred to as the fibrous zeolites (Gottardi and Galli 1985).

Three different framework topologies exist based upon the cross-linking of the T_5O_{10} tetrahedral chains (Figs. 2d-f), leading to three subgroups: the natrolite group (NAT) (natrolite, mesolite, scolecite, paranatrolite, and gonnardite), thomsonite (THO), edingtonite (EDI) and kalborsite (EDI). Structure projections on the **ab**-plane look very similar for the NAT, THO, and EDI frameworks, with the main difference being the type and location of the channel occupants (Figs. 3 and 4, below). These differences in channel contents are also related to cross-linking of the T_5O_{10} chains, Si/Al content, and (Si,Al) ordering in the chains.

Table 5. Zeolite classification scheme of Gottardi and Galli (1985). [This scheme is used in this chapter.] Listed next to each heading is Breck's associate SBU. This index has not been updated with the new data presented in this chapter; it includes some discredited names.

fibrous zeolites (T_5O_{10})
- natrolite, tetranatrolite, paranatrolite, mesolite, scolecite
- thomsonite
- edingtonite
- gonnardite

single connected 4-ring chains (single 4-ring)
- analcime, wairakite, viséite, hsianghualite
- laumontite, leonhardite
- yugawaralite
- roggianite

doubly connected 4-ring chains
- gismondine, garronite, amicite, gobbinsite
- phillipsite, harmotome
- merlinoite
- mazzite
- paulingite

6-rings (single & double 6 rings)
- gmelinite
- chabazite, willhendersonite
- levyne
- erionite
- offretite
- faujasite

mordenite group (T_8O_{16})
- mordenite
- dachiardite
- epistilbite
- ferrierite
- bikitaite

heulandite group ($T_{10}O_{22}$)
- heulandite, clinoptilolite
- stilbite, stellerite, barrerite
- brewsterite

Unknown structures
- cowlesite
- goosecreekite
- parthéite

The T_5O_{10} chains may be cross-linked in various ways (Alberti and Gottardi 1975, Smith 1983, Malinovskii et al. 1998), but only three connection types have been verified among natural zeolites to form natrolite, thomsonite, and edingtonite group zeolites (Fig. 2). The difference in the three arrangements shown in Figure 2 is the amount of translation of the individual chains with respect to each another as they cross-link to form the three-dimensional framework. Edingtonite is the simplest of the three cases. There are no relative translations between the cross-linking chains (Fig. 2f). Cross-linking of the tetrahedral chains in thomsonite appears similar to that in edingtonite when viewed down the [100] direction, with the difference being that thomsonite has a higher tetrahedral Al content than edingtonite. However, when viewed down the [010] direction, the chains are translated 1/8 *c*, approximately 1.65 Å, (Fig. 2e). In the natrolite group, the chains are also translated about 1.65 Å with respect to each other (Fig. 2d); however, in this structure every adjacent chain is translated with respect to its nearest neighbor, unlike in thomsonite where the translation only occurs in the (010) plane. In the crystal structures analyzed to date, (Si,Al) appears ordered in mesolite and scolecite, ordered to slightly disordered in natrolite, and completely disordered in paranatrolite, and gonnardite (Ross et al. 1992). With this in mind, Alberti et al. (1995) recently proposed some refinements on the classification of this group based on (Si,Al) order-disorder.

All of the framework structures for this group of zeolites contain channels parallel to the **c**-axis. Naturally, these channels must contain sufficient cations to charge balance the framework. The dominant cations occurring in this group are Na, Ca, or Ba. Differing amounts of H_2O also occur within these channels. The channel cations bond both to

framework oxygens and to oxygens associated with channel H_2O molecules. The channels are formed by elliptical rings of eight tetrahedra and vary in size for the three different frameworks. As Ross et al. (1992) noted, the size and shape of the [001] channels vary as a function of the cross-linking of the tetrahedral chains, with edingtonite having the largest channels, thomsonite intermediate, and the natrolite group the smallest channels. Thus, edingtonite would be expected to house larger cations than natrolite, for example, which indeed is the case.

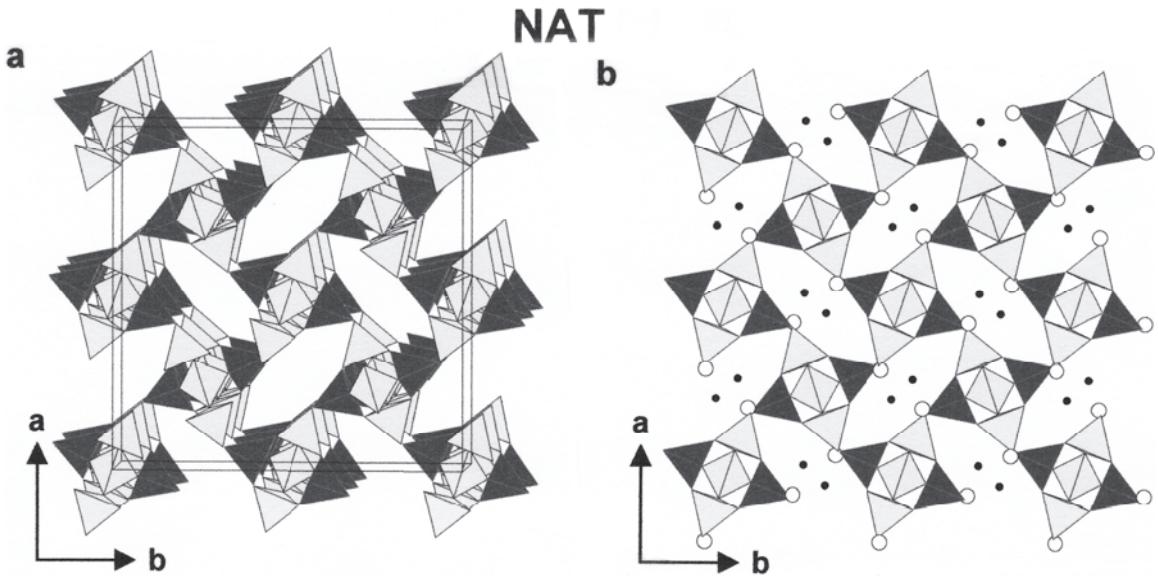

Figure 3. Projections of the natrolite-group structures. (a) The natrolite framework projected on (001) and slightly tilted out of the (001) plane with the **a**-axis vertical and the **b**-axis horizontal. The projection shows the unit cell, the elliptical [001] channels, and a view down the cross-linked T_5O_{10} chains. (b) The natrolite structure projected on (001) with the **a**-axis vertical, showing the framework and channel contents. The Na atoms (small black circles) near the channel center are related to each other by a 2_1 screw in the [001] channel center. H_2O molecules (white circles) are located nearer the channel edges.

Natrolite group (NAT): natrolite, scolecite, mesolite, gonnardite, paranatrolite

The NAT framework of these five zeolites (Fig. 3a) has maximum space group symmetry $I4_1/amd$ assuming complete disorder of (Si,Al). Ordering of Si and Al in the framework lowers this symmetry to $I4_1md$ because previously equivalent tetrahedra become distinct. Distortion of the framework (e.g. tetrahedral rotation caused by addition of channel cations) further reduces this symmetry to $I42d$, the space group for gonnardite. Symmetric and nonsymmetric addition of channel cations further reduces the symmetry to $Fdd2$ (natrolite and mesolite) and $F1d1$ (scolecite). The special arrangement of extraframework cations, responsible for the lowered symmetry of these minerals, may also cause characteristic twinning (Akizuki and Harada 1988).

Natrolite (NAT), $Na_{16}[Al_{16}Si_{24}O_{80}]\cdot 16H_2O$, is orthorhombic, space group $Fdd2$, a = 18.29, b = 18.64, c = 6.59 Å, Z = 1. The structure of natrolite was first proposed by Pauling (1930) and then determined by Taylor et al. (1933). Since then, many other refinements have been made, ranging from low-temperature neutron studies (Artioli et al. 1984) to dehydration studies (Peacor 1973, Bakakin et al. 1994, Joswig and Baur 1995, Baur and Joswig 1996). (See Gottardi and Galli 1985, Ross et al. 1992 and Alberti et al. 1995, for other reviews). Low-temperature neutron refinements have also allowed for

location of the H atoms within the channel and for determination of (Si,Al) ordering (e.g. Artioli et al. 1984). Natrolite's framework consists of ordered cross-linked chains of Si and Al tetrahedra as shown in Figure 3a when viewed down the **c**-axis or when viewed with the **c**-axis vertical (Fig. 2d). Of these three closely related zeolite species, natrolite, mesolite, and scolecite, natrolite shows the highest degree of (Si,Al) disorder. Several refinements have been performed on strongly (Si,Al) disordered natrolites (Alberti and Vezzalini 1981a, Krogh Andersen et al. 1990).

When viewed down the **c**-axis, each channel contains two Na and two H_2O molecules (Fig. 3b). A 2_1 screw axis at the center of each channel leads to a spiral of Na atoms up or down the channel. Each Na is six-coordinated to four framework oxygens and two H_2O molecules. These coordination polyhedra share edges and run parallel to the **c**-axis. A natural K-rich natrolite has K on a new extraframework site close to an H_2O position in regular natrolite (Meneghinello et al. 1999).

Natrolite (unit-cell volume = 2250 $Å^3$) is completely dehydrated at 548 K leading to anhydrous natrolite with a volume = 1785 $Å^3$ and space group *F*112 (Joswig and Baur 1995). At 823 K the unit-cell volume increases to 1960 $Å^3$ (Baur and Joswig 1996) and the space group becomes again *Fdd*2, the same symmetry as found for hydrated natrolite. High-pressure studies are reported by Belitsky et al. (1992). Structures of ion-exchanged natrolite varieties were presented by Baur et al. (1990) and Stuckenschmidt et al. (1992, 1996).

Scolecite (NAT), $Ca_8[Al_{16}Si_{24}O_{80}]\cdot 24H_2O$, is monoclinic, space group *F*1*d*1, a = 18.51, b = 18.98, c = 6.53 Å, β = 90.64°, Z = 1 (Adiwidjaja 1972, Joswig et al. 1984, Stuckenschmidt et al. 1997, Kuntzinger et al. 1998). Neutron diffraction studies at room temperature and at 20 K (Joswig et al. 1984, Kvick et al. 1985) enabled the location of H atoms and showed the framework structure to be ordered. The *F*1*d*1 space group setting (Joswig et al. 1984) permits a direct comparison with the structure of other T_5O_{10} zeolite species because it retains the **c**-axis parallel to the T_5O_{10} chains, whereas the standard *Cc* setting (Kvick et al. 1985) places the **a**-axis parallel to the chains.

The reduction in symmetry from orthorhombic (*Fdd*2) to monoclinic (*F*1*d*1) is related to the symmetry of the channel cation distribution. The 2_1 axes in natrolite do not occur in scolecite because there is only one Ca per channel. The other Na site is replaced by an H_2O molecule, so each channel of scolecite contains one Ca site and three H_2O molecules (Fig. 3c). All Na in natrolite has been replaced by Ca and additional H_2O by the following substitution: $Ca + H_2O \rightarrow 2Na$, thereby maintaining charge balance. Each Ca is seven-coordinated to four framework oxygens and three channel H_2O molecules. These coordination polyhedra do not share edges with each other, as is the case for the Na polyhedra in natrolite. Phase transformations at high hydrostatic pressures were investigated by Bazhan et al. (1999).

Mesolite (NAT), $Na_{16}Ca_{16}[Al_{48}Si_{72}O_{240}]\cdot 64H_2O$, is orthorhombic, space group *Fdd*2, a = 18.405, b = 56.65, c = 6.544 Å, Z = 1 (Adiwidjaja 1972, Artioli et al. 1986a) with a structure similar to natrolite. Mesolite possesses the same space group and similar unit-cell parameters as natrolite, except the b cell edge is tripled. There is complete (Si,Al) ordering in the framework.

Mesolite has two distinct channel types: one contains two Na's and two H_2O molecules and is similar to the channels in natrolite, and the other channel contains one Ca and three H_2O molecules and is similar to the channels in scolecite (Fig. 3d). One plane of Na channels alternates with two planes of Ca channels. These planes are parallel to (010), and this symmetric arrangement of channels results in the tripling of the b cell

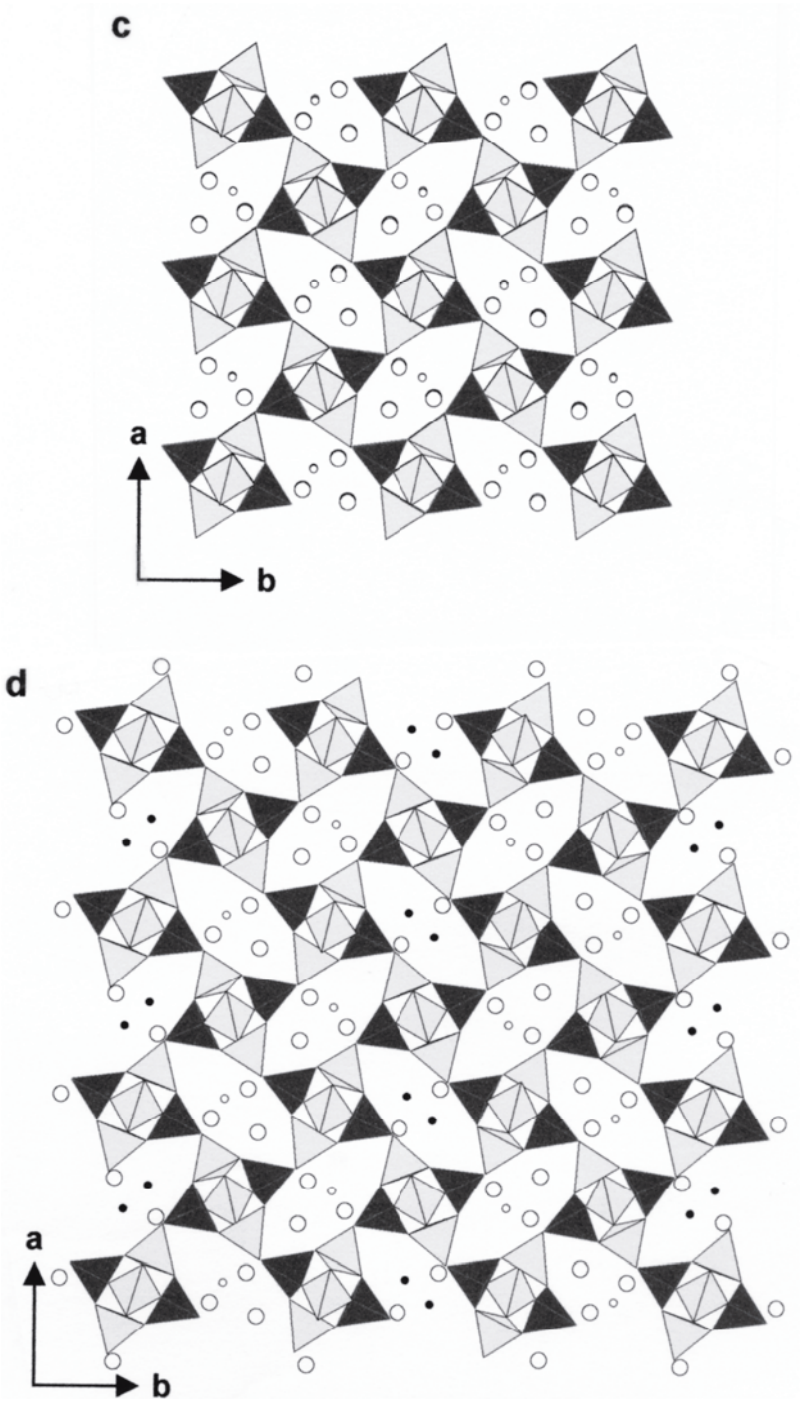

Figure 3, contined. Projections of the natrolite-group structures. (c) The scolecite structure projected on (001) with the **a**-axis vertical, showing the framework and channel contents. A single Ca atom (small white circles) occurs in the [001] channel and has moved closer to the channel center than the Na site in natrolite. Three H_2O molecules (larger white circles) occur in the channel. Two of these are similar to those found in natrolite but have moved away from the channel edge. A new H_2O site occurs in the channel center near the position of one of the Na atoms in natrolite. (d) The mesolite structure projected on (001) with the **a**-axis vertical, showing the Na sites (small black circles), which are similar to those found in natrolite, and the Ca sites (small white circles), which are similar to those found in scolecite. The H_2O positions (larger white circles) are also similar to those found in natrolite and scolecite. There is an ordered arrangement of one "natrolite channel strip" and two "scolecite channel strips" shown vertically, resulting in a tripling of the **b**-axis.

edge, as mentioned above. Structural distortions and extraframework cation arrangement upon dehydration are discussed by Ståhl and Thomasson (1994). Above 598 K mesolite becomes X-ray amorphous.

Gonnardite (NAT) has a highly variable composition, approximated by $(Na,Ca)_{6\text{-}8}[(Al,Si)_{20}O_{40}]\cdot 12H_2O$ (Foster 1965). Alberti et al. (1995) proposed a distinction between gonnardite and tetranatrolite (Chen and Chao 1980) based upon their Si/Al content. However, recently tetranatrolite was discredited (Artioli and Galli 1999) because no valid chemical or crystallographic parameter (Coombs et al. 1998) can be used to distinguish gonnardite from tetranatrolite. Gonnardite is tetragonal, space group $I\bar{4}2d$, a = 13.21, c = 6.62 Å, Z = 1 (Mazzi et al. 1986, Mikheeva et al. 1986, Artioli and Torres Salvador 1991). Only one type of channel exists in gonnardite. However, this one channel type is an "average" of the Na-channel in natrolite and the Ca-channel in scolecite. This average channel contains disordered (Ca,Na) atoms on the two metal sites shown in Figure 4a. The atomic environment surrounding any Na in gonnardite is similar to Na in natrolite. The atomic environment surrounding any Ca in gonnardite is similar to Ca in scolecite. However, for a Na vertically adjacent to a Ca parallel to the **c**-axis, the coordination of Na would increase because of extra channel H_2O located nearer the middle of the [001] channels (Mazzi et al. 1986).

Paranatrolite (NAT), $Na_{16}[Al_{16}Si_{24}O_{80}]\cdot 24H_2O$, has a simplified formula identical to natrolite with the exception of additional H_2O (Chao 1980). The symmetry is pseudo-orthorhombic, a = 19.07, b = 19.13, c = 6.580 Å, Z = 1, but may be monoclinic or triclinic (Chao 1980). Separate species status of paranatrolite is debatable and the mineral may be regarded as over-hydrated gonnardite or natrolite (Coombs et al. 1998). The extra H_2O may fit into channel sites which are vacant in natrolite and are located between the Na sites (Mazzi et al. 1986, Gabuda and Kozlova 1997). These Na sites are related by a 2_1 screw; thus, vacancies exist between them parallel to the **c**-axis. These are the same sites occupied by H_2O in scolecite but they are located nearer the middle of the channel (Fig. 3c).

Thomsonite (THO) and edingtonite (EDI) frameworks

Thomsonite (THO), $Na_4Ca_8[Al_{20}Si_{20}O_{80}]\cdot 24H_2O$, is orthorhombic, space group *Pncn*, a = 13.09, b = 13.05, c = 13.22 Å, Z = 1 (Alberti et al. 1981, Ståhl et al. 1990). The structure of thomsonite was first determined by Taylor et al. (1933) and solved in space group *Pbmn* with a = 13.0, b = 13.0, c = 6.6 Å. The doubling of c (Alberti et al. 1981, Ståhl et al. 1990) is a result of (Si,Al) ordering in the T_5O_{10} chains which are parallel to the **c**-axis (Fig. 2b). Gottardi and Galli (1985) and Tschernich (1992) gave *Pcnn* as the space group setting for thomsonite. *Pcnn* and *Pncn* differ by the choice of the **a**- and **b**-axes. For *Pcnn*, $a < b$, whereas for *Pncn*, $a > b$. The framework consists of cross-linked chains of T_5O_{10} tetrahedra as shown in Figure 2e and explained in detail above. The major channels in thomsonite are parallel to [001], and Ca, Na, and H_2O reside in them. Two types of these channels with different channel occupants can be distinguished. In one channel, there is a fully occupied site with either Na or Ca in equal amounts. In the other channel, Ca occupies a split position about 0.5 Å apart and thus can only be 50% occupied (Fig. 4b). Ross et al. (1992) emphasized that the (Na,Ca) polyhedra share edges parallel to the **c**-axis and that the Ca polyhedra alternate with vacancies. Na and Ca are disordered over these edge-sharing polyhedra (Ståhl et al. 1990). The cation in the edge-sharing (Na,Ca) polyhedron is eight-coordinated with four framework oxygens and four channel H_2O molecules, whereas the isolated Ca polyhedron is six-coordinated with four framework oxygens and two channel H_2O molecules. There are four different H_2O sites, two in the channel containing the (Na,Ca) polyhedron and the other two nearer the channel edge (Fig. 4b).

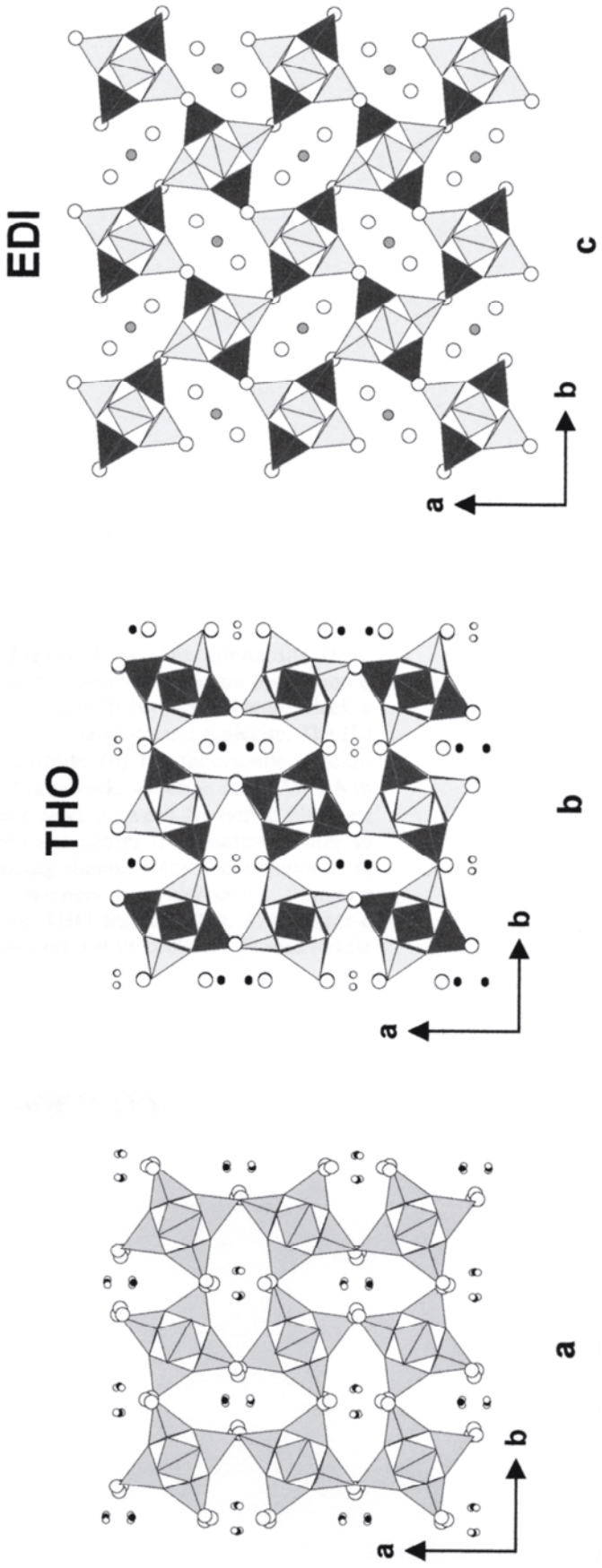

Figure 4. (a) The gonnardite structure projected on (001) with the **a**-axis vertical, showing the disordered framework (i.e. no distinction between the tetrahedra) and channel contents. Each [001] channel can contain both Na atoms (small black circles) and Ca atoms (small white circles) similar to the cation locations in natrolite and scolecite. The H_2O sites (larger white circles) are located nearer the channel edges as in natrolite. (b) The thomsonite structure projected on (001) with the **a**-axis vertical showing the ordered Si/Al framework, which is more Al-rich than the previous fibrous zeolites. There is an even distribution of channel types between Na (small black circles) and Ca (small white circles). H_2O molecules (larger white circles) are nearer the channel center in the Na-containing channels and nearer the edge in the Ca-containing channels. (c) The edingtonite structure projected on (001) with the **a**-axis vertical. Note that the [001] channels are wider in this fibrous zeolite framework than in any of the previous frameworks (i.e. NAT or THO frameworks). This larger-diameter [001] channel houses a Ba (or Sr or Ca) atom (gray-shaded circle) at its center. H_2O sites (white circles) exist both in the [001] channel and near its edge.

Edingtonite (EDI), $Ba_2[Al_4Si_6O_{20}]\cdot 8H_2O$, is either orthorhombic, space group $P2_12_12_1$, a = 9.55, b = 9.67, c = 6.523 Å, Z = 1 Å (Taylor and Jackson 1933, Galli 1976, Kvick and Smith 1983, Belitsky et al. 1986) or tetragonal (Mazzi et al. 1984) space group $P\bar{4}2_1m$, a = 9.581, c = 6.526 Å. Based on optical observations, Akizuki (1986) also discussed triclinic growth sectors in edingtonite. Orthorhombic edingtonites are (Si,Al) ordered, whereas (Si,Al) disorder increases the symmetry to tetragonal. Kvick and Smith (1983) used neutron diffraction to locate the H positions. The framework of edingtonite consists of cross-linked chains of T_5O_{10} tetrahedra as shown in Figure 2f and explained in detail above. The Ba atoms are located in the center of [001] channels on a two-fold axis (Fig. 4c) and are ten-coordinated to six framework oxygens and four H_2O molecules. The coordination polyhedra alternate with vacancies parallel to the **c**-axis similar to the Ca polyhedra in mesolite, scolecite, and thomsonite. There are two H_2O sites in each [001] channel, one located nearer the center and the other nearer the channel's edge (Fig. 4c). Ståhl and Hanson (1998) studied the *in situ* dehydration process using X-ray synchrotron powder-diffraction data and monitored the breakdown of the structure between 660 and 680 K.

Kalborsite (EDI), $K_6B(OH)_4Cl[Al_4Si_6O_{20}]$, is tetragonal, space group $P\bar{4}2_1c$, a = 9.851, c = 13.060 Å, Z = 2 (Malinovskii and Belov 1980). The framework exhibits a well-ordered (Si,Al) distribution. Doubling of the **c**-axis relative to edingtonite occurs due to ordering of $[B(OH)_4]^-$ tetrahedra and Cl^-, both bonded to extraframework K, along the [001] channels. $[B(OH)_4]^-$ and Cl^- sites correspond to the Ba sites in edingtonite. The different size of $[B(OH)_4]^-$ and Cl^- anions causes different distortions of two adjacent cages.

ZEOLITES WITH CHAINS OF CORNER-SHARING FOUR-MEMBERED RINGS INCLUDING THOSE WITH FINITE UNITS OF EDGE-SHARING FOUR-MEMBERED RINGS AND RELATED STRUCTURES

This group is an extension of that defined by Gottardi and Galli (1985) as "zeolites with singly connected 4-ring chains." It is an extension because of several newly described frameworks for natural zeolites.

Analcime, wairakite, pollucite, leucite, ammonioleucite, hsianghualite (ANA)

All minerals listed in this subgroup have the ANA (analcime) framework topology with the maximum space group symmetry *Ia*3*d* which may be lowered due to tetrahedral cation ordering and the extraframework cation arrangement. Four-membered tetrahedral rings, the SBU for this group, form chains in three dimensions, yielding a complex tetrahedral framework. The channel openings are formed by strongly distorted eight-membered rings (aperture 1.6 × 4.2 Å). The channels run parallel to <110> producing six channel directions.

Analcime (ANA), $Na_{16}[Al_{16}Si_{32}O_{96}]\cdot 16H_2O$, crystallizes in various space groups. A stoichiometric analcime according to the above formula was refined in the cubic space group *Ia*3*d* with a = 13.73 Å, Z = 1 (e.g. Ferraris et al. 1972). Such an analcime has a statistical (Si,Al) distribution with only one symmetry-independent tetrahedron. All Na sites within the structural voids are occupied. Na is six-coordinated by four framework oxygens and two H_2O molecules (Fig. 5a). Yokomori and Idaka (1998) and Takaishi (1998) provided structural evidence that the ideal topological symmetry of analcime is not cubic but trigonal $R\bar{3}$ with a = 11.909 Å, α = 109.51°. In general, analcime has split X-ray reflections and non-cubic optical properties (Akizuki 1981a). These non-cubic crystals are always polysynthetically twinned (e.g. Mazzi and Galli 1978). The symmetry

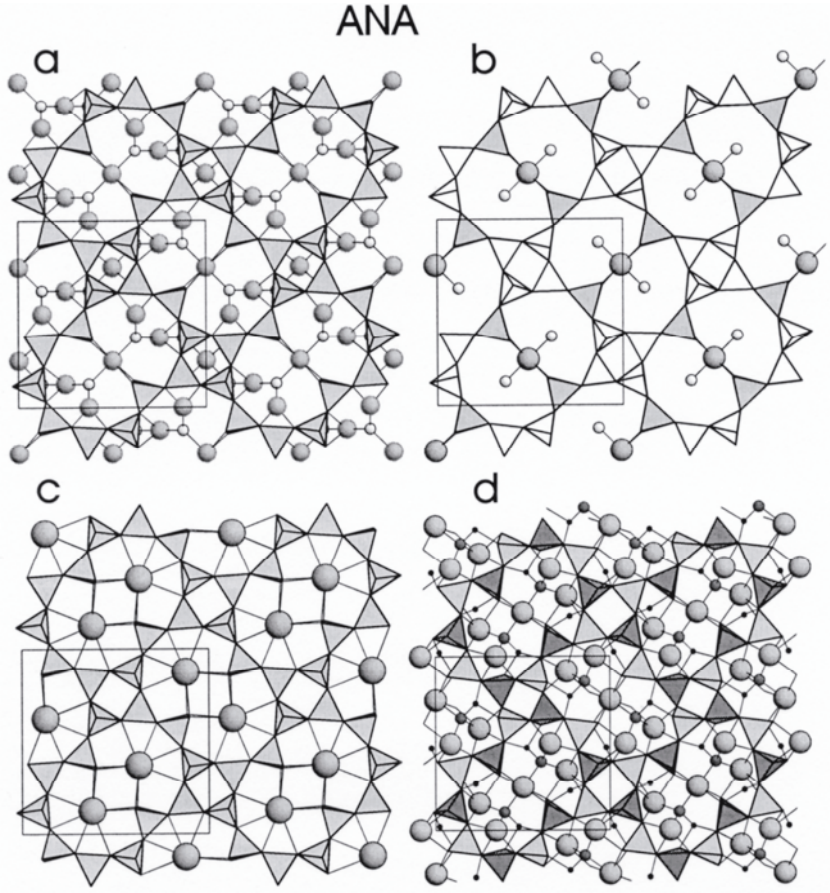

Figure 5. The ANA framework projected parallel to [001] from z ≈ 0 to z ≈ 1/4 with unit-cell outlines. (a) In the cubic analcime structure (*Ia3d*) all tetrahedra show the same shading and are randomly occupied by 2/3 Si and 1/3 Al. Large spheres represent extraframework Na; smaller spheres are H_2O molecules. (b) In the monoclinic (*I*2/*a*) structure of wairakite two different shadings of tetrahedra are distinguished: dark tetrahedra are occupied by Al, and light tetrahedra bear Si. Between the apices of two AlO_4 tetrahedra, Ca (larger spheres) occupies a cavity position. Ca is additionally bonded to two H_2O molecules (small circles). (c) In the cubic (*Ia3d*) structure of pollucite all tetrahedra have the same shading, characterizing a random (Si,Al) distribution as in cubic analcime. Large spheres representing Cs or K occupy the same sites as H_2O in analcime. (d) In the cubic ($I2_13$) structure of hsianghualite light tetrahedra are occupied by Si, and dark tetrahedra by Be illustrating the perfect alternation between Si and Be. Larger spheres in the structural cavities are Ca, intermediate spheres are F, and small circles are Li. Li is tetrahedrally coordinated by three framework oxygens and one fluorine. However, in this truncated portion of the structure not all ligands coordinating Li are shown.

lowering is caused by partial (Si,Al) ordering (Teertstra et al. 1994a, Kato and Hattori 1998) accompanied by extraframework cation order. Four main types of symmetries are observed: cubic *Ia3d*, tetragonal $I4_1/acd$ with $a > c$, tetragonal $I4_1/acd$ with $c > a$, and orthorhombic (*Ibca*) with all the intermediate varieties (Mazzi and Galli 1978); Hazen and Finger (1979) even reported monoclinic or triclinic symmetry. Due to tetrahedral tilting, analcime undergoes several phase transitions with increasing pressure and becomes triclinic at 12 kbar (Hazen and Finger 1979). The dehydration dynamics and the accompanied structural distortions up to 921 K were studied by Cruciani and Gualtieri (1999).

Wairakite (ANA), $Ca_8[Al_{16}Si_{32}O_{96}]\cdot 16H_2O$, with near end-member composition (Aoki and Minato 1980) is monoclinic, *I*2/*a*, $a = 13.699$, $b = 13.640$, $c = 13.546$ Å, $\beta = 90.51°$, $Z = 1$. As found for most analcimes, wairakite exhibits fine lamellar twinning

which probably formed as a consequence of a cubic to monoclinic phase transition (Coombs 1955). Liou (1970) showed the existence of a tetragonal disordered phase between 300 and 460°C. The transformation from this phase to ordered (monoclinic) wairakite is very sluggish. Compared with analcime, wairakite has only half the channel cations due to substitution of Ca^{2+} for $2Na^{+}$. These eight Ca ions exhibit an ordered distribution on the sixteen available positions (Fig. 5b), which also correlates with increased (Si,Al) order (Takéuchi et al. 1979). Monoclinic wairakite has six symmetry independent tetrahedral sites. Four are occupied by Si and two by Al. Ca is six-coordinated to four oxygen atoms, associated with two AlO_4 tetrahedra, and two H_2O molecules.

Pollucite (ANA), $Cs_{16}[Al_{16}Si_{32}O_{96}]$, is not often regarded as a zeolite mineral (Gottardi and Galli 1985) because the end-member formula is anhydrous (Teertstra and Černý 1995). However, pollucite forms a complete solid solution series with analcime. Thus, most members of this series are H_2O bearing (e.g. Teertstra et al. 1992). Pollucite possesses a structural framework (space group *Ia3d*, a = 13.69 Å, Z = 1, for the composition $Cs_{12}Na_4[Al_{16}Si_{32}O_{96}]\cdot 4H_2O$) analogous to cubic analcime with (Si,Al) disorder (Beger 1969). Teertstra et al. (1994a,b) reported some degree of short-range (Si,Al) ordering as observed by ^{27}Al and ^{29}Si MAS NMR spectroscopy. Cs in pollucite (Fig. 5c) occupies the same sites as H_2O in cubic analcime. If pollucite has an analcime component, H_2O and Cs are statistically distributed over the same site.

Leucite (ANA), $K_{16}[Al_{16}Si_{32}O_{96}]$, was previously not regarded a zeolite mineral (Gottardi and Galli 1985, Tschernich 1992) because it is anhydrous and in nature does not seem to form extended solid solution series with either one of the hydrous minerals of this group. Leucite undergoes a cubic-tetragonal phase transition at approximately 600°C. The structure of high-temperature cubic leucite (space group *Ia3d*, a = 13.0 Å, Z = 1) has a statistical (Si,Al) distribution (Peacor 1968), as in cubic pollucite and analcime (Fig. 5c). Extraframework K in cubic leucite occupies the same site as Cs in pollucite, leading to a twelve-fold K coordination with six K-O distances of 3.35 Å and additional six K-O distances of 3.54 Å. When a twinned crystal is heated above 600°C, it transforms to cubic symmetry, but when cooled again, the crystal develops twins with the same proportions and twin boundaries as before (e.g. Korekawa 1969, Mazzi et al. 1976, Palmer et al. 1988). Grögel et al. (1984) and Palmer et al. (1989) suggested the formation of an intermediate tetragonal phase (space group $I4_1/acd$). The room-temperature structure of leucite was refined by Mazzi et al. (1976) in the tetragonal space group $I4_1a$ with a = 13.09, c = 13.75 Å, yielding essentially the same (Si,Al) disorder as in the cubic phase. The major difference between the two phases is the coordination of K. At high temperature (cubic leucite), K is coordinated to twelve oxygens. In tetragonal leucite, the K-bearing cavity is compressed, and K becomes six-coordinated with K-O = 3Å. The strong thermal vibration of K at high temperature requires a larger cavity volume. However, with decreasing temperature the thermal motion becomes less dominant, and the structure changes to an energetically more favorable environment for K. Several NMR studies (e.g. Phillips and Kirkpatrick 1994) have shown that the framework of leucite exhibits some degree of short-range (Si,Al) ordering (in analogy to pollucite). The hypothesis that such ordering could trigger the cubic to tetragonal phase transition was rejected by Dove et al. (1993) using static lattice-energy calculations.

Ammonioleucite (ANA), $(NH_4)_{16}[Al_{16}Si_{32}O_{96}]$, was described as a natural transformation product (ion exchange) of analcime (Hori et al. 1986). Thus, the framework characteristics of analcime are still preserved (Moroz et al. 1998). Ammonioleucite is reported to be tetragonal, space group $I4_1ad$, a = 13.214, c = 13.713 Å, Z = 1.

Hsianghualite (ANA), $Li_{16}Ca_{24}F_{16}[Be_{24}Si_{24}O_{96}]$, crystallizes in the cubic space group $I2_13$ with a = 12.864 Å, Z = 1 (Rastsvetaeva et al. 1991), which is due to (Be,Si) order (Fig. 5d) different from the symmetry of other cubic structures (*Ia*3*d*) of the analcime type. Ca, Li, and F occur as extraframework ions. Ca is eight-fold coordinated by six framework oxygens and two fluorines. Li occupies a site close to the cavity wall and is tetrahedrally coordinated by three framework oxygens and one fluorine. Fluorine is four-coordinated with three bonds to Ca and one to Li. The synthetic compound $Cs_{16}[Be_8Si_{40}O_{96}]$ (ANA) has a pollucite structure and crystallizes in space group *Ia*3*d*, a = 13.406 Å with (Si,Be) disorder (Torres-Martinez et al. 1984).

Kehoeite, doranite, and viséite, originally described with an ANA framework, have been discredited (White and Erd 1992, Teertstra and Dyer 1994, Di Renzo and Gabelica 1995).

Laumontite (LAU)

Fully hydrated laumontite (LAU) has the simplified formula $Ca_4[Al_8Si_{16}O_{48}]\cdot 18H_2O$ (Armbruster and Kohler 1992, Artioli and Ståhl 1993, Ståhl and Artioli 1993). Before these studies, it was assumed that fully hydrated laumontite contained $16H_2O$ pfu (e.g. Coombs 1952, Pipping 1966, Gottardi and Galli 1985). When laumontite is exposed to low humidity, it partially dehydrates at room temperature to a variety named "leonhardite" (Blum 1843, Delffs 1843) with the simplified formula $Ca_4[Al_8Si_{16}O_{48}]\cdot 14H_2O$ (e.g. Coombs 1952, Pipping 1966, Armbruster and Kohler 1992, Artioli et al. 1989). This dehydration can be reversed by soaking the sample in H_2O at room temperature (e.g. Coombs 1952, Armbruster and Kohler 1992) and directly observed with the polarizing microscope by the variation in extinction angle which changes with degree of hydration (Coombs 1952).

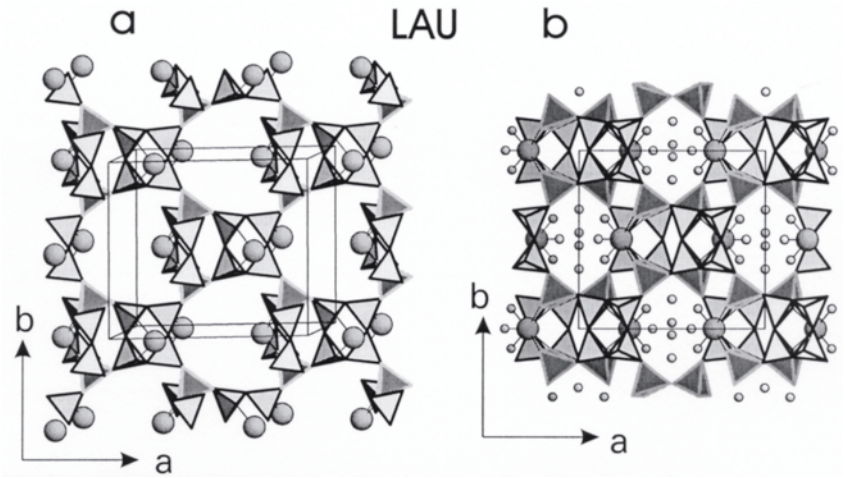

Figure 6. Polyhedral drawings of the laumontite (LAU) framework; AlO_4 tetrahedra have light edges, SiO_4 tetrahedra have dark edges, and spheres represent Ca. (a) Portion of the framework projected approximately on (001) to emphasize the indented shape of the channels parallel to the **c**-axis. (b) Projection along the **c**-axis (channel direction); there are two types of H_2O molecules (small spheres): those coordinating Ca and those in the center of the channels connected to other H_2O molecules and to the channel wall by hydrogen bonds. Note that the AlO_4 tetrahedra are not connected to each other as could be interpreted from this projection.

Various structural studies of laumontite with different degrees of hydration (between 10.8 and 18 H_2O pfu) show that the framework topology remains unchanged and can be described in *C*2/*m* symmetry (Artioli et al. 1989, Armbruster and Kohler 1992, Artioli and Ståhl 1993, Ståhl and Artioli 1993). The framework exhibits two different types of four-membered rings, those where Si and Al alternate and those formed by only SiO_4

tetrahedra. Large channels run parallel to the **c**-axis (Fig. 6a) confined by ten-membered rings (aperture 4.0 × 5.3 Å). Ca occupies a four-fold site on a mirror plane within the **c**-extended channels and is coordinated by three H_2O molecules and four oxygens, belonging to AlO_4 tetrahedra (Fig. 6b).

Room-temperature unit-cell parameters for fully hydrated laumontite with $18H_2O$ are a = 14.863, b = 13.169, c = 7.537 Å, β = 110.18°, Z = 1 (Ståhl and Artioli 1993), whereas the $14H_2O$ variant has a = 14.75, b =13.07, c = 7.60 Å, β = 112.7°, Z = 1 (Pipping 1966). Coombs (1952) found no piezoelectric effect for laumontite and leonhardite but a strong pyroelectric effect. Thus, it may be concluded that the structure lacks a center of symmetry and the space group is either *C*2 or *Cm*. Ståhl and Artioli (1993) discussed the possibility of a locally ordered H_2O superstructure leading to lowering of symmetry. The simplest model would lead to doubling of the *a*-axis with space group *P*2. Armbruster and Kohler (1992) and Ståhl et al. (1996) investigated the dehydration of laumontite. The complicated clustering of H_2O and accompanying phase transitions in laumontite with varying degrees of hydration were studied by Gabuda and Kozlova (1995) using NMR ^{1}H and ^{27}Al spectroscopy between 200 and 390 K.

Fersman (1909) introduced the term "primary leonhardite" for the composition $Na_{1.24}K_{1.59}Ca_{2.55}[Al_{8.18}Fe^{3+}_{0.03}Si_{15.86}O_{48}]\cdot 14H_2O$, later confirmed by Pipping (1966). This "primary leonhardite," with more than five channel cations pfu, neither dehydrates nor rehydrates at room temperature. The excess of channel cations compared with ordinary laumontite indicates that "primary leonhardite" has additional extraframework cation sites (Baur et al. 1997, Stolz and Armbruster 1997) which are occupied by H_2O molecules in fully hydrated laumontite. This also explains why "primary leonhardite" cannot be further hydrated and why it shows no indication of weathering as usual for exposed laumontite. The species name 'leonhardite' was recently discredited (Wuest and Armbruster 1997) because 'leonhardite' is just a partially dehydrated variety of laumontite.

Yugawaralite (YUG)

The framework topology of yugawaralite (YUG), $Ca_2[Al_4Si_{12}O_{32}]\cdot 8H_2O$, space group *C*2/*m* symmetry is reduced to the acentric space group *Pc*, a = 6.72, b = 13.93, c = 10.04 Å, β = 111.1°, Z = 1, due to complete (Si,Al) ordering (Kerr and Williams 1967, 1969; Leimer and Slaughter 1969, Eberlein et al. 1971, Kvick et al. 1986). The mineral is thus piezo- and pyroelectric (Eberlein et al. 1971). Symmetry reduction to *P*1 has been reported on the basis of optical measurements (Akizuki 1987a).

Four-membered rings of tetrahedra are occupied by three Si and one Al in an ordered fashion (Fig. 7a). The structure possesses two types of channel systems confined by eight-membered rings. One channel system extends parallel to the **a**-axis (aperture 2.8 × 3.6 Å), and the other is parallel to the **c**-axis (aperture 3.1 × 5.0 Å). Ca resides at the intersection of the two types of channels and is bonded to four framework oxygens and four H_2O molecules. A neutron single-crystal structure refinement at 13 K (Kvick et al. 1986) located the proton positions. The dehydration of yugawaralite, including an accompanying phase transition at ~200°C, was studied by Gottardi and Galli (1985) and Alberti et al. (1994).

Goosecreekite (GOO)

Goosecreekite (GOO), $Ca_2[Al_4Si_{12}O_{32}]\cdot 10H_2O$, is monoclinic, space group $P2_1$, a = 7.401, b = 17.439, c = 7.293 Å, β = 105.44°, Z = 1. The framework consists of almost completely ordered (Si,Al) tetrahedra (Rouse and Peacor 1986). The assignment of goosecreekite to this group is rather arbitrary, as it has a 6-2 SBU (Meier et al. 1996). However, the structure can also be constructed from corner- and edge-sharing four-membered rings. Strongly deformed eight-membered rings (aperture 4.0 × 2.8 Å) confine

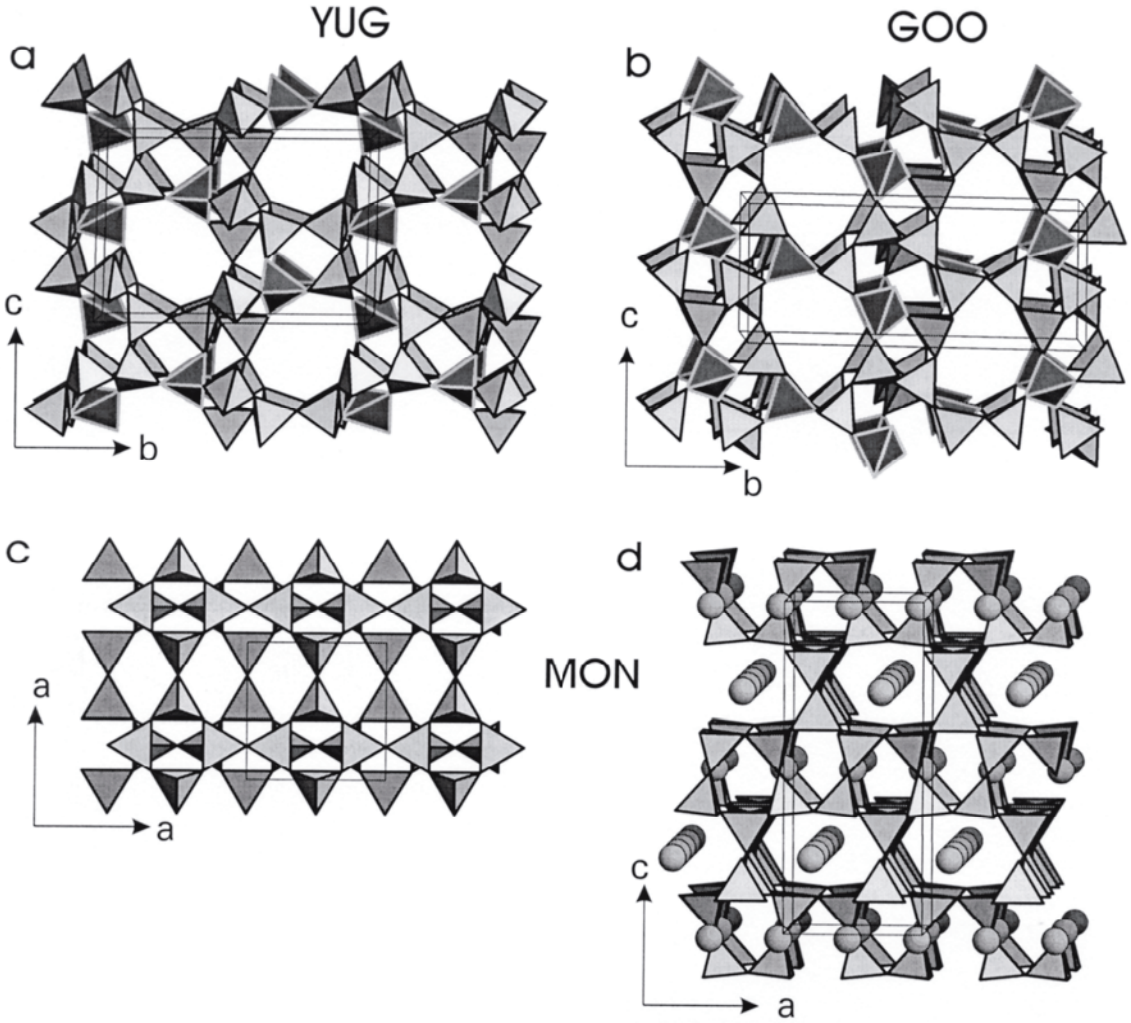

Figure 7. (a) Framework of yugawaralite (YUG) projected approximately along the **a**-axis. SiO_4 tetrahedra have black edges, and AlO_4 tetrahedra have light edges. (b) Framework of goosecreekite (GOO) projected approximately along the **a**-axis. SiO_4 tetrahedra have black edges, and AlO_4 tetrahedra have light edges. (c) A portion of the tetragonal substructure of montesommaite (MON) projected on (001). The framework is built by linked (001) layers consisting of four- and eight-membered rings. (d) The tetragonal substructure of montesommaite (MON) projected approximately along the **a**-axis. Spheres represent (K,Na) sites.

channels parallel to the **a**-axis (Fig. 7b) which are connected by additional eight-ring channels (aperture 2.7 × 4.1 Å) running zigzag-wise parallel to the **b**-axis. Eight-membered ring channels also run parallel to the **c***-axis. Ca is located roughly at the intersection of these channels and bonds to two framework oxygens and five H_2O molecules. All H_2O molecules are bonded to Ca.

Montesommaite (MON)

Montesommaite (MON), $(K,Na)_9[Al_9Si_{23}O_{64}]\cdot 10H_2O$, was described as being closely allied to merlinoite and gismondine (Rouse et al. 1990, Alberti 1995). However, in the more rigorous classification used in this chapter, montesommaite must be assigned to the group with chains of corner-sharing four-membered rings and not the "edge-sharing four-membered rings." Montesommaite is orthorhombic, space group, *Fdd*2, a = 10.099, b = 10.099, c = 17.307 Å, Z = 1, but it is nearly tetragonal, pseudo $I4_1/amd$ (a = 7.141, c = 17.307 Å). The tetragonal substructure was solved (Rouse et al. 1990) by

analogy to Smith's (1978) hypothetical model 38 and refined from semi-quantitative powder diffraction data. The framework can be constructed by linking (001) sheets, formed by four- and eight-membered rings (Fig. 7c). The structure (Fig. 7d) has straight eight-membered ring channels running parallel to the **a**- and **b**-axes (aperture 3.6 Å). K is in eight-fold coordination by six framework oxygens and two H_2O molecules.

Roggianite (-RON)

Roggianite (-RON) with the simplified formula $Ca_2[Be(OH)_2Al_2Si_4O_{13}]\cdot 2.5H_2O$ crystallizes in space group *I*4/*mcm*, *a* = 18.370, *c* = 9.187 Å, Z = 8 (Passaglia and Vezzalini 1988, Giuseppetti et al. 1991). The crystal structure (Giuseppetti et al. 1991) shows a well-ordered (Si,Al,Be) distribution and is characterized by large twelve-membered tetrahedral rings (aperture 4.2 Å) forming channels parallel to the **c**-axis (Fig. 8a). These channels bear three types of partially occupied, disordered H_2O sites but no cations. A special structural and chemical feature of roggianite is the existence of framework OH groups terminating the two corners of a BeO_4 tetrahedron. All interrupted framework structures, including roggianite, are marked by a dash in front of the framework code. Ca occupies a narrow cage and bonds within 2.4 Å to six framework oxygens. Two additional framework oxygens sites are 2.9 Å from Ca; thus, the coordination may be described as 6+2. Voloshin et al. (1986) described an alleged new mineral with the unapproved name "ginzburgite" which is identical to roggianite.

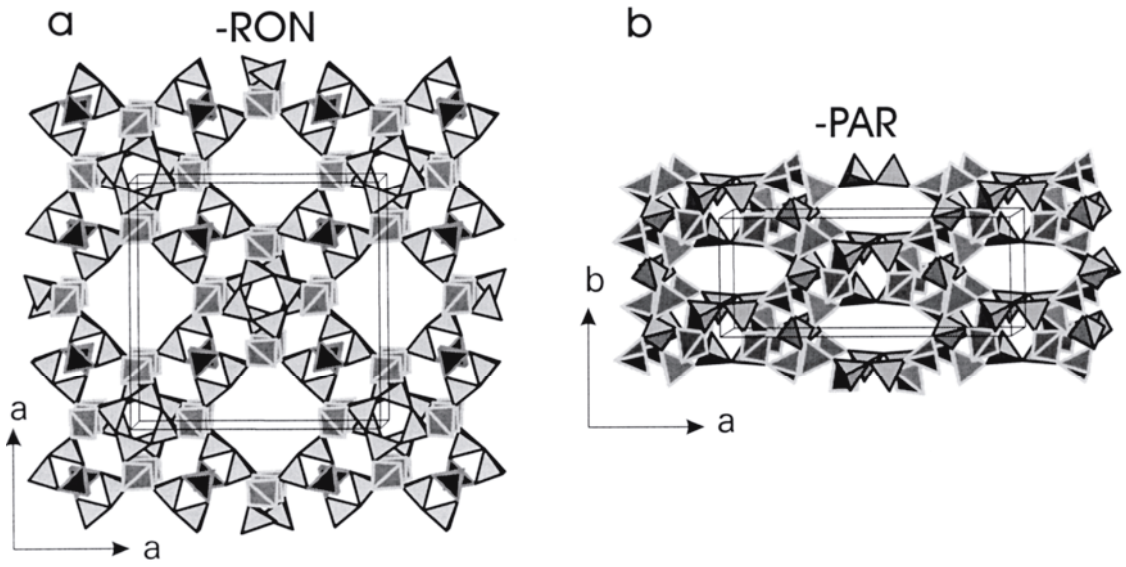

Figure 8. (a) Framework of roggianite (-RON) projected approximately along the **c**-axis (channel direction). SiO_4 tetrahedra are light with dark rims, AlO_4 tetrahedra are gray with light rims, and $BeO_2(OH)_2$ tetrahedra are black with light rims. H_2O molecules (not shown) fill the wide structural channels, whereas Ca (not shown) occupies a narrow cage close to the $BeO_2(OH)_2$ tetrahedra. (b) Framework of parthéite (-PAR) projected approximately along the **c**-axis. SiO_4 tetrahedra have black edges, and AlO_4 tetrahedra have light edges.

Parthéite (-PAR)

Parthéite (-PAR), $Ca_2[Al_4Si_4O_{15}(OH)_2]\cdot 4H_2O$, is monoclinic, space group *C*2/*c*, *a* = 21.555, *b* = 8.761, *c* = 9.304 Å, β = 91.55°, Z = 4. The structure (Engel and Yvon 1984) exhibits a completely ordered (Si,Al) distribution. Due to the presence of OH groups, the framework is interrupted at every second AlO_4 tetrahedron. The framework can be constructed from corner-sharing four-rings with intercalated finite units of three edge-

sharing four-rings. Thus, strictly speaking, the framework of parthéite is a hybrid between two different structural units of Gottardi and Galli (1985). Strongly compressed channels (Fig. 8b) exist parallel to the **c**-axis delimited by ten-membered rings (aperture 6.9 × 3.5 Å). Ca in these channels has a distorted cube-like coordination formed by six framework oxygens and two H_2O molecules.

ZEOLITES WITH CHAINS OF EDGE-SHARING FOUR-MEMBERED RINGS

Zeolite minerals with the gismondine (GIS), phillipsite (PHI), and merlinoite (MER) framework have the same double crankshaft as their main building block (Fig. 9a). A double crankshaft is formed by alternating four-membered rings with four tetrahedral apices pointing up (U) and four tetrahedral apices pointing down (D). Thus, in the chain direction the arrangement can be described as UUDDUUDD. These four-membered rings are connected by edge-sharing to chains leading to a corrugated ribbon resembling a crankshaft with a periodicity of ~10 Å. If this tetrahedral double crankshaft is projected along the direction of extension, it appears as a four-membered ring. Smith (1978) and Sato (1979) showed that there are seventeen possibilities to connect the double crankshaft to a framework. Only three of these have been observed in zeolite minerals. A review of these hypothetical and observed structures is provided by Sato and Gottardi (1982). Different types of double crankshafts are found for mazzite, perlialite, and boggsite (Fig. 9b,c).

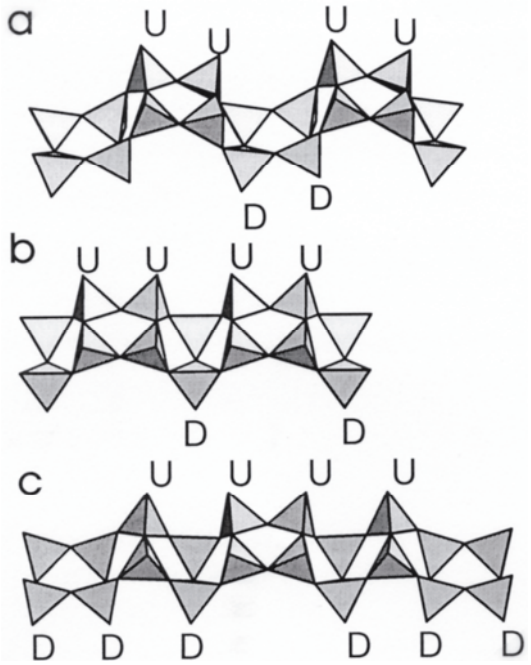

Figure 9. (a) Double crankshaft (GIS, PHI, and MER) formed by alternating four-membered rings with four tetrahedral apices pointing upward and downward. These rings share edges to form infinite chains with a periodicity of approximately 10 Å. Along the chain direction, the orientation of tetrahedral apices is defined as UUDDUUDD (U = up, D = down). A double crankshaft projected along the extension direction appears as a four-membered ring. (b) Chains of edge-sharing four-membered rings in mazzite and perlialite have the sequence of tetrahedral apices UUDUUD (U = up, D = down) leading to a periodicity of approximately 7.5 Å. (c) Chains of edge-sharing four-membered rings in boggsite have the sequence of tetrahedral apices DDUDUUDUDD (D = down, U = up) or vice versa leading to a periodicity of approximately 20 Å.

Gismondine, garronite, amicite, gobbinsite (GIS)

All minerals in this subgroup have the GIS (gismondine) framework topology, which has the maximum space group symmetry $I4_1/amd$. The channels running parallel to the **a**- and **b**-axes are confined by eight-membered rings (aperture 3.0 × 4.7 Å). Only the structure of the high-silica variety of the synthetic zeolite Na-P (GIS) preserves the topological symmetry $I4_1/amd$ (Hakanson et al. 1990). There are two systems of double crankshafts (along the **a**- and **b**-axes) related by a 4_1 axis forming the GIS framework (Fig. 10a). If the tetrahedra are alternately occupied by Si and Al (gismondine and amicite), the symmetry is lowered at least to orthorhombic *Fddd*. Additional symmetry

lowering occurs due to the distribution of channel cations and H_2O molecules.

Gismondine (GIS), $Ca_4[Al_8Si_8O_{32}]\cdot 16H_2O$, has a completely (Si,Al) ordered framework with space group $P2_1/c$, a = 10.02, b = 10.62, c = 9.84 Å, β = 92.5°, Z = 1, with the pseudo-4_1 axis parallel to the **b**-axis. Ca is displaced from the center of the cavity at the intersection of the eight-membered ring channels and is attached to one side of the eight-membered ring (Fig. 10a). Ca is coordinated to two framework oxygens and four H_2O molecules (Fischer and Schramm 1971, Rinaldi and Vezzalini 1985). Artioli et al. (1986b) located all proton positions by single-crystal neutron diffraction at 15 K and found two statistically distributed configurations for the Ca coordination. In the more frequent configuration (70%), Ca is six-coordinated. In the other variant (30%), one H_2O molecule splits to two new sites; thus, the coordination becomes seven-fold. Upon partial dehydration gismondine undergoes several phase transitions accompanied by symmetry reduction (Reeuwijk 1971, Vezzalini et al. 1993, Milazzo et al. 1998). Structure refinements on cation-exchanged varieties were performed by Bauer and Baur (1998).

Garronite (GIS), $NaCa_{2.5}[Al_6Si_{10}O_{32}]\cdot 13H_2O$, may be considered the (Si,Al) disordered equivalent of gismondine. Artioli (1992) applied the Rietveld method to X-ray powder diffraction data to study the structures of two garronite samples and found the space group to be lowered to $I\bar{4}m2$ with a = 9.9266, c = 10.3031 Å, Z = 1. The symmetry lowering from $I4_1/amd$ to $I\bar{4}m2$ is explained in terms of cation and H_2O arrangements in the structural cavities. There seems to be an indication of partial (Si,Al) ordering. Four partially occupied H_2O sites, two partially occupied nearby Ca sites, and one Na site were located. The short distances preclude simultaneous occupation of Ca and Na sites. Orthorhombic symmetry has been proposed by Nawaz (1983) and Howard (1994). Garronite can only partly be dehydrated and the framework collapses above 254°C. Partially dehydrated phases have decreased symmetry with space groups $I2/a$ and $P4_12_12$ (Schröpfer and Joswig 1997, Marchi et al. 1998).

Amicite (GIS), $Na_4K_4[Al_8Si_8O_{32}]\cdot 10H_2O$, has perfect (Si,Al) order like gismondine but with space group $I2$, a = 10.226, b = 10.422, c = 9.884 Å, β = 88.32°, Z = 1 (Alberti and Vezzalini 1979). The pseudo-4_1 axis generates two sets of double crankshafts parallel to the **b**-axis. Na and K are well ordered in two completely occupied sites. Na is six-coordinated by three framework oxygens and three H_2O molecules. K is seven-coordinated by four framework oxygens and three H_2O molecules. In amicite, two of the gismondine Ca sites are occupied by Na with two additional Na sites. K sites in amicite are occupied in gismondine by H_2O. Three filled H_2O sites are bonded to channel cations. One additional H_2O site is only half occupied and shows a long distance (2.9 Å) to Na. Amicite can be completely dehydrated without destruction of the framework (Vezzalini et al. 1999).

Gobbinsite (GIS), $Na_5[Al_5Si_{11}O_{32}]\cdot 11H_2O$, could only be studied on the basis of X-ray powder data (Nawaz and Malone 1982, McCusker et al. 1985, Artioli and Foy 1994). McCusker et al. (1985) refined the structure of $Ca_{0.6}Na_{2.6}K_{2.2}[Al_6Si_{10}O_{32}]\cdot 12H_2O$ in space group $Pmn2_1$, a = 10.108, b = 9.766, c = 10.171 Å, Z =1, using the Rietveld method and geometric constraints for the framework. The pseudo-4_1 axis in gobbinsite is parallel to the **c**-axis. Ordering of Si and Al is not apparent but cannot be ruled out. The Na sites (more than half occupied) are five-coordinated by three framework oxygens and two H_2O molecules and occupy an eight-membered ring perpendicular to the **a**-axis. K (less than half occupied) is located in an eight-membered ring perpendicular to the **b**-axis and is coordinated by two framework oxygens and one H_2O molecule. Orthorhombic symmetry occurs because of the cation distribution.

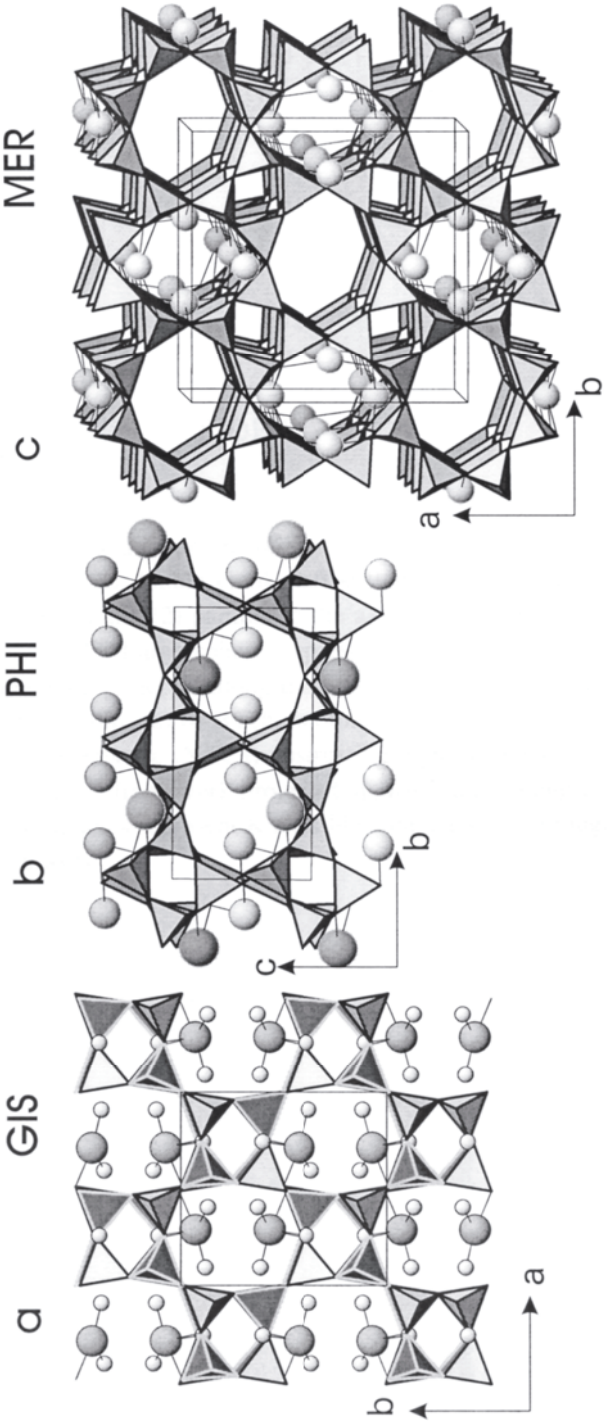

Figure 10. (a) The gismondine (GIS) framework projected along the **c**-axis. The pseudo-4_1 axis is parallel to the **b**-axis. Two double crankshaft systems can be seen: (1) along the direction of projection (four-membered rings) and (2) parallel to the **a**-axis. Tetrahedra with light edges are filled with Al; those with black edges by Si. Large spheres represent Ca; small spheres are fully occupied H_2O. (b) The phillipsite (PHI) framework projected along the **a**-axis, parallel to the extension of double crankshafts. Large spheres represent K (phillipsite) or Ba (harmotome) which block eight-membered ring channels parallel to the **c**-axis. Small spheres are (Na,Ca) obstructing eight-membered ring channels parallel to the **b**-axis. (c) The merlinoite (MER) framework projected approximately along the **c**-axis parallel to the extension of double crankshafts. Spheres represent K sites blocking passages through eight-membered ring channels parallel to the **a**- and **b**-axes.

Phillipsite (PHI) and merlinoite (MER) frameworks

Phillipsite (PHI), $K_2(Ca_{0.5},Na)_4[Al_6Si_{10}O_{32}]\cdot 12H_2O$, and **harmotome** (PHI), $Ba_2(Ca_{0.5},Na)[Al_5Si_{11}O_{32}]\cdot 12H_2O$, form a solid-solution series. The true space group of phillipsite and harmotome is still under debate. Recent X-ray and neutron single-crystal structure refinements between 15 and 293 K confirm the centric space group $P2_1/m$ for harmotome (Stuckenschmidt et al. 1990) proposed by Rinaldi et al. (1974). There are, however, hints of acentricity (space group $P2_1$ or even $P1$), indicated by piezoelectricity (Sadanaga et al. 1961) and optical domains (Akizuki 1985). Room-temperature unit-cell parameters are a = 9.869, b = 14.139, c = 8.693 Å, β = 124.81°, Z = 1, for harmotome, $Ba_{1.92}Ca_{0.46}K_{0.07}[Al_{4.65}Si_{11.26}O_{32}]\cdot 12H_2O$, and a = 9.865, b = 14.300, c = 8.668 Å, β = 124.20°, Z = 1, for phillipsite, $K_{2.0}Ca_{1.7}Na_{0.4}[Al_{5.3}Si_{10.6}O_{32}]\cdot 13.5H_2O$ (Rinaldi et al. 1974). Both structures have similar cation and H_2O distributions within the structural channels (Fig. 10b), and Ba and K occupy more or less the same site. Three types of channels confined by eight-membered rings of tetrahedra exist, one parallel to the **a**-axis (aperture 3.6 Å), one parallel to the **b**-axis (aperture 4.3 × 3.0 Å), and another parallel to the **c**-axis (aperture 3.3 × 3.2 Å). The double crankshafts run parallel to the **a**-axis (Fig 10b). Ordering of (Ca,Na) vacancies combined with (Si,Al) order might be responsible for symmetry lowering as discussed above. Stuckenschmidt et al. (1990) proposed a partially ordered (Si,Al) distribution, whereas Rinaldi et al. (1974) stated that the near uniformity of T-O distances gives little or no suggestion of (Si,Al) order. Ba in harmotome is coordinated to four H_2O molecules and seven framework oxygens. Only one of these four H_2O molecules is weakly fixed by hydrogen bonds; the others are strongly disordered. Two additional strongly disordered H_2O molecules reside in the structural channels and are not bonded to cations (Stuckenschmidt et al. 1990). Similar H_2O disorder is also found in phillipsite (Rinaldi et al. 1974). Stacking faults on (100) and (010) by a slip of $a/2$ or $b/2$ are possible in all frameworks with the double crankshaft. Thus, as a result of $a/2$ faults, sedimentary phillipsite may be composed of phillipsite and merlinoite domains (Gottardi and Galli 1985). Rietveld refinements of Sr- and Cs-exchanged phillipsites were reported by Gualtieri et al. (1999a,b).

Merlinoite (MER), simplified $K_5Ca_2[Al_9Si_{23}O_{64}]\cdot 24H_2O$, is pseudo-tetragonal, space group $I4/mmm$ but the true structure is orthorhombic $Immm$ with a = 14.116, b = 14.229, c = 9.946 Å, Z = 1 (Galli et al. 1979). The framework has a statistical (Si,Al) distribution and contains channels, confined by eight-membered rings, parallel to the **a**-axis (aperture 3.5 × 3.1 Å) and the **b**-axis (aperture 3.6 × 2.7 Å). Eight-membered double and single rings delimit channels (aperture 5.1 × 3.4 Å and 3.3 × 3.3 Å) parallel to the **c**-axis. The double crankshafts also run parallel to the **c**-axis. The framework topology of merlinoite (Fig. 10c) is identical to the synthetic barium chloroaluminosilicate (Solov'eva et al. 1972) which is tetragonal. K and Ba occupy the center of two deformed eight-membered rings connecting a small and a large cage. Additional partially occupied and disordered cation positions were located within the larger cage. Two fully and six partially occupied H_2O sites were located in merlinoite (Galli et al. 1979). Structure refinements of natural merlinoite varieties, $NaK_5Ba_3[Al_{12}Si_{20}O_{64}]\cdot 20H_2O$, $Immm$ with a = 14.099, b = 14.241, c = 10.08 Å, Z =1 (Baturin et al. 1985), and $Na_5K_7[Al_{12}Si_{20}O_{64}]\cdot 24H_2O$, $Immm$ with a = 14.084, b = 14.264, c = 10.112 Å, Z = 1 (Yakubovich et al. 1999) also yielded strongly disordered extraframework cation and H_2O arrangements.

Mazzite (MAZ) and perlialite (LTL)

In contrast to the double crankshafts in which alternately two tetrahedral apices point up and down along the chain direction, the edge-sharing four-ring chains in mazzite and perlialite have the sequence of two tetrahedral apices up and one down or vice versa

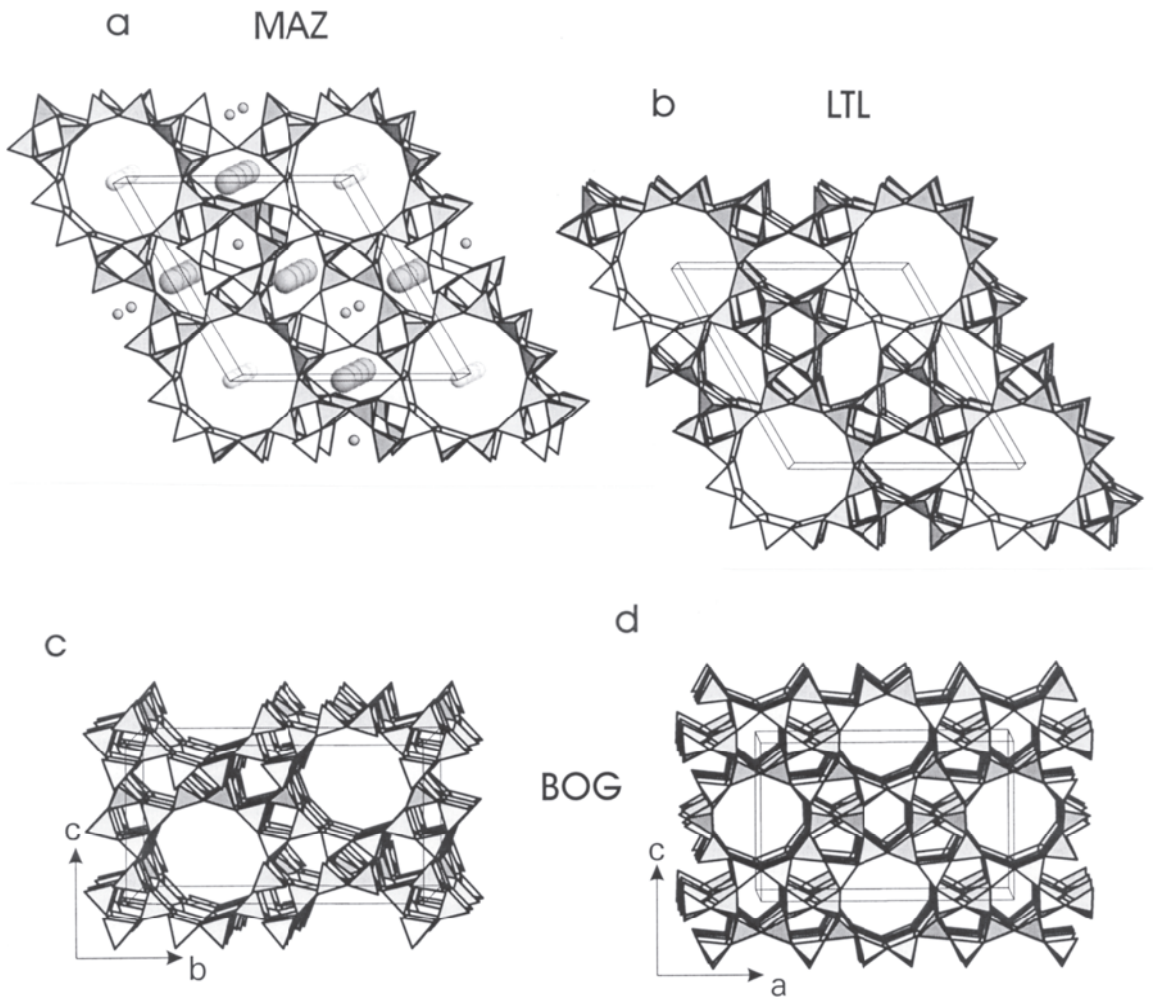

Figure 11. (a) The mazzite (MAZ) framework projected approximately along the **c**-axis, parallel to the edge-sharing four-membered ring chains. Notice the six-membered single ring and the twelve-membered double ring in contrast to perlialite (LTL). Small spheres are Mg, intermediate spheres are Ca, and large spheres are K. (b) The perlialite (LTL) framework projected approximately along the **c**-axis. Notice the six-membered double rings and twelve-membered single rings in contrast to mazzite. (c) The boggsite (BOG) framework projected approximately along the **a**-axis, parallel to the crankshafts (d) The boggsite (BOG) framework projected approximately along the **b**-axis.

(Fig. 9b), leading to a periodicity of about 7.5 Å.

Mazzite (MAZ), $K_{2.5}Mg_{2.1}Ca_{1.4}Na_{0.3}[Al_{10}Si_{26}O_{72}]\cdot 28H_2O$, is hexagonal, space group $P6_3/mmc$, a = 18.392, c = 7.646 Å, Z = 1 (Galli 1975). Two types of channels run parallel to the **c**-axis (Fig. 11a). One is confined by twelve-membered rings of tetrahedra (aperture 7.4 Å), the other by eight-membered rings (aperture 5.6 × 3.4 Å). T-O distances are consistent with (Si,Al) disorder. Mg occurs in a "gmelinite-type" cage (Fig. 1b) and is six-coordinated by H_2O molecules. Galli (1975) speculated that the Mg-H_2O complex acts as a template for the formation "gmelinite-type cages" (Fig. 1b). An additional cation site (occupancy approximately 50%) is mainly occupied by K and is situated in the distorted eight-membered rings. K is octahedrally coordinated by four framework oxygens and two H_2O molecules. Ca is located in the center of the large channels running parallel to the **c**-axis and is surrounded by disordered H_2O molecules. The walls of the

large channels are lined with H_2O molecules, and the cations sit at regular intervals in the middle of these H_2O pipes (Galli 1975). Dehydration of mazzite and accompanying cation diffusion was investigated by Rinaldi et al. (1975b) and Alberti and Vezzalini (1981b).

Perlialite (LTL), $K_9Na(Ca,Sr)[Al_{12}Si_{24}O_{72}]\cdot 15H_2O$, is hexagonal, space group *P*6/*mmm*, $a = 18.54$, $c = 7.53$ Å, $Z = 1$. The framework topology (Artioli and Kvick 1990) is the same as for synthetic Linde Type L (LTL) as determined by Barrer and Villiger (1969). Two types of channels run parallel to the **c**-axis. One is bounded by twelve-membered rings (aperture 7.1 Å), and the other is bounded by strongly compressed eight-membered rings (aperture 3.4 × 5.6 Å). T-O distances give no indication of (Si,Al) order. When comparing the structural drawings for mazzite and perlialite (Fig. 11a,b) projected parallel to the **c**-axis, strong similarities are evident. However, in perlialite six-membered double rings connect the sheets, whereas six-membered single rings occur in mazzite. Thus, in perlialite six-membered double rings connect two cancrinite-type cages (Fig. 1a), and in mazzite six-membered single rings link two gmelinite cages (Fig. 1b). The powder sample of perlialite used for structure refinement (Artioli and Kvick 1990) was separated with Tl-malonate (heavy liquid). Thus, perlialite became partly ion-exchanged and approached the composition $K_8Tl_4[Al_{12}Si_{24}O_{72}]\cdot 20H_2O$. K was located in the cancrinite cage (fully occupied) and in the center of the six-membered double rings (occupancy 20%). Cations in the large channels bonded to six framework oxygens of the eight-membered rings and additional H_2O molecules which fill the interior of the twelve-membered ring channels. Notice the different arrangement of cations and H_2O in the wide channels compared with mazzite. The second most preferred extraframework site (fully occupied) is in the compressed eight-membered rings, forming channels parallel to the **c**-axis.

Boggsite (BOG)

Boggsite (BOG), $Ca_8Na_3[Al_{19}Si_{77}O_{192}]\cdot 70H_2O$, is orthorhombic, space group *Imma*, $a = 20.236$, $b = 23.798$, $c = 12.798$ Å, $Z = 1$. A third type of chain of edge-sharing four-membered rings is found in boggsite. The up (U) and down (D) orientation of the tetrahedral apices follows the sequence DDUDUUDUDD (Fig. 9c), thus leading to the 20 Å periodicity along the **a**-axis. The structural framework (Pluth and Smith 1990) is characterized by wide channels parallel to the **a**-axis (Fig. 11c) confined by twelve-membered rings (aperture 7.0 Å). Each twelve-membered ring channel along the **a**-axis has offset ten-membered ring windows (Fig. 11d) into left and right channels parallel to the **b**-axis (aperture 5.8 × 5.2 Å). The (Si,Al) distribution is random. Extraframework cations and H_2O molecules form a highly disordered ionic solution that lacks systematic bonding to the framework.

Paulingite (PAU)

Paulingite (PAU) with the simplified structural formula $Na_{14}K_{36}Ca_{59}Ba_2[Al_{173}Si_{499}O_{1344}]\cdot 550H_2O$ is cubic, space group *Im*3*m*, $a = 35.09$ Å, $Z = 1$. The complicated and large framework (Gordon et al. 1966, Andersson and Fälth 1983, Bieniok et al. 1996, Lengauer et al. 1997) is characterized by channels confined by eight-membered rings of tetrahedra (aperture 3.8 Å) running parallel to the **a**-axis. No (Si,Al) order was detected. Seven different polyhedral cages occur in paulingite (Bieniok et al. 1996). Bieniok (1997) studied the dehydration and accompanying structural distortion.

ZEOLITES WITH SIX-MEMBERED RINGS

Smith and Bennet (1981) provided a review of the 98 most simple nets built by parallel six-membered rings linked by four-membered rings into the infinite set of ABC-6

nets. In addition to the zeolites gmelinite, chabazite, willhendersonite, levyne, erionite, offretite, and bellbergite, the zeolite-related minerals of the cancrinite group (afghanite, bystrite, cancrinite, cancrisilite, davyne, franzinite, giuseppettite, hydroxycancrinite, liottite, microsommite, pitiglianoite, quadridavyne, sacrofanite, tiptopite, tounkite, vishnevite, and wenkite) and the minerals of the sodalite group (bicchulite, hauyne, kamaishilite, lazurite, nosean, sodalite, and tugtupite) belong to this family. One of the characteristics of minerals in this structural family is stacking faults in the sequence of the six-membered double or single rings. In X-ray single-crystal photographs, these faults lead to some diffuse reflections parallel to the stacking direction. The importance of these stacking faults in this group is evident when one considers that gmelinite and offretite have infinite channels confined by twelve-membered rings; any stacking faults will thus block the channels. Following the classification of Gottardi and Galli (1985), faujasite and pahasapaite are also included in this group. Faujasite has six-membered double-rings not in one but in four planes, and pahasapaite has six-membered single rings.

Because cancrinites and sodalites are not reviewed in this chapter, at least the fundamentals of these frameworks will be briefly explained. Cancrinite can be constructed from six-membered rings stacked in an ab sequence (small letters are used to denote six-membered single rings), whereas sodalite has an abc stacking sequence of the ring units. The term "cancrinite-like" has been applied to feldspathoids that do not have the abc sequence of sodalite (e.g. liottite: ababac, and franzinite: cabcbacb). For further discussion, and references consult Smith and Bennet (1981).

Gmelinite (GME)

Gmelinite (GME), $(Na,K,Ca_{0.5},Sr_{0.5})_8[Al_8Si_{16}O_{48}]\cdot 22H_2O$, is hexagonal, space group $P6_3/mmc$, a = 13.621 to 13.805, c = 9.964 to 10.254 Å, Z = 1, depending on chemistry. The tetrahedral framework (Fig. 12c) consists of parallel stacks of six-membered double rings in the sequence ABAB (Fischer 1966, Galli et al. 1982, Malinovskii 1984, Vigdorchik and Malinovskii 1986, Vezzalini et al. 1990, Sacerdoti et al. 1995). The (Si,Al)-disordered structure exhibits channels parallel to the **c**-axis confined by twelve-membered rings (aperture 7.0 Å) which are connected perpendicular to the **c**-axis by eight-membered rings (aperture 3.9 × 3.6 Å). Two extraframework cation positions occur, with most cations located in the gmelinite cage (C1) between two six-membered double rings stacked parallel to the **c**-axis. These cations are coordinated by three framework oxygens and three H_2O molecules. Another cation site (C2) is in the large channel close to the eight-membered ring and is coordinated to three framework oxygens and four H_2O molecules. H_2O is strongly disordered with up to eight H_2O sites. Depending on the occupancy and type of cation in C2, the gmelinite framework undergoes a deformation involving lengthening parallel to the **c**-axis and shortening parallel to the **a**-axis (Vezzalini et al. 1990). Crystal structure refinements of exchanged varieties and accompanying structural distortions were discussed by Vigdorchik and Malinovskii (1986) and Sacerdoti et al. (1995). If the stacking of the six-membered double rings exhibits faults (e.g. ABCABC), a disordered intergrowth with chabazite results, leading to diffuse streaks in X-ray photographs along the **c**-axis (Fischer 1966).

Chabazite and willhendersonite (CHA)

Chabazite (CHA), $(Ca_{0.5},Na,K)_4[Al_4Si_8O_{24}]\cdot 12H_2O$, has a framework structure consisting of parallel stacks of six-membered double rings in the sequence ABC (Fig. 12b). Thus, a new type of cage (the chabazite cage) is typical of this structure (Fig. 1c). Large channels confined by twelve-membered rings characteristic of gmelinite are not formed in chabazite. The largest channels perpendicular to [001] (hexagonal setting) are confined by eight-membered rings (aperture 3.8 × 3.8 Å). The framework topology of

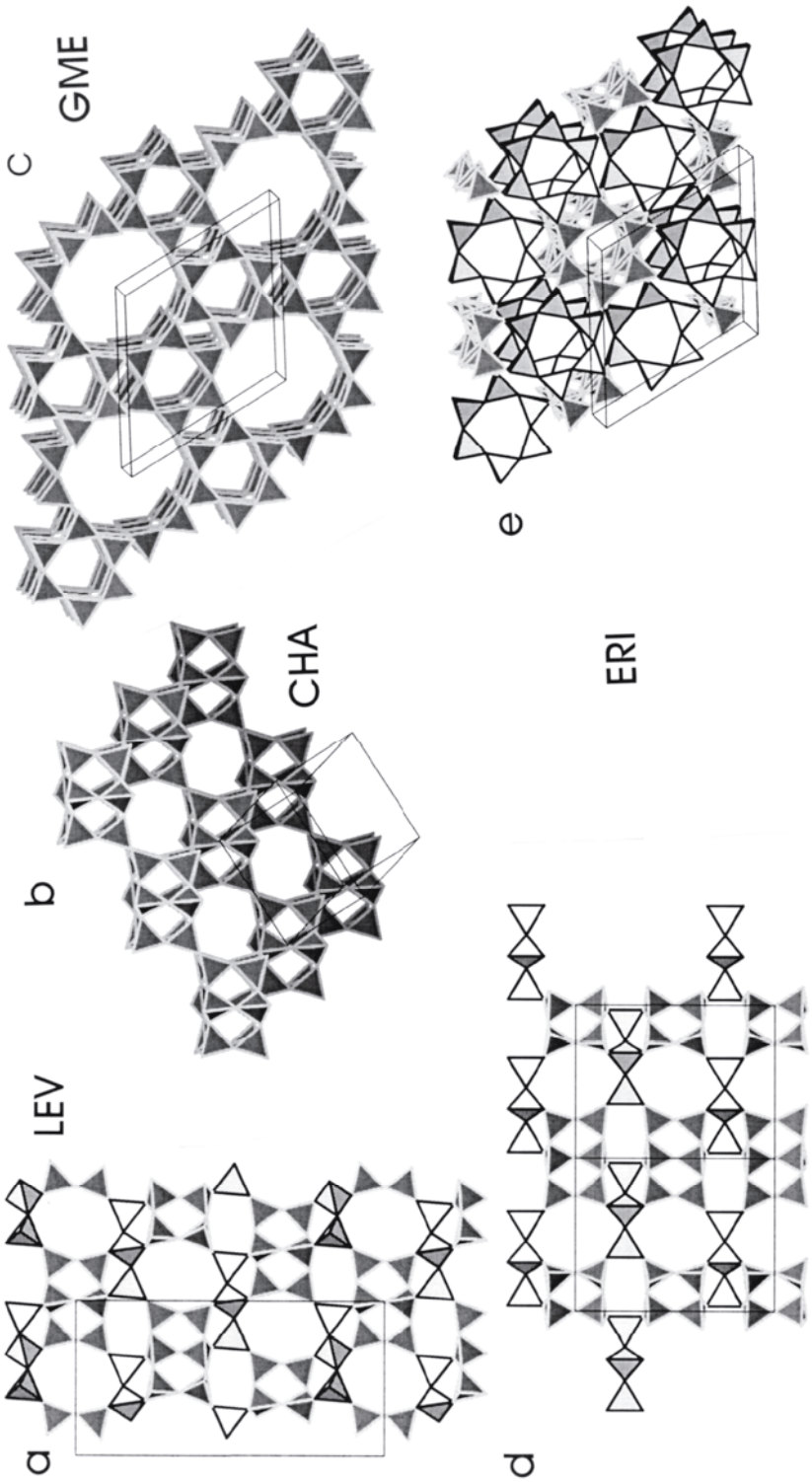

Figure 12. Polyhedral drawings of zeolite structures composed of single (dark rims) and double six-membered rings (light rims). Single rings are denoted with small letters, and double rings with capital letters. (a) The levyne (LEV) framework projected approximately along the **a**-axis. The structure consists of rings stacked in an AbCaBcA sequence parallel to the **c**-axis. (b) The chabazite (CHA) framework with rhombohedral unit-cell outlines. The structure consists of six-membered double rings stacked in an ABC sequence. (c) The gmelinite (GME) framework projected approximately along the **c**-axis. The structure consists of six-membered double rings stacked in an ABAB sequence parallel to the **c**-axis. (d) The erionite (ERI) framework projected parallel to [110]. The stacking sequence of rings is AbAc parallel to the **c**-axis. (e) The erionite framework projected approximately along the **c**-axis.

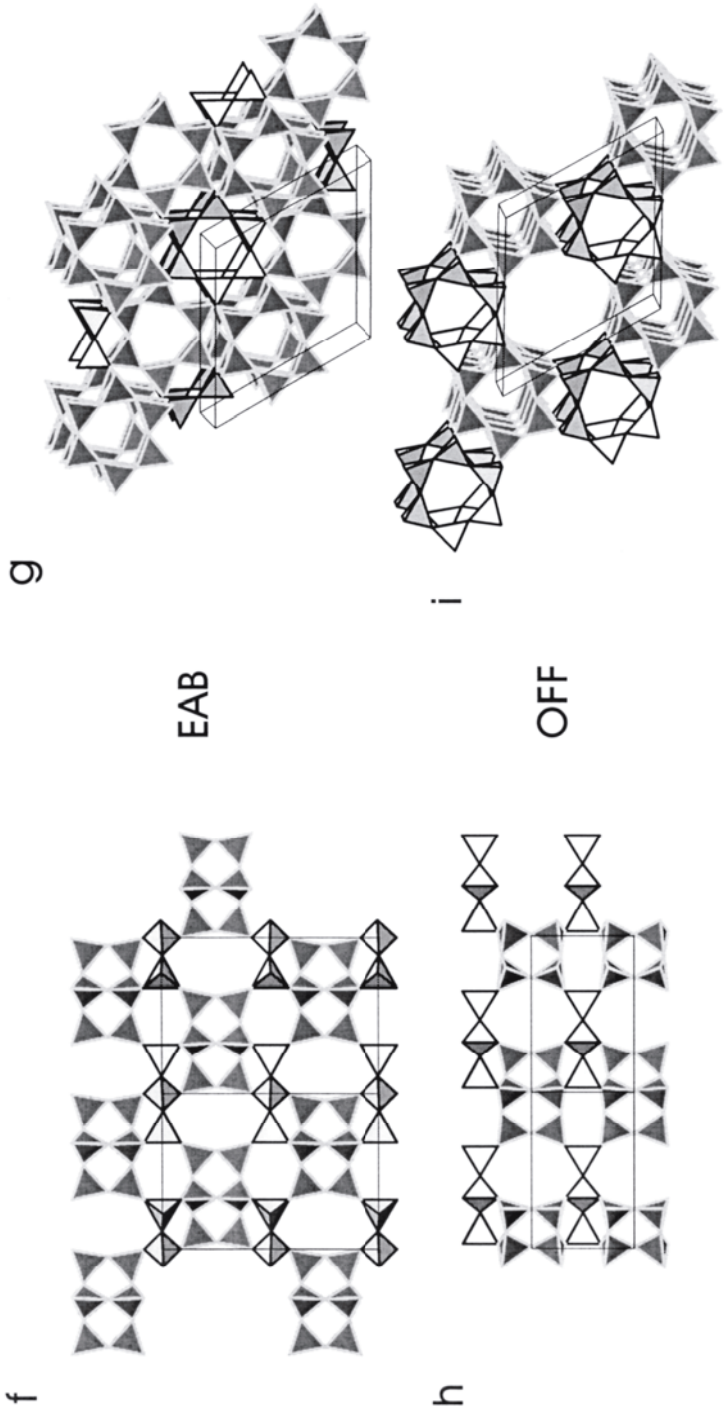

Figure 12, continued. Polyhedral drawings of zeolite structures composed of single (dark rims) and double six-membered rings (light rims). Single rings are denoted with small letters, and double rings with capital letters. (f) The bellbergite (EAB) framework projected parallel to [110]. The structure consists of six-membered rings stacked in an aBaC sequence parallel to the **c**-axis. (g) The bellbergite (EAB) framework projected approximately along the **c**-axis. (h) The offretite (OFF) framework projected parallel to [110]. The structure consists of six-membered rings stacked in an AbAb sequence parallel to the **c**-axis. (i) The offretite (OFF) framework projected approximately along the **c**-axis.

CHA is rhombohedral $R\bar{3}m$, which has also been attributed to chabazite (space group $R\bar{3}m$, a = 9.40 Å, α = 94.3°, Z = 1). Based primarily on optical observations, the symmetry of chabazite is known to be lower than rhombohedral, leading to complicated twinning (Akizuki 1981b). Mazzi and Galli (1983) separated optically homogeneous domains of four chabazite crystals from different localities and performed structure refinements in triclinic ($P1$) and rhombohedral space groups. In the six independent tetrahedra sites (in $P1$), some (Si,Al) ordering was observed. However, this ordering pattern was different in the four cases investigated. Mazzi and Galli (1983) suggested that chabazite may have randomly arranged domains with perfect (Si,Al) ordering. By use of ^{29}Si NMR spectroscopy, Engelhardt and Michel (1987) confirmed the variable (Si,Al) distribution in natural chabazites.

A series of cation-exchange experiments (Na, K, Ag, Cs, Ca, Sr, Ba, Cd, Mn, Co, and Cu), accompanied by structure refinements of the hydrated and dehydrated chabazites, were reviewed by Smith (1988). Four channel cation sites were distinguished (e.g. Alberti et al. 1982). C1 is located on the three-fold axis in the center of the double six-ring. C1 is not occupied in the Na- and K- forms but is partly occupied in natural, Ca-, and Sr-forms. C2 is the major cation site and is located on the three-fold axis, above or below the double six-membered rings, bonding to three framework oxygens of the ring and additional H_2O sites. C3 with usually low occupancy is located on the three-fold axis at the center of the chabazite cage. C4 is nearly in the center of the eight-membered rings, forming windows between the large cages. H_2O molecules mainly complete the C2 coordination and are additionally disordered over various sites with medium to low occupancies. Butikova et al. (1993) described structure refinements of a natural Ca-rich chabazite and its dehydrated form at 250°C. They observed strong structural distortions at high temperature and diffusion of cations to new sites, thus confirming results of Belokoneva et al. (1985).

Willhendersonite (CHA), $K_2Ca_2[Al_6Si_6O_{24}]\cdot 10H_2O$, also has the CHA tetrahedral framework topology (Peacor et al. 1984), but the structure has an Si/Al ratio of 1.0 and almost perfect (Si,Al) ordering, reducing the symmetry from $R\bar{3}m$ to $R\bar{3}$. A further symmetry reduction to triclinic $P\bar{1}$, a = 9.206, b = 9.216, c = 9.500 Å, α = 92.34, β = 92.70, γ = 90.12°, Z = 1, occurs (Tillmanns et al. 1984), which is caused by the ordered distribution of cations and H_2O molecules within the structural voids, and distortion of the framework due to cations which are too small to fill specific sites. In willhendersonite the six-membered rings are strongly compressed which leads to a different coordination of the C2 site (C2') discussed for chabazite. This C2' site occupied by Ca is seven-coordinated to four framework oxygens and three H_2O molecules. In spite of the Si/Al and K/Ca ratio of 1.0, Na and Ca are strongly disordered. The structure of Ca-endmember willhendersonite (space group $P1$) with slightly reduced (Si,Al) ordering was reported by (Vezzalini et al. 1997a).

Levyne (LEV)

Levyne (LEV), $(Ca_{0.5},Na,K)_6$ $[Al_6Si_{12}O_{36}]\cdot 18H_2O$, is rhombohedral, space group $R\bar{3}m$, a = 13.338, c = 23.014 Å, Z = 1. The structure (Merlino et al. 1975, Sacerdoti 1996) is built by alternating six-membered double-rings with six-membered single rings (Fig. 12a). The stacking sequence is AbCaBcA, where capital letters represent the double rings and small letters the single rings. The structure exhibits three equivalent channel systems perpendicular to the three-fold axis confined by eight-membered rings (aperture 3.6 × 4.8 Å). There is no indication of (Si,Al) ordering in the data of Merlino et al. (1975). However, Sacerdoti (1996) reported 35% Al on T1 and 25% Al on T2 based on three refinements. Five cation positions are known. The most important, C1, is above or

below the six-membered double rings where the cation is six-coordinated to three framework oxygens and three H_2O molecules. C2 is in the center of the cage coordinated only to H_2O molecules. C5 is in the center of the six-membered ring, and C3 and C4 are between C2 and C5.

Erionite (ERI)

Erionite (ERI), $K_2(Na,Ca_{0.5})_8[Al_{10}Si_{26}O_{72}]\cdot 28H_2O$, is hexagonal, space group $P6_3/mmc$, a = 13.26, c = 15.12 Å, Z = 1 (Kawahara and Curien 1969, Schlenker et al. 1977a, Alberti et al. 1997, Gualtieri et al. 1998). The structure is built by alternating six-membered single (small letters) and six-membered double rings (capital letters) stacked in the AbAc sequence (Fig 12d). The single rings are preferred by Al (Gualtieri et al. 1998). The crystals are characterized by offretite stacking faults leading locally to the AbAb sequence (Fig. 12h). Three equivalent channel systems run perpendicular to the **c**-axis and are bounded by eight-membered rings (aperture 3.6 × 5.1 Å; Fig. 12d). Three types of cages characterize this zeolite: a six-membered double ring (empty), a cancrinite cage (preferred by K), and an erionite cage (Fig. 1e) with dispersed Ca, Na, and Mg. Dehydration (Schlenker et al. 1977a) leads to internal ion-exchange, where Ca migrates into the cancrinite cage and K moves to the center of the eight-membered ring, blocking the windows. As in most zeolites constructed by six-membered rings, stacking faults reduce the crystal quality of erionite (Millward et al. 1986). Samples from Sasbach (Kaiserstuhl, Germany) represent continuous transitions from offretite to erionite (Rinaldi 1976).

Bellbergite (EAB)

Bellbergite (EAB), $(K,Ba,Sr)_2Sr_2Ca_2(Ca,Na)_4[Al_{18}Si_{18}O_{72}]\cdot 30H_2O$, is hexagonal, with possible space groups $P6_3/mmc$, $P\,6\,2c$, or $P6_3mc$, a = 13.244, c = 15.988 Å, Z = 1 (Rüdinger et al. 1993). The unit-cell parameters are quite similar to those of erionite. The structure has the EAB framework (Meier and Groner 1981) with the aBaC stacking sequence of six-membered single (small letters) and double rings (capital letters). Thus, the structure is related to erionite (AbAc) in such a way that single and double rings are interchanged (Fig. 12d,f). This leads to the same cages as found in erionite (i.e. six-membered double rings, cancrinite cage, and erionite cage). Three identical channel systems run perpendicular to the **c**-axis (Fig. 12f), bounded by eight-membered rings (aperture 3.6 × 5.1 Å). The structure was refined in space group $P6_3/mcc$, and no (Si,Al) ordering was found (Rüdinger et al. 1993). Alberti (1995) speculated that stacking faults or symmetry lower than $P6_3/mmc$ may explain the (Si,Al) disorder which is unusual for framework silicates with an Si/Al ratio of 1.

Offretite (OFF)

Offretite (OFF), $KCaMg[Al_5Si_{13}O_{36}]\cdot 15H_2O$, is hexagonal, space group $P\bar{6}\,m2$, a = 13.29, c = 7.58 Å, Z = 1 (Gard and Tait 1972, Mortier et al. 1976a,b; Alberti et al. 1996a, Gualtieri et al. 1998). The structure is built by alternating six-membered single (small letters) and six-membered double rings (capital letters) stacked in the AbAb sequence (Fig. 12h). The crystals are characterized by erionite stacking faults leading locally to the AbAc sequence. With regard to zeolitic properties, the major difference between offretite and erionite are channels confined by twelve-membered rings of tetrahedra (aperture 6.7 × 6.8 Å) running parallel to the **c**-axis in offretite (Fig. 12i) which are blocked by single six-membered rings in erionite (Fig. 12e). Three equivalent channel systems bounded by eight-membered rings (aperture 3.6 × 4.9 Å) run perpendicular to the **c**-axis and interconnect the main channels. Four types of cages characterize this zeolite: six-membered double rings (empty or very low occupancy), cancrinite cage (preferred by K),

a gmelinite cage (Fig. 1b) filled with Mg surrounded by disordered H_2O, and the wide channels whose centers are occupied by Ca-H_2O complexes. Si and Al are disordered over the two tetrahedral sites (Alberti et al. 1996a). Dehydration (Mortier et al. 1976a,b) leads to internal ion-diffusion.

Offretite is commonly intergrown with erionite either in macrodomains (Rinaldi 1976) or as cryptodomains detected by single-crystal study (Mortier et al. 1976a). Application of transmission electron-microscopy combined with structural data clearly showed that the Mg concentration is the major factor controlling whether erionite or offretite is formed (Gualtieri et al. 1998). A chabazite-offretite epitaxial overgrowth was found by Passaglia and Tagliavini (1994).

Faujasite (FAU)

Faujasite (FAU), $Na_{20}Ca_{12}Mg_8[Al_{60}Si_{132}O_{384}]\cdot 235H_2O$, is cubic, space group $Fd3m$, a = 24.60 Å, Z = 1 (Bergerhoff et al. 1958, Baur 1964). Faujasite is actually a rare zeolite, but it is well known, because it has the same framework topology (FAU) as Linde X and Linde Y, synthetic counterparts used as sorbants and catalysts. A review of structural work on synthetic counterparts (Linde X and Linde Y), on ion-exchanged faujasite, and on ion-exchanged and dehydrated faujasite was provided by Smith (1988). Properties of natural and synthetic faujasite were discussed by Stamires (1973). Faujasite corresponds to the most open framework of all natural zeolites. About half of the unit-cell

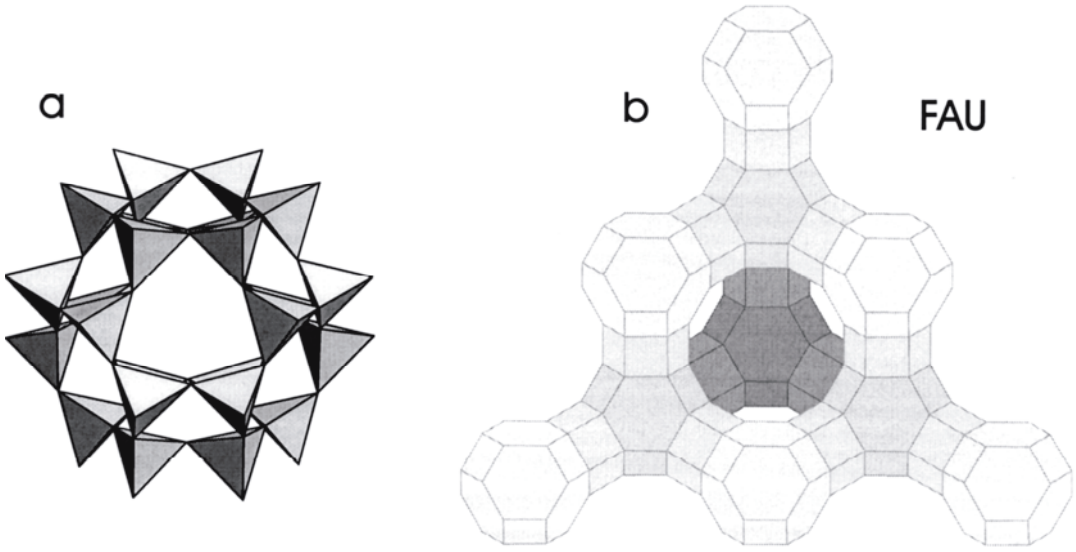

Figure 13. (a) The sodalite cage (β-cage) characteristic of faujasite (FAU) and Linde Type A (LTA). (b) Portion of the faujasite structure viewed parallel to [111] with β-cages represented by polyhedra. The cages are connected by six-membered double rings.

space is void in the dehydrated form. The structure consists of sodalite cages (Fig. 13a; truncated octahedra, β-cages) connected in a cubic manner over six-membered double rings. Thus, wide intersecting channels are formed parallel to <111> with an aperture of 7.4 Å (Fig. 13b). Approximately 50% of the cations reside in the sodalite cage bonded to three framework oxygens of the six-membered rings and additional H_2O molecules. The remaining cations and H_2O molecules are disordered in the large cavities. The same β-cages also exist in the important synthetic product Linde Type A (LTA). In the LTA framework, the β-cages are connected by four-membered double rings in a cubic fashion (Fig. 13c).

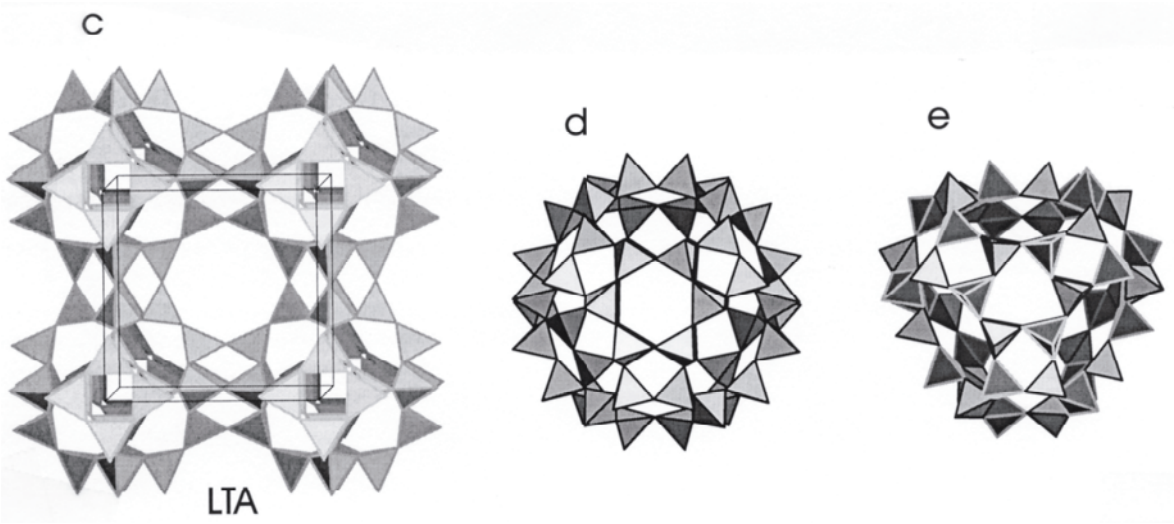

Figure 13. (c) The Linde Type A (LTA) framework viewed approximately along the **a**-axis with β-cages connected by four-membered double rings. (d) The α-cage (symmetry *m*3*m*) as found in hydrated zeolite rho (RHO). (e) The α-cage (symmetry 23) as found in pahasapaite. BeO_4 tetrahedra have light rims and PO_4 tetrahedra have dark rims.

Pahasapaite (RHO)

Pahasapaite (RHO), $(Ca_{5.5}Li_{3.6}K_{1.2}Na_{0.2})Li_8[Be_{24}P_{24}O_{96}]\cdot 38H_2O$, is cubic, space group $I23$, a = 13.781 Å, Z = 1 (Rouse et al. 1987). The structure (Rouse et al. 1989) contains ordered BeO_4 and PO_4 tetrahedra forming a three-dimensional array of distorted truncated cubo-octahedra or α-cages (Fig. 13d,e) connected via double eight-membered rings (aperture 2.2 × 2.2 Å). There are two identical, interpenetrating systems of cages related by the *I*-centering of the lattice. Similar α-cages also exist in paulingite. Pahasapaite has a distorted zeolite rho framework. The wide cages have a diameter of about 8 Å. Hydrated zeolite rho has the maximum symmetry $Im\bar{3}m$, which is reduced to $I\bar{4}3m$ in dehydrated zeolite rho and to $I23$ in pahasapaite due to (Be,P) ordering. Eight Li and 32 H_2O molecules reside within the cages. The remaining six H_2O molecules and 10.5 cations block the passages of double eight-rings between two cages. When pahasapaite is dehydrated (Corbin et al. 1991), the unit-cell volume decreases by 14% due to H_2O loss and increases for the dehydrated form by ~1% between 25°C and 400°C (Parise et al. 1994).

ZEOLITES OF THE MORDENITE GROUP

Structures assigned to this subgroup can be built from single five-membered rings with an attached tetrahedron (i.e. SBU: 5-1). These structures contain sheets built by six-membered rings (6^3 nets) which are often highly puckered (Fig. 14a,b,c). In the classical tetrahedral sheet of six-membered rings found in mica, all tetrahedral apices point in the same direction; thus, a framework cannot be constructed. However, frameworks can be built from sheets where half of the tetrahedral apices point upward and half point downward. These are the common structural principles of mordenite (MOR), dachiardite (DAC), epistilbite (EPI), ferrierite (FER), and bikitaite (BIK) (Meier 1978). This sheet concept has the advantage that cation and H_2O diffusion can be more easily explained for these structures because the sheets are not permeable in the temperature range of zeolite applications. Furthermore, the sheets help define the perfect cleavage and morphology of these zeolites. For a more thorough derivation of this group, refer to Meier (1978), Gottardi and Galli (1985), and van Koningsveld (1992).

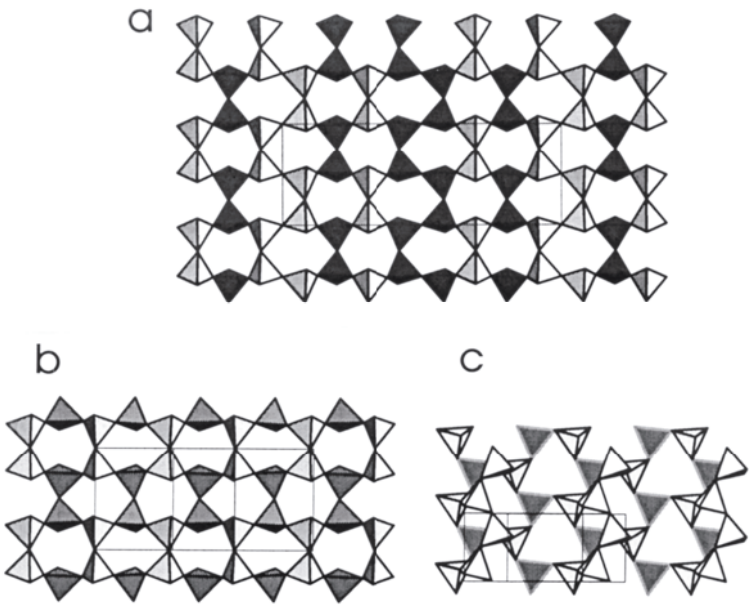

Figure 14. Sheets built by six-membered rings in the mordenite group. (a) (100) sheet in mordenite; half of the tetrahedral apices are pointing up and half are pointing down. (b) (100) sheet in dachi-ardite. Sheets with the same arrangement of tetrahedral apices also exist parallel to (010) in epistilbite and parallel to (100) in ferrierite. (c) The tridymite-type sheet parallel to (001) in bikitaite. The sheet is decorated with pyroxene-type tetrahedral chains extending parallel to the **b**-axis. Tetrahedra in the chains are filled with Si; those in the sheet of triclinic bikitaite are filled alternately with Si (light tetrahedra with black rims) and Al (dark tetrahedra with light rims).

Mordenite (MOR), $(Na_2,K_2,Ca)_4[Al_8Si_{40}O_{96}]\cdot 28H_2O$, is orthorhombic, space group $Cmc2_1$ (notice the topological symmetry, space group *Cmcm* which is used in several studies), a = 18.11, b = 20.46, c = 7.52 Å, Z = 1 (Meier 1961, Alberti et al. 1986, Shiokawa et al. 1989, Passaglia et al. 1995). The symmetry lowering from *Cmcm* to $Cmc2_1$ is necessary to properly model a T-O-T angle which is 180° in *Cmcm*. Apparent T-O-T angles of 180° are energetically unfavorable (e.g. Meier and Ha 1980, Gibbs 1982) and are often a result of either an incorrect space group assignment or oxygen disorder (Alberti 1986). The lowering to the acentric space group $Cmc2_1$ in mordenite is also reflected in the distribution of extraframework cations (Alberti et al. 1986). Gramlich-Meier (1981) modeled an (Si,Al) ordered mordenite framework in the monoclinic space group *Cc* and obtained two distinct conformeric solutions. There is considerable evidence that these structural variants exist side by side as domains and since twinning is also likely, a mordenite crystal could contain up to eight different domains (Meier et al. 1978).

The mordenite structure can be envisioned as puckered sheets formed by six-membered rings parallel to (100), which define the perfect (100) cleavage (Fig. 14a). The sheets are linked by four-membered rings in a way that twelve-membered rings (aperture 6.5 × 7.0 Å) and strongly compressed eight-membered rings remain at the seam, forming channels parallel to the **c**-axis (Fig. 15a). Another set of compressed eight-membered rings (aperture 2.6 × 5.7 Å) interconnects the wide channels parallel to the **b**-axis. Judging from T-O distances, the four-membered rings are slightly enriched in Al (e.g. Alberti 1997). Cations in mordenite mainly occupy three sites. Two of these sites are close to the four-membered Al-enriched rings and are located in the connecting channels parallel to the **b**-axis; the A site centers the strongly compressed eight-membered ring channels, whereas the D site is near the center of the eight-membered ring, giving access to the wide channel. The E site is in the large channels.

Gottardi and Galli (1985) and Smith (1988) reviewed ion-exchanged mordenites. In dehydrated K- and Ba-exchanged mordenites (Mortier et al. 1978, Schlenker et al. 1978), the symmetry lowers to *Pbcn*. Temperature-dependent (between 20 and 450°C) structural studies on Ca-exchanged natural mordenite were published by Elsen et al. (1987). Song (1999) studied crystal defects in mordenites which may result in channel blockage.

Maricopaite (-MOR), $Pb_7Ca_2[Al_{12}Si_{36}(O,OH)_{100}]\cdot n(H_2O, OH)$ (Peacor et al. 1988), is orthorhombic, space group *Cm*2*m*, *a* = 19.434, *b* =19.702, *c* = 7.538 Å, Z = 1. The structure exhibits a rather random (Si,Al) distribution and is closely related to mordenite but has an interrupted framework (emphasized by the structure code –MOR) in which 17% of the TO_4 groups are three-fold connected (Rouse and Peacor 1994). This difference has several consequences; in maricopaite there are no four- and eight-membered rings parallel to (001). A strongly compressed channel apparently bounded by eight-membered rings still appears in projections parallel to the **c**-axis. Inspection of Figure 15b discloses that the apparent rings are composed of staggered half rings, one half at z = 0 and the other half at z = 1/2. Thus, the voids are considerably larger than in mordenite. Notice that the elongation of the compressed channels is parallel to the **a**-axis in mordenite but is parallel to the **b**-axis in maricopaite. The compressed channels confined by the staggered half rings (Fig. 15b) are obstructed by two types of $Pb_4(O,OH)_4$ clusters which appear to act as a template for this unusual type of void. Two Pb atoms bond to the same framework oxygen; thus, the bond valence sum for this oxygen is satisfied without connection to an additional TO_4 tetrahedron, causing an interrupted framework. However, Pb sites are only partially occupied. Thus, if Pb is locally absent, a proton (H) balances the framework oxygen valence sum.

Dachiardite (DAC), $(Na,K,Ca_{0.5})_4[Al_4Si_{20}O_{48}]\cdot 18H_2O$, is monoclinic, space group *Cm*, *a* = 18.676, *b* = 7.518, *c* = 10.246 Å, β =107.87°, Z = 1. However, all available structure refinements (Gottardi and Meier 1963, Vezzalini 1984, Quartieri et al. 1990) have been performed in the higher space group *C*2/*m*. Vezzalini (1984) and Quartieri et al. (1990) detected two types of domains (called A and B) in an equal ratio, resulting in the average symmetry *C*2/*m*. These domains form to avoid energetically unfavorable 180° T-O-T angles (e.g. Meier and Ha 1980, Gibbs 1982), similar to the symmetry

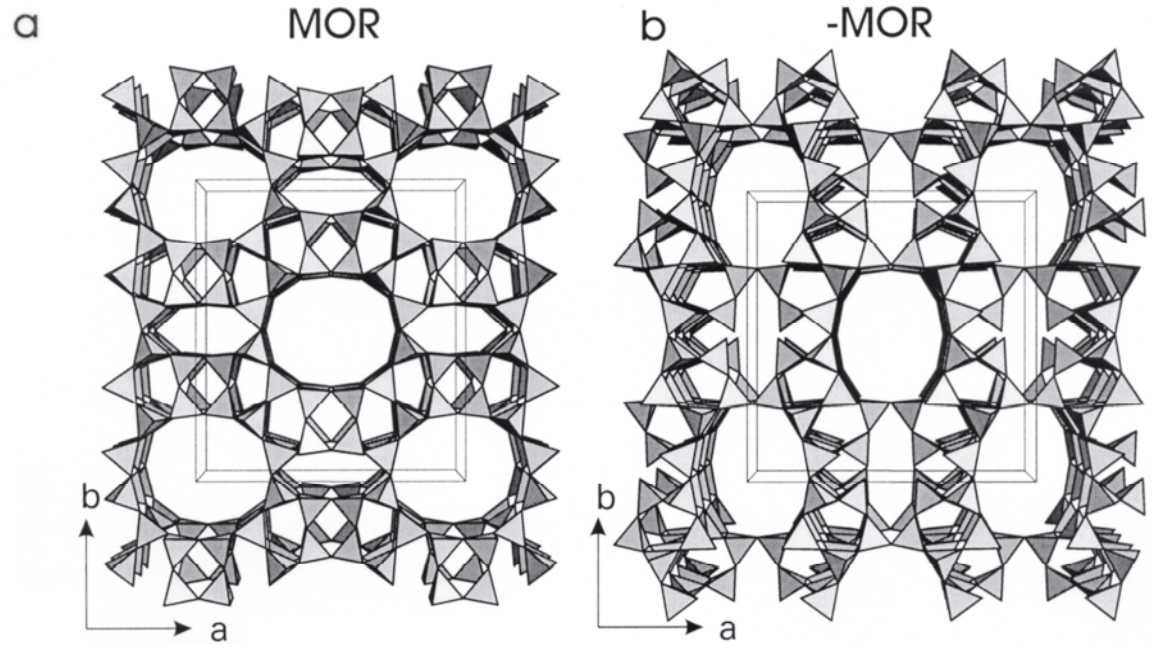

Figure 15. (a) The mordenite (MOR) framework projected along the **c**-axis. The sheets of six-membered rings parallel to (100) are linked parallel to the **a**-axis by four-membered rings. (b) The maricopaite (-MOR) framework projected along the **c**-axis. The unit-cell origin is shifted by 1/2 along the **a**-axis to facilitate better comparison with mordenite. In contrast to mordenite there are no four-membered rings due to the interrupted framework in maricopaite.

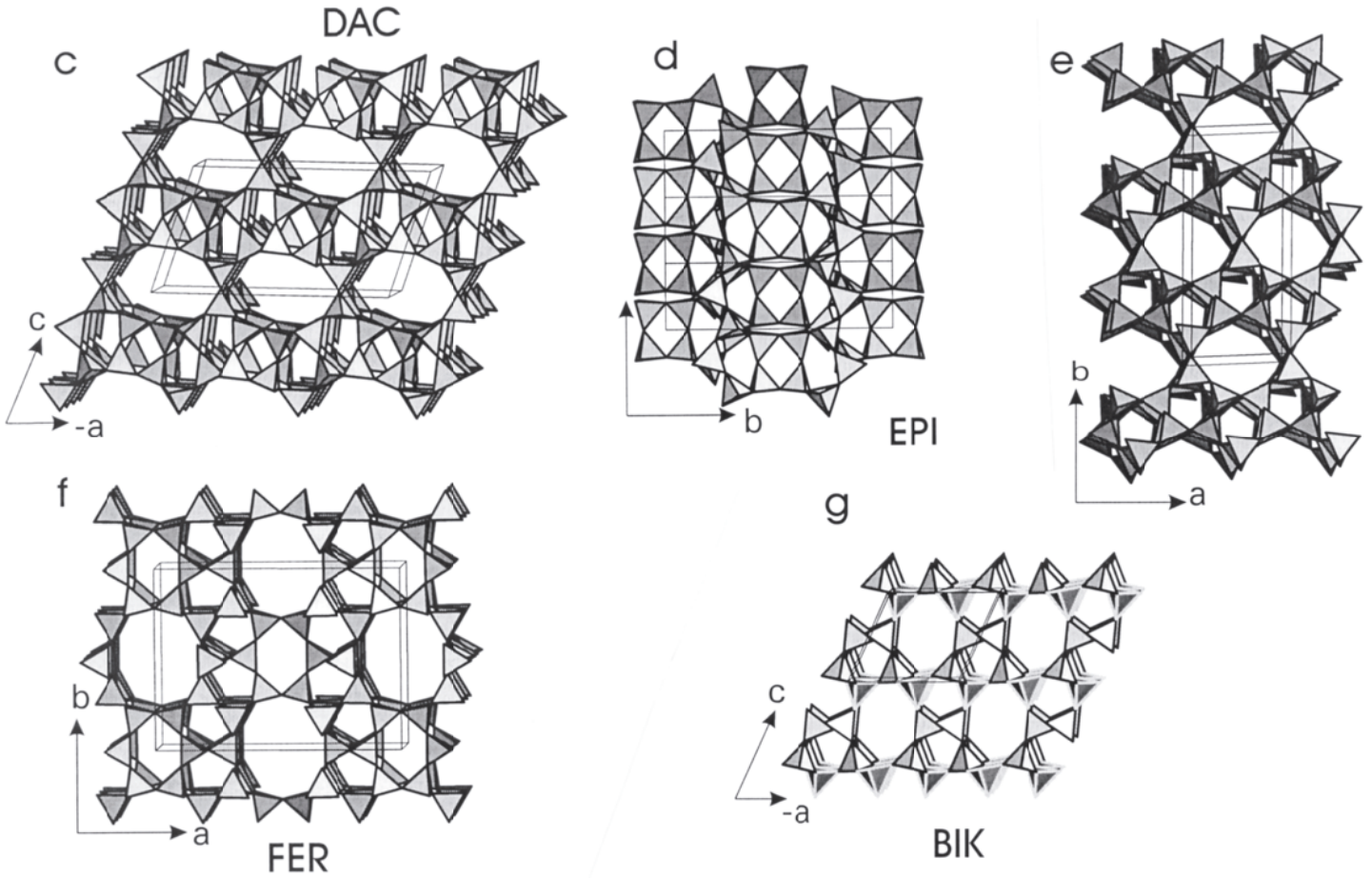

Figure 15, continued. (c) The dachiardite (DAC) framework projected approximately along the **b**-axis. The sheets of six-membered rings parallel to (100) are linked parallel to the **a**-axis by four-membered rings. (d) The epistilbite (EPI) framework projected on (100). The sheets of six-membered rings parallel to (010) are linked parallel to the **b**-axis by four-membered rings obstructing the ten-membered ring channels. (e) The epistilbite (EPI) framework projected approximately along the **c**-axis. (f) The ferrierite (FER) framework projected approximately along the **c**-axis. The sheets of six-membered rings parallel to (100) are linked parallel to the **a**-axis by six-membered rings. (g) The bikitaite (BIK) framework (triclinic variety) projected parallel to the **b**-axis. The sheets of six-membered rings parallel (001) are linked by tetrahedral chains. Light tetrahedra with dark rims are filled with Si; dark tetrahedra with light rims are filled with Al.

lowering in mordenite (described above) and epistilbite (discussed below). Out of the few occurrences of dachiardite (e.g. Tschernich 1992), only the samples from Elba (Gottardi and Meier 1963, Vezzalini 1984) and from Hokiya-dake, Japan (Quartieri et al. 1990) give sharp single-crystal X-ray reflections. All other investigated samples yield diffuse peaks and streaking (Alberti 1975a, Gellens et al. 1982) caused by severe disorder and twinning. Actually, the mineral "svetlozarite" proposed by Maleev (1976) was shown by Gellens et al. (1982) to be a twinned dachiardite with stacking faults and twin domains only a few unit-cells in size. Quartieri et al. (1990) identified two types of dachiardite frameworks (normal dachiardite and modified dachiardite) within the same crystal. They assumed that alternating small domains of different size or possibly a high density of stacking faults caused domain formation.

The dachiardite framework can be constructed from cross-linking slightly puckered sheets parallel to (100) formed by six-membered rings (Figs. 14b and 15c). Two of these sheets are linked parallel to the **a**-axis by four-membered rings. Thus, roughly elliptical channels confined by ten-membered rings (aperture 5.3 × 3.4 Å) are formed parallel to the **b**-axis. These channels are additionally connected by channels through eight-membered rings (aperture 3.7 × 4.8 Å) running parallel to the **c**-axis. The structural difference between mordenite and dachiardite can best be envisioned by the arrangement of tetrahedra pointing up and down within the six-membered ring sheets (compare Fig. 14a and b with Fig. 15a and c). In the Elba dachiardite, two extraframework cation positions are distinguished; C1 is at the intersection of the *b* (ten-membered ring) and *c* (eight-membered ring) channels and is coordinated by three framework oxygens and five H_2O molecules. C2 is in the channel parallel to the **c**-axis, with a distance >3.3 Å to the framework oxygen atoms.

Epistilbite (EPI), $Ca_3[Al_6Si_{18}O_{48}]\cdot 16H_2O$, is monoclinic, space group *C*2, or triclinic, space group *C*1, $a = 9.08$, $b = 17.74$, $c = 10.15$ Å, $\alpha = 90$, $\beta = 124.58$, $\gamma = 90°$, $Z = 1$. Older refinements (Kerr 1964, Merlino 1965, Perrotta 1967) were done in space group *C*2/*m*, which led to a correct description of the tetrahedral connectivity. Slaughter and Kane (1969) and Alberti et al. (1985) analyzed low-symmetry (*C*2) domains in the structure. Alberti et al. (1985) recognized that these domains (named A and B) form to avoid energetically unfavorable T-O-T angles of 180°. In contrast to dachiardite (Vezzalini 1984), these domains do not occur in a 1:1 ratio. Yang and Armbruster (1996b) showed that these domains can be explained by a twin-like (010) mirror plane. Furthermore, they found that epistilbite from Gibelsbach, Fiesch (Valais, Switzerland) is triclinic (*C*1) as a result of (Si,Al) ordering and extraframework cation distribution. Previously Akizuki and Nishido (1988) suggested triclinic symmetry based on optical studies.

The structure of epistilbite possesses the same up and down orientation of tetrahedra within the sheets of six-membered rings as in dachiardite (Fig. 14b). The sheets parallel to (010), which define the perfect (010) cleavage, are also connected by four-membered rings (Fig. 15d). However, in the **c** direction the four-membered rings alternate at different x levels (shifted by 1/2) and block the ten-membered rings. Open channels are confined by eight-membered rings (aperture 3.7 × 5.2 Å) extending parallel to [001] (Fig. 15e). In triclinic epistilbite, four Ca positions are located in a cage confined by the ten-membered rings of tetrahedra. Two of these sites are related to the other two sites by a pseudo two-fold axis; thus, only two sites can be occupied simultaneously because of short Ca-Ca distances. Ca has a square antiprismatic coordination with five H_2O molecules and three framework oxygens. A strong correlation exists between the Al distribution in the neighboring tetrahedra and the occupancy of the four possible Ca sites.

Ferrierite (FER), $(Na,K)Mg_2Ca_{0.5}[Al_6Si_{30}O_{72}]\cdot 20H_2O$, may be orthorhombic, space group *Immm*, a = 19.18, b =14.14, c = 7.5 Å, Z = 1, which agrees with the maximum symmetry of the framework topology (Vaughan 1966, Gramlich-Meier et al. 1984). Gramlich-Meier et al. (1985) refined the structure of a monoclinic variety of ferrierite (Mg-poor) in space group $P2_1/n$ (standard setting $P2_1/c$), a =18.89, b = 14.18, c = 7.47 Å, β = 90°. In contrast to the orthorhombic structure, monoclinic ferrierite has no T-O-T angles of 180°. In light of the discussion on the mordenite, dachiardite, and epistilbite structures, it may be speculated that lower symmetry is a general feature of all ferrierites (Alberti 1986, Alberti and Sabelli 1987). Alberti and Sabelli (1987) refined the structure of Mg-rich ferrierite from Monastir (Sardinia) in space group *Immm* but provided strong evidence, based on disorder of the $Mg(H_2O)_6$ extraframework complex, that the true space group is *Pnnm*, which leads to a relaxation of the 180° T-O-T angle. Thus, the straight T-O-T angle must only be apparent because of fractional statistical occupation. The monoclinic symmetry (Gramlich-Meier et al. 1985) seems to be specific for the Mg-poor variety. Both monoclinic and orthorhombic ferrierite have an essentially random (Si,Al) distribution. Electron diffraction patterns of orthorhombic ferrierite display pronounced streaking parallel to $[010]^*$ and $[110]^*$ caused by contraction and expansion faults (Gramlich-Meier et al. 1984, Smith 1986).

The structure of ferrierite (Fig. 15f) can be envisioned as corrugated six-membered ring sheets (parallel to (100)) with the same arrangement of up and down tetrahedra as in dachiardite and epistilbite (Fig. 14b). However, the sheets in ferrierite, which also define the perfect cleavage, are connected parallel to the **a**-axis by six-membered rings and not by four-membered rings as in the previous two structures. This arrangement leads to channels parallel to the **c**-axis formed by ten-membered rings (aperture 5.4 × 4.2 Å) interconnected by channels, parallel to the **b**-axis, confined by eight-membered rings (aperture 4.8 × 3.5 Å). Mg forms a disordered $Mg(H_2O)_6^{2+}$ complex wedged in between six-membered rings in the channels parallel to the **b**-axis. Alkali ions are disordered in the wide channels parallel to the **c**-axis.

Bikitaite (BIK), $Li_2[Al_2Si_4O_{12}]\cdot 2H_2O$, is either triclinic, space group $P1$, a = 8.607, b = 4.954, c = 7.597 Å, α = 89.90, β = 114.43, γ = 89.99°, Z = 1 (Bissert and Liebau 1986, Ståhl et al. 1989, Quartieri et al. 1999), or monoclinic, space group $P2_1$, a = 8.61, b = 4.96, c = 7.60 Å, β = 114.5°, Z = 1 (Kocman et al. 1974, Bissert and Liebau 1986). The framework of bikitaite can be constructed from puckered six-membered ring sheets of the tridymite type, where up and down tetrahedra alternate (Fig. 14c). These sheets parallel to (001) have pyroxene tetrahedral chains above and below extending parallel to the **b**-axis which connect two neighboring sheets (Fig 15g). The orientation of the sheets agrees with the observed morphology and perfect cleavage. The structure is characterized by channels parallel to the **b**-axis delimited by deformed eight-membered rings (aperture 2.8 × 3.7 Å). Half of the tetrahedra in the six-membered ring sheets are occupied by Al (well ordered in triclinic and disordered in monoclinic bikitaite), whereas tetrahedra in the pyroxene chains are only occupied by Si. Its is not understood as yet whether short range (Si,Al) ordering is preserved within the sheets of monoclinic bikitaite (Bissert and Liebau 1986). Li is close to the walls of the *b*-extended channels and bonds to three framework oxygens of Al tetrahedra and to one H_2O molecule. The arrangement of H_2O molecules forming hydrogen-bonded H_2O chains parallel to the **b**-axis was investigated by Ståhl et al. (1989) and Quartieri et al. (1999).

$T_{10}O_{20}$ ZEOLITES: THE TABULAR ZEOLITES

The building blocks for this group of zeolites are chains of $T_{10}O_{20}$ $(Al,Si)O_4$ tetrahedra running parallel to the **a**-axis (Breck 1974). These chains are in turn cross-

linked in the (010) plane to form three different framework topologies (Figs. 16-18). This cross-linking results in several types of channels that are all interconnected and are in the (010) plane. For all the $T_{10}O_{20}$ zeolites, the periodicity perpendicular to the (010) plane (i.e. the length of *b*) is similar and approximately 18 Å. The $T_{10}O_{20}$ units are more difficult to visualize than the T_5O_{10} units for the fibrous zeolites, and in a similar manner, these $T_{10}O_{20}$ chains control the morphology of these zeolites. The tabular nature results from a very rigid structure parallel to the **a**-axis, based on the $T_{10}O_{20}$ chains, and their cross-linking parallel to the **c**-axis is much stronger than their cross-linking parallel to the **b**-axis. Thus, all the zeolites in this subgroup exhibit a tabular morphology and in general exhibit perfect (010) cleavage because of the weakness imparted to the structure in the **b** direction. For an in-depth discussion of the SBU's for this group, see Alberti (1979).

Heulandite and clinoptilolite (HEU)

Both heulandite, $(Na,K)Ca_4[Al_9Si_{27}O_{72}]\cdot 24H_2O$, and clinoptilolite, $(Na,K)_6[Al_6Si_{30}O_{72}]\cdot 20H_2O$, possess the same tetrahedral framework (labeled HEU) and form a solid-solution series sometimes referred to as the heulandite group zeolites. Heulandite is defined as a series having Si/Al < 4.0, and clinoptilolite as a series having Si/Al ≥ 4.0 (Coombs et al. 1998). A detailed discussion on differences and similarities between heulandite and clinoptilolite is provided by Bish (this volume).

The crystal structures of heulandite and clinoptilolite are mostly described to be monoclinic, space group *C*2/*m*, *a* = 17.7, *b* = 17.8, *c* = 7.4 Å, β = 116.4°, *Z* = 1 (e.g. Alberti 1975b, Koyama and Takéuchi 1977, Bresciani-Pahor et al. 1980, Alberti and Vezzalini 1983, Hambley and Taylor 1984, Smyth et al. 1990, Armbruster and Gunter 1991, Armbruster 1993, Gunter et al. 1994, Cappelletti et al. 1999). However, lower symmetries such as *Cm*, and $C\bar{1}$ have also been reported (Alberti 1972, Merkle and Slaughter 1968, Gunter et al. 1994, Yang and Armbruster 1996a, Sani et al. 1999, Stolz et al. 2000a,b). The HEU framework (Figs. 16a,b) contains three sets of intersecting channels all located in the (010) plane. Two of the channels are parallel to the **c**-axis - the A channels are formed by strongly compressed ten-membered rings (aperture 3.0 × 7.6 Å), and the B channels are confined by eight-membered rings (aperture 3.3 × 4.6 Å). The C channels are parallel to the **a**-axis, or [102] and are also formed by eight-membered rings (aperture 2.6 × 4.7 Å).

Alberti (1972) concluded that the true probable lower symmetry of heulandite cannot reliably be extracted from X-ray single-crystal data because of strong correlations of *C*2/*m* pseudo-symmetry related sites during the least-squares procedure. Thus, *C*1, $C\bar{1}$, *Cm*, *C*2, and *C*2/*m* are possible space groups for heulandite and clinoptilolite. Akizuki et al. (1999) determined by optical methods and X-ray diffraction that a macroscopic heulandite crystal is composed of growth sectors displaying triclinic and monoclinic symmetry where the triclinic sectors are explained by (Si,Al) ordering on the crystal faces. Yang and Armbruster (1996a) and Stolz et al. (2000a,b) stated that, due to correlation problems, symmetry lowering in heulandite can only be resolved from X-ray data when investigated in cation-exchanged samples where the distribution of extraframework cations also reflects the lower symmetry.

Differing degrees of (Si,Al) ordering over the five distinct tetrahedral sites (assuming *C*2/*m* space group) have been reported for both heulandite and clinoptilolite. In all refinements, the tetrahedron with the highest Al content, T2, joins the "sheets" of $T_{10}O_{20}$ groups by sharing their apical oxygens (Figs. 16a-c). A neutron diffraction study by Hambley and Taylor (1984) located the majority of the H atoms and found (Si,Al) ordering values similar to other *C*2/*m* refinements. Additional (Si,Al) ordering, due to lower symmetry ($C\bar{1}$ or *Cm*), was resolved by Yang and Armbruster (1996a), Sani et al.

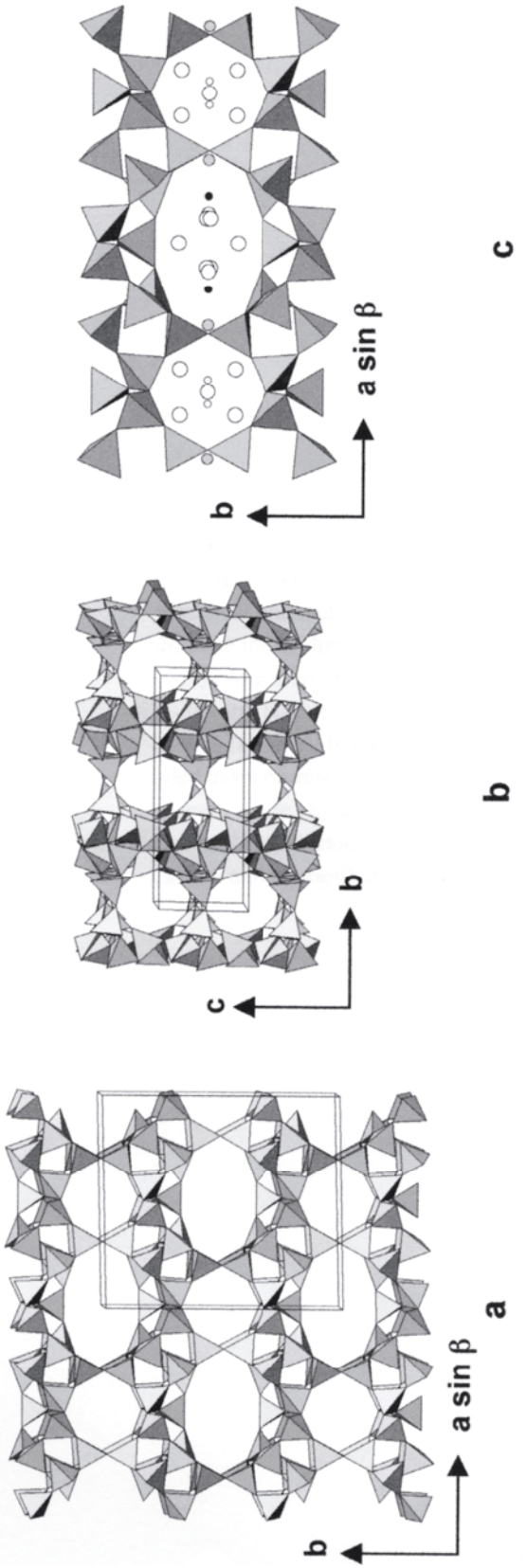

Figure 16. The heulandite structure. (a) A (001) projection looking down the **c**-axis with the **b**-axis vertical, showing the elliptical ten-membered A rings forming one set of [001] channels and the near circular eight-membered rings forming the smaller B channels along [001]. (b) A (100) projection looking down the **a**-axis with the **c**-axis vertical, showing the C channels which are parallel to [100] and are formed by elliptical eight-membered rings. (c) A (001) projection of heulandite looking down the **c**-axis with the **b**-axis vertical, showing three different cation sites and H_2O molecules from a sample refinement. The A channel (elliptical rings) has two different metal sites. The small black dot represents a channel cation site usually occupied by Na, and the larger gray-shaded atom represents a lower-populated site which normally contains K. In the smaller circular B channel, the small white circles represent a site usually occupied by Ca. The larger white circles represent H_2O molecules. In the A channel, these H_2O sites are usually partially occupied and their locations are variable for heulandite and clinoptilolite. (Data for these projections taken from Gunter et al. 1994.)

(1999), and Stolz et al. (2000a,b).

Two main channel cation sites have been reported by all researchers and at least two more sites of lower occupancy have been reported by others (e.g. Sugiyama and Takéuchi 1986, Armbruster and Gunter 1991, Armbruster 1993). These sites usually contain Na, Ca, K, and Mg, with Na and K predominantly close to the intersection of the A and C channels and Ca located in the B channel (Fig. 16b). The Na site in the A channel often also contains Ca, whereas the Ca site in the B channel is usually Na free. K and Na occur at nearby sites but K is more centered in the C channel (Fig. 16b). Both can be distinguished by their different distances from the framework (Fig. 16c). Na, K, and Ca ions are on the (010) mirror plane, present in *C*2/*m* or *Cm* symmetry, and they coordinate to framework oxygens and channel H_2O molecules. In one refinement, Na was nine-coordinated to four framework oxygens and five strongly disordered and partially occupied channel H_2O molecules, whereas both Ca and K were eight-coordinated to four framework oxygens and four channel H_2O molecules (Gunter et al. 1994). Mg commonly resides in the center of the A channel, coordinated only to six disordered H_2O molecules (Koyama and Takéuchi 1977, Sugiyama and Takéuchi 1986, Armbruster 1993).

Heulandite and clinoptilolite contain differing amounts of H_2O as a function of their extraframework-cation chemistry (Bish 1988, Yang and Armbruster 1996a) and hydration state. The H_2O molecules occurring in the B channel (coordinated to Ca; Fig. 16c) are usually fully occupied, whereas those occurring in the A channel are usually only partially occupied (Koyama and Takéuchi 1977, Armbruster and Gunter 1991). The structural mechanism of dehydration and accompanying framework distortions were studied by Alberti (1973), Alberti and Vezzalini (1983), Armbruster and Gunter (1991) and Armbruster (1993).

Stilbite, stellerite, barrerite (STI)

The three zeolites belonging to this group all possess the same framework, labeled STI in reference to stilbite, which was the first described and most common zeolite in this group. The maximum symmetry possible for this framework is *Fmmm*, which is the space group for stellerite. Barrerite is also orthorhombic but with lower space group symmetry *Amma*, and stilbite is monoclinic, space group *C*2/*m*. In fact, the difference between minerals in this group is based on symmetry, which is controlled by the channel cations. For instance, the mineral is considered stilbite if it is monoclinic, it is considered stellerite if it is Ca-dominant and orthorhombic, and it is considered barrerite if it is Na-dominant and orthorhombic. Interestingly, Ca-exchanged barrerite increases symmetry to *Fmmm* (Sacerdoti and Gomedi 1984), whereas Na-exchanged stellerite maintains *Fmmm* symmetry (Passaglia and Sacerdoti 1982).

Two sets of connected channels occur in the STI framework. One channel extends parallel to the **a**-axis (Fig. 17) and is confined by a ten-membered ring (aperture 4.9 × 6.1 Å). The other channel (aperture 2.7 × 5.6 Å) is located along [101] for monoclinic STI frameworks or [001] for orthorhombic structures and is confined by an eight-membered ring (Fig. 17). As stated above, both of these channels are in the (010) plane, creating a structural weakness across this plane leading to perfect (010) cleavage and a tabular habit.

Stilbite (STI) has the simplified formula $NaCa_4[Al_9Si_{27}O_{72}]\cdot 30H_2O$ and is usually monoclinic, space group *C*2/*m*, a = 13.64, b = 18.24, c = 11.27 Å, β = 128.0°, Z = 1 (Galli and Gottardi 1966, Slaughter 1970, Galli 1971). To better compare monoclinic stilbite with orthorhombic stellerite and barrerite, Quartieri and Vezzalini (1987) chose a different space group setting for stilbite, *F*2/*m*, to obtain a pseudo-orthorhombic unit cell

with a = 13.617, b = 18.249, c = 17.779 Å, β = 90.7°. Optical studies of stilbite have shown that within one macroscopic single-crystal, monoclinic (*F*2/*m*) and orthorhombic (*Fmmm*) domains coexist depending on the growth direction (Akizuki and Konno 1985). Akizuki et al. (1993) also studied the symmetry of different growth sectors in stilbite by single-crystal diffraction and refined the structure of an orthorhombic {001} growth sector yielding space group *Fmmm*, a = 13.616, b = 18.238, c = 17.835 Å within a chemically homogeneous crystal. This structure represents a disordered variant of the monoclinic *F*2/*m* structure of stilbite where the higher symmetry occurs on a submicroscopic scale rather than microscopically as in {101} growth sectors. Galli

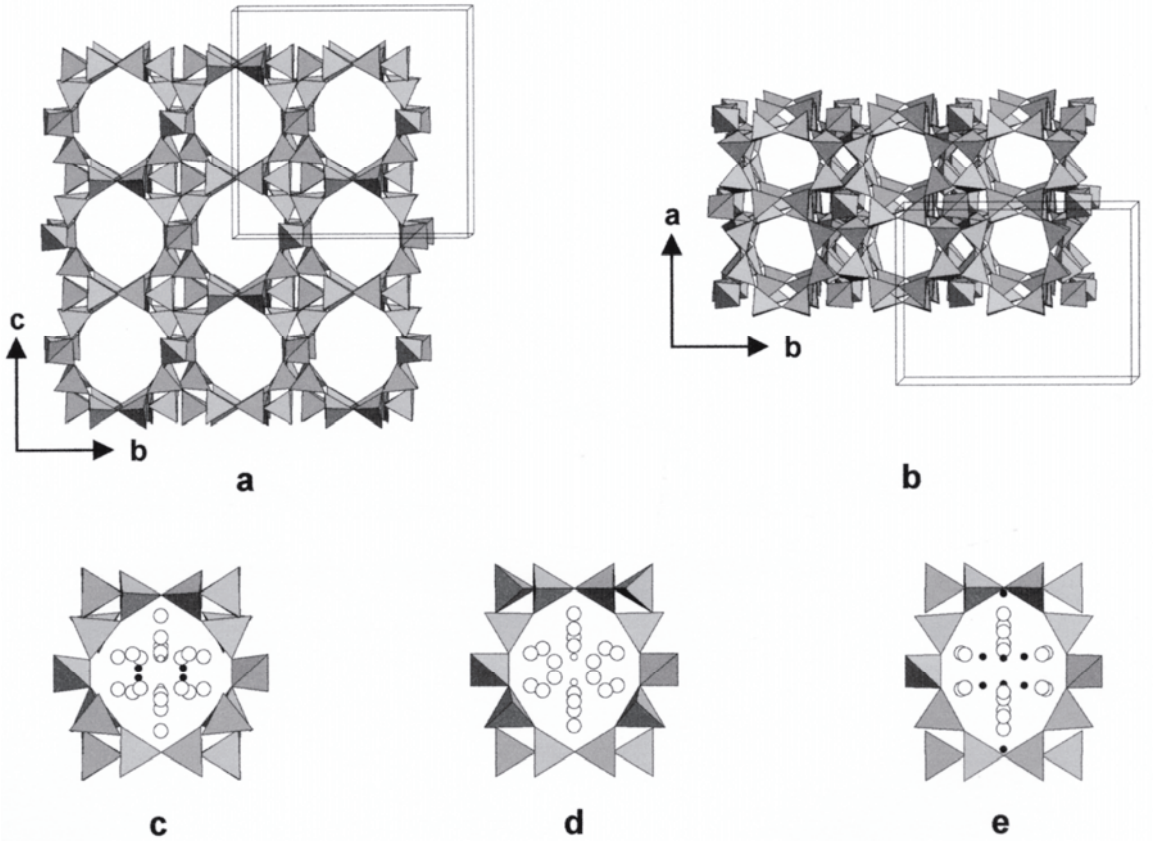

Figure 17. Stilbite-group zeolites framework and channel contents. Projections c-e are on (100) looking down the **a**-axis with the **c**-axis vertical. The small black circles represent Na atoms, the small white circles are Ca atoms, and the larger white circles are H_2O molecules. (a) A (100) projection looking down the **a**-axis with the **c**-axis vertical, showing the elliptical ten-membered rings forming [100] channels. (b) A (001) projection looking down the **c**-axis with the **a**-axis vertical, showing the eight-membered rings forming the smaller set of [001] channels. These drawings are based upon a pseudo-orthorhombic unit cell choice, space group *F2/m* used by Quartieri and Vezzalini (1987) instead of the more standard choice of *C2/m* for stilbite. Using the pseudo-orthorhombic unit cell allows easier comparison among the three zeolites with this framework. Thus, the projected unit cell better fits orthorhombic stellerite and barrerite, than does stilbite. If *C2/m* were chosen, then the [001] channels in the right drawing would be relabeled to [101] channels. (c) Stilbite (Quartieri and Vezzalini 1987) contains both Ca and Na; the Ca sites are nearer the center of the [100] channel and are located on a (010) mirror plane, and the Na sites are located on both sides of the mirror plane near the channel center. (d) Stellerite (Miller and Taylor 1985) contains only Ca; the Ca sites are the same as in stilbite, but H_2O has occupied the Na sites in stilbite. (e) Barrerite (Galli and Alberti 1975b) contains only Na. Na has occupied the Ca sites in stilbite and stellerite. Na sites of stilbite have moved a little, and a new Na site occurs near the channel edge on the (010) mirror plane.

(1971) and Akizuki et al. (1993) implied complete (Si,Al) disorder based upon average T-O distances. Slaughter (1970) and Quartieri and Vezzalini (1987) assumed pronounced (Si,Al) ordering, with Al contents varying between 11 and 40% in the different tetrahedral sites.

All refinements done in monoclinic symmetry yielded one fully occupied Ca site located near the middle of the ten-membered ring parallel to the **a**-axis (Fig. 17c). Ca is bonded only to channel H_2O molecules and not to framework oxygens. Galli (1971) and Quartieri and Vezzalini (1987) found one partially occupied Na site that is seven-coordinated to two framework oxygens and five channel H_2O molecules. Slaughter (1970) interpreted the Ca site to contain a small amount of Na and found three partially occupied Na sites and another undifferentiated partially occupied metal site. The dehydration dynamics of stilbite was studied by Cruciani et al. (1997) using synchrotron X-ray powder diffraction.

Stellerite (STI) is the Ca-dominant end member of this group with the simplified formula $Ca_4[Al_8Si_{28}O_{72}]\cdot 28H_2O$ and orthorhombic symmetry, space group *Fmmm*, a = 13.55, b = 18.26, c = 17.80 Å, Z = 1 (Galli and Alberti 1975a, Miller and Taylor 1985). The neutron diffraction data of Miller and Taylor (1985) disclosed slight (Si,Al) ordering with individual tetrahedral Al contents ranging from 10 to 30%.

Stellerite has only one fully occupied, or nearly fully occupied, Ca channel cation site (Fig. 17d) (Galli and Alberti 1975a, Miller and Taylor 1985). Ca is coordinated only to channel H_2O molecules and not to framework oxygens. Similar to stilbite, the $Ca(H_2O)$ complex is hydrogen bonded to the framework oxygens (Miller and Taylor 1985). There are seven partially occupied H_2O sites in the structure with occupancies between 0.2 and 0.8 (Galli and Alberti 1975a, Miller and Taylor 1985).

Barrerite (STI), $Na_8[Al_8Si_{27}O_{72}]\cdot 26H_2O$, is orthorhombic, space group *Amma*, a = 13.64, b = 18.20, c = 17.84 Å, Z = 1, and has (Si,Al) disordered over five distinct tetrahedral sites (Galli and Alberti 1975b, Sacerdoti et al. 1999). Five partially occupied channel cations sites can be resolved. Two of these sites are similar to the Ca site in stilbite and stellerite and have the highest Na occupancies, 0.72 and 0.62 (Galli and Alberti 1975b). The other two sites are somewhat similar to the Na sites in stellerite, with lower occupancies, 0.14 and 0.25. The fifth site is specific to barrerite, with an occupancy of 0.25 (Galli and Alberti 1975b). Figure 17e shows the channel cation distribution. Galli and Alberti (1975b) also found 14 channel H_2O sites ranging in occupancy from 0.2 to 0.91. The cation and H_2O distribution in barrerite is thus quite complex and may vary from sample to sample (Galli and Alberti 1975b, Sacerdoti et al. 1999). Upon dehydration barrerite transforms to heat-collapsed phases characterized by major changes in the framework (Alberti and Vezzalini 1978, Sani et al. 1998).

Bresterite (BRE)

Brewsterite (BRE) with the simplified formula $(Sr,Ba,Ca)_2[Al_4Si_{12}O_{32}]\cdot 10H_2O$ is monoclinic, space group $P2_1/m$, a = 6.793, b = 17.57, c = 7.76 Å, β = 94.54°, Z = 1 (Perrotta and Smith 1964, Schlenker et al. 1977b, Artioli et al. 1985, Cabella et al. 1993). As in all tabular zeolites, there are two sets of interconnecting channels in the framework. Eight-membered rings (aperture 2.8 × 5.0 Å) form channels parallel to the **a**-axis (Fig. 18), and a second set of eight-membered rings (aperture 2.8 × 4.1 Å) forms channels parallel to the **c**-axis (Fig. 18). Schlenker et al. (1977b) found partial (Si,Al) ordering in the four unique tetrahedral sites; three of the sites contain 30 to 40% Al and the fourth site contains no Al (i.e. it is fully occupied by Si). Neutron diffraction data by Artioli et al. (1985) confirmed this partial (Si,Al) ordering. Based upon optical studies, brewsterite

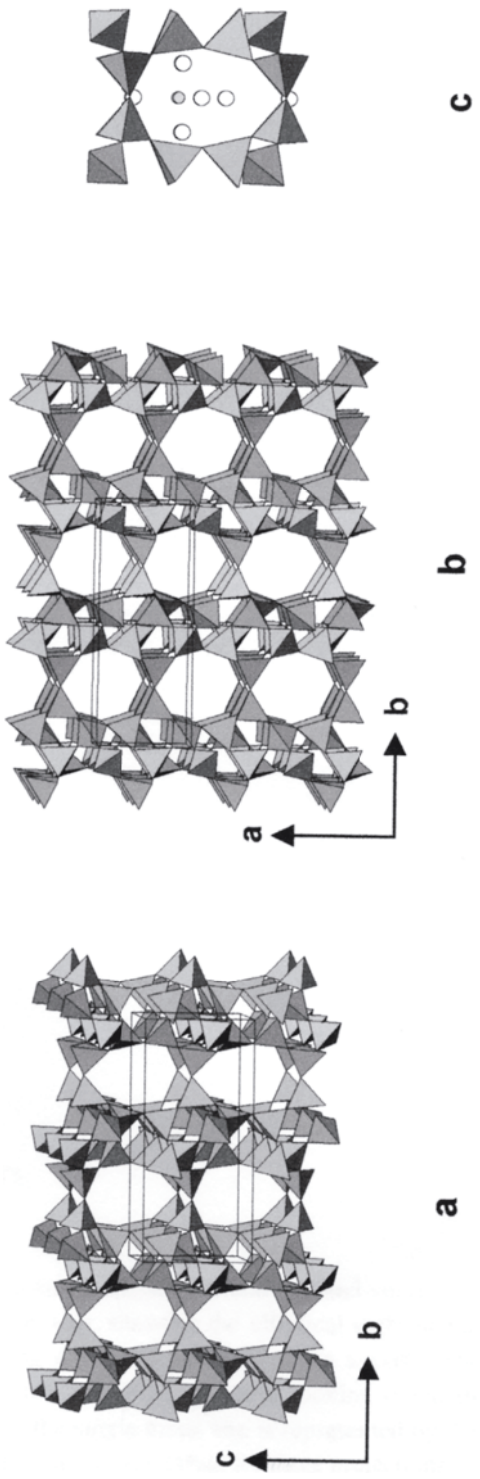

Figure 18. Brewsterite framework and channel contents. (a) A (100) projection looking down the **a**-axis with the **c**-axis vertical, showing the elliptical eight-membered rings forming [100] channels. (b) A (001) projection looking down the **c**-axis with the **a**-axis vertical, showing eight-membered rings which form [001] channels. (c) A (100) projection looking down the **a**-axis with the **c**-axis vertical, showing the channel contents; the single metal site is represented by the smaller gray-shaded circle, and the larger white circles are the H_2O molecules. (Data for these projections obtained from Artioli et al. 1985.)

is triclinic (Akizuki 1987b). This reduction in symmetry may be explained by an ordering of (Si,Al) depending on the growth direction. Recently Akizuki et al. (1996) refined the crystal structures of various growth sectors and found triclinic symmetry (space group *P*1). Akizuki et al. (1996) determined slightly different (Si,Al) distributions for tetrahedral sites related to each other by a pseudomirror plane.

All structure refinements located only one fully occupied channel-cation position. The site is located in the middle of the [100] channels and is nine-coordinated to four framework oxygens and five channel H_2O molecules (Fig. 18c). Artioli et al. (1985) also located the H positions in the channels based on neutron diffraction data. Upon dehydration up to 684 K, brewsterite loses eight of its ten H_2O molecules accompanied by diffusion of the channel cations and framework distortion (Ståhl and Hanson 1999). In a dehydration experiment with 24h equilibration in vacuum at 550 K, Alberti et al. (1999) observed statistical breaking of T-O-T bonds and formation of an altered tetrahedral topology.

OTHER RARE OR STRUCTURALLY POORLY DEFINED ZEOLITES

Lovdarite (LOV), $K_4Na_{12}[Be_8Si_{28}O_{72}]\cdot 18H_2O$, (Men'schikov et al. 1973, Khomyakov et al. 1975) is orthorhombic, space group *Pma*2, a = 39.576, b = 6.9308, c = 7.1526 Å, Z = 1 (Merlino 1990). The structure consists of a framework of ordered Si and Be tetrahedra and is characterized by channels running parallel to the **a**-axis through eight-membered rings (aperture 3.6 × 3.7 Å) and running parallel to the **b**-axis through strongly deformed nine-membered rings (aperture 3.2 × 4.4 Å). A special feature are three-membered rings formed by one BeO_4 and two SiO_4 tetrahedra. Na is five-coordinated by four framework oxygens and one H_2O molecule; K is nine-coordinated by six framework oxygens and three H_2O molecules. Diffraction patterns suggest that lovdarite may consist of distinct disordered domains (Merlino 1990).

Weinebeneite (WEI), $Ca_4[Be_{12}P_8O_{32}(OH)_8]\cdot 16H_2O$ (Walter 1992), space group *Cc*, a = 11.987, b = 9.707, c = 9.633 Å, β = 95.76°, Z = 1, has a tetrahedral framework formed by PO_4 and BeO_4 tetrahedra. Four-membered rings of alternating PO_4 and BeO_4 tetrahedra build a two-dimensional network. These layers are composed of crankshafts forming four- and eight-membered rings (Fig. 19) and resemble layers in the gismondine framework (GIS). In weinebeneite, two such layers are oriented parallel to (100) and are shifted relative to each other by b/2 and connected by additional BeO_4 tetrahedra (Fig. 19). This arrangement leads to three-membered rings (P-Be-Be) which are unknown in framework silicates but have been described before in the beryllosilicate lovdarite (Merlino 1990). The framework oxygens connecting two Be tetrahedra are actually OH groups; thus, the framework remains uninterrupted. Ca is situated in structural channels parallel to the **c**-axis and is confined by ten-membered rings and is coordinated by three framework oxygens and four H_2O molecules. One H_2O molecule is positionally disordered.

Gaultite (VSV), $Na_4[Zn_2Si_7O_{18}]\cdot 5H_2O$, (Ercit and van Velthuizen 1994) is orthorhombic, space group *F*2*dd*, a = 10.211, b = 39.88, c = 10.304 Å, Z = 8 and has a framework structure composed of ordered ZnO_4 and SiO_4 tetrahedra forming strongly deformed eight- and nine-membered ring channels along [101]. The eight-membered ring channel is filled with chains of edge-sharing NaO_6 octahedra built by framework oxygens and H_2O molecules. The nine-membered ring channels host disordered Na and H_2O. The framework can be constructed from stacks along **b** of two-dimensional nets composed of four- and eight-membered rings (similar as in weinebeneite, Fig. 19) with periodic insertions of tetrahedra between the sheets. The framework also has characteristic three-membered rings formed by two SiO_4 and one ZnO_4 tetrahedra.

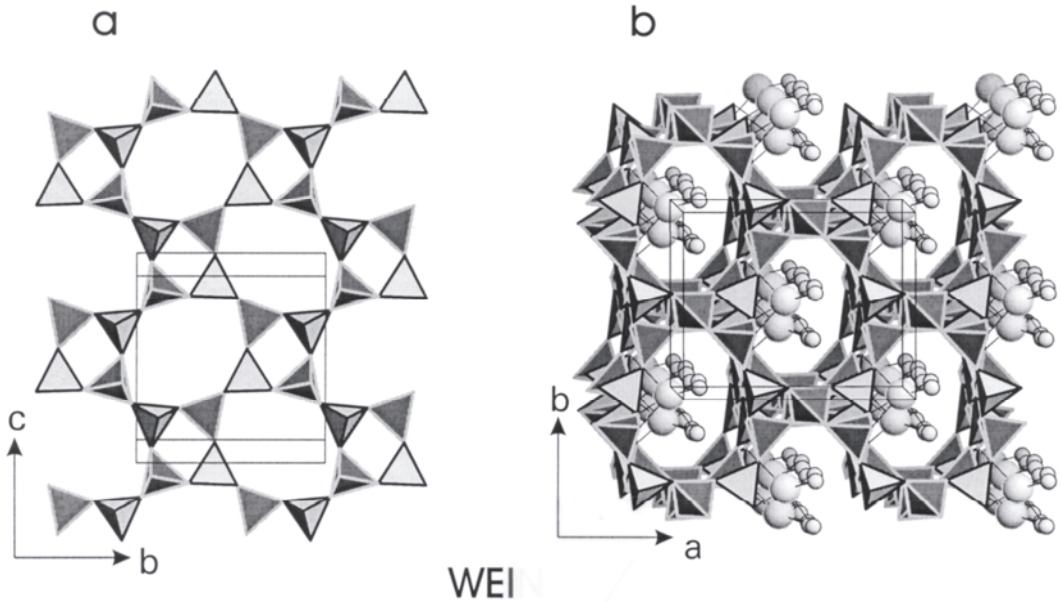

Figure 19. The tetrahedral framework of weinebeneite. BeO_4 tetrahedra have light edges; PO_4 tetrahedra have black edges. (a) The tetrahedral four-ring layer in weinebeneite projected on (100). (b) The weinebeneite framework projected approximately along the **c**-axis**.** The (100) tetrahedral sheets are linked by intercalated BeO_4 tetrahedra. Large spheres are Ca, and small spheres are fully occupied H_2O sites.

Chiavennite (-CHI), $CaMn[Be_2Si_5O_{13}(OH)_2]\cdot 2H_2O$, and **tvedalite**, $(Ca,Mn)_4[Be_3Si_6O_{17}(OH)]\cdot 4.3H_2O$ are beryllosilicates (Bondi et al. 1983, Raade et al. 1983, Larsen et al. 1992). Chiavennite (-CHI) is orthorhombic, space group *Pnab*, a = 8.729, b = 31.33, c = 4.903 Å, Z = 4. The crystal structure (Tazzoli et al. 1995) is characterized by an interrupted framework where BeO_4 tetrahedra share only three vertices. Channels parallel to the **c**-axis are confined by nine-membered rings (aperture 3.3 × 4.3 Å). Mn occurs as an extraframework cation and is six-coordinated by four oxygens and two OH groups of the framework. Ca is eight-coordinated by four oxygens, two OH groups, and two H_2O molecules. A possible structure model of tvedalite with a *C*-centered orthorhombic lattice a = 8.7, b = 23.1, c = 4.9 Å derived from chiavennite was given by Alberti (1995).

Tschernichite (BEA), $Ca[Al_2Si_6O_{16}]\cdot 8H_2O$ (Boggs et al. 1993, Galli et al. 1995). The X-ray powder pattern could be indexed on a tetragonal unit cell with a = 12.88 and c = 25.01 Å, Z = 8. From the similarity of the X-ray powder patterns of zeolite beta and that of tschernichite, it is assumed that tschernichite is its natural analog (Smith et al. 1991). Zeolite beta occurs in two polymorphs which appear to be stacked in a random sequence in tschernichite (Alberti 1995). Zeolite beta is characterized by two types of channels parallel to the **a**-axis and to the **c**-axis confined by twelve-membered rings.

Gottardiite (NES), $Na_{2.5}K_{0.2}Mg_{3.1}Ca_{4.9}[Al_{18.8}Si_{117.2}O_{272}]\cdot 93H_2O$ (Galli et al. 1996) is orthorhombic, space group *Cmca*, a = 13.698, b = 25.213, c = 22.660 Å, Z = 1 (Alberti et al. 1996b), and represents a natural analog of the framework topology (NES) found for synthetic NU-87 (Shannon et al. 1991). The topological symmetry is *Fmmm*, which is reduced to *Cmca* in gottardiite to avoid energetically unfavorable T-O-T angles of 180°. NU-87 is monoclinic, space group $P2_1/c$ (a = 14.32, b = 22.38, c = 25.09 Å, β = 151.5°). The structure (Fig. 20a) consists of sheets parallel to (001) formed by 5^46^2 and 5^4 polyhedral units (e.g. 5^46^2 designates a polyhedron, built by tetrahedra, which is confined by four pentagons and two hexagons). Each (001) sheet is bonded to an analogous sheet

through four-membered rings, parallel to the sheets, leading to a two-dimensional channel system parallel to (001). Ten-membered ring channels run parallel to the **a**-axis and twelve-membered ring channels extend zigzag-wise parallel to the **b**-axis. Both channel types are connected by ten-membered ring windows. Extraframework ions and molecules are strongly disordered and positioned close to the center of the channels.

Terranovaite (TER), $Na_{4.2}K_{0.2}Mg_{0.2}Ca_{3.7}[Al_{12.3}Si_{67.7}O_{160}]\cdot>29H_2O$ (Galli et al. 1997a) is orthorhombic with average space group *Cmcm*, a = 9.747, b = 23.880, c = 20.068 Å, Z = 1. The structure (Fig. 20b,c) is characterized by chains built of five-membered rings (pentasil chains) and by a two-dimensional ten-membered ring channel system parallel to (010). The structure represents a new topology not found in any other synthetic or natural zeolite.

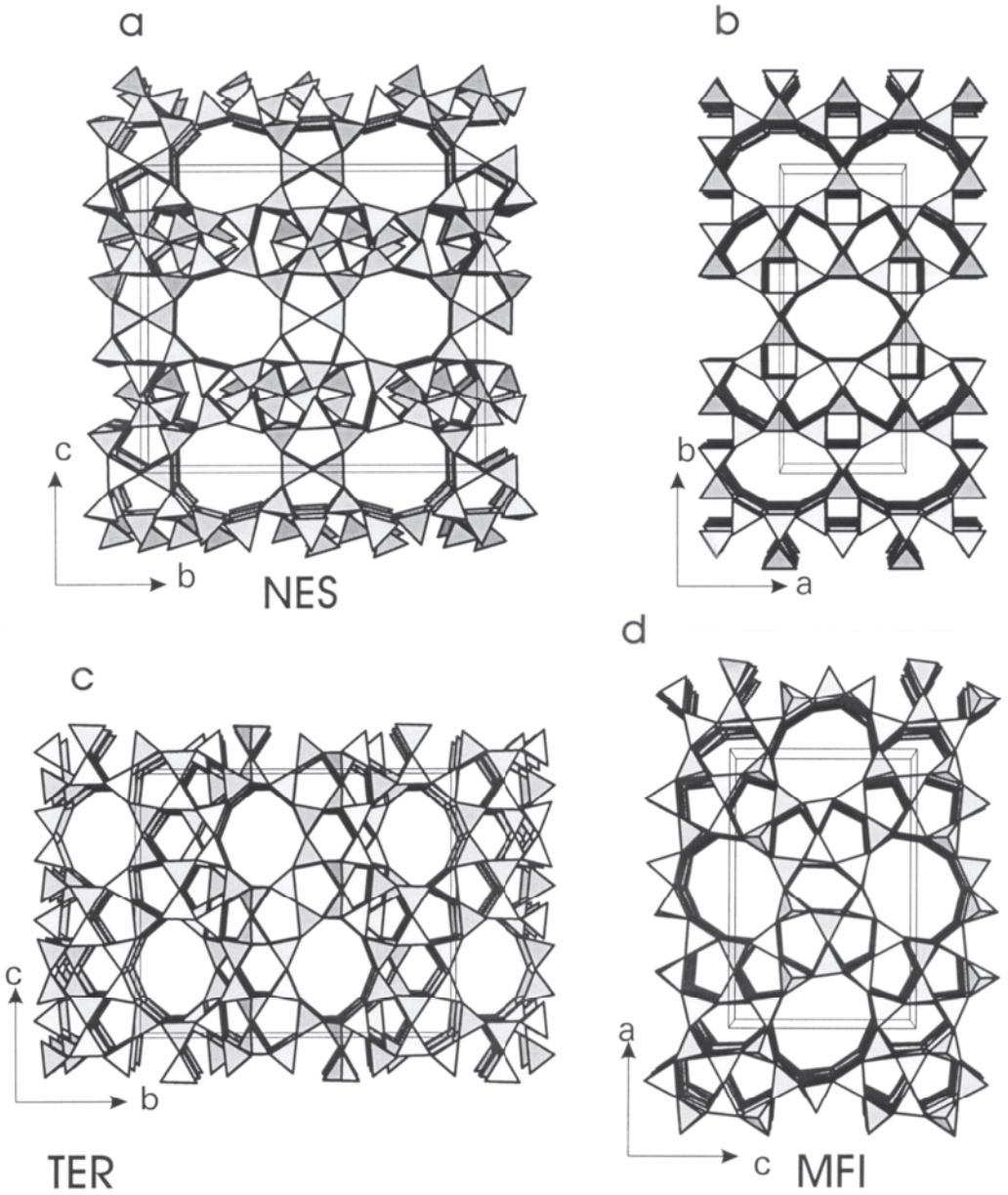

Figure 20. (a) The gottardiite (NES) framework projected approximately along the **a**-axis. Dense sheets extend parallel to (001). (b) The terranovaite (TER) framework projected along the **c**-axis. (c) The terranovaite framework projected along the **a**-axis. (d) The mutinaite (MFI) framework projected along the **b**-axis.

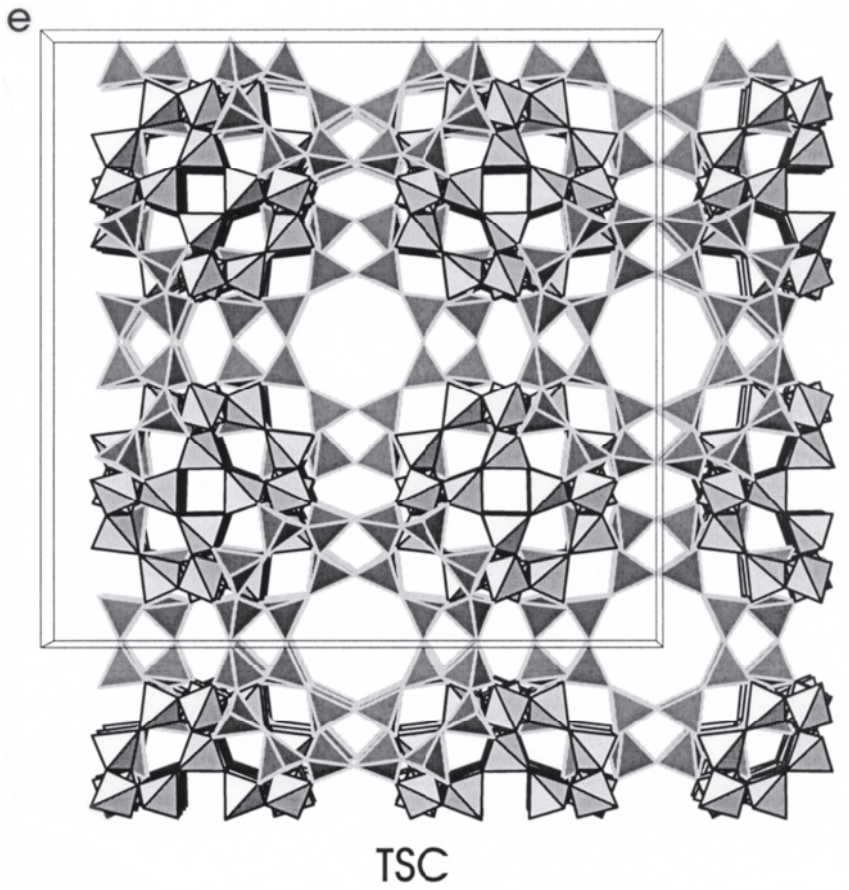

Figure 20, continued. (e) The tschörtnerite (TSC) framework projected parallel to the **a**-axis. T1-type tetra-hedra forming the sodalite cage (β-cage) have dark rims, T2-type tetrahedra forming the α-cage have light rims. The new 96-membered tschörtnerite cage is built by both T1 and T2 tetrahedra.

Mutinaite (MFI), $Na_{2.76}K_{0.11}Mg_{0.21}Ca_{3.78}[Al_{11.20}Si_{84.91}O_{192}]\cdot 60H_2O$ (Galli et al. 1997b) is the natural counterpart of ZSM-5 (Kokotailo et al. 1978), space group *Pnma*, a = 20.201, b = 19.991, c = 13.469 Å, Z = 1 (Vezzalini et al. 1997b). The structure (Fig. 20d) is characterized by chains built of five-membered rings (pentasil chains) and of ten-membered ring channels parallel to [100] and [010]. T-O bond distances are compatible with a disordered (Si,Al) distribution. Channel cations and H_2O molecules are strongly disordered.

Tschörtnerite (TSC), $Ca_4(K,Ca,Sr,Ba)_3Cu_3(OH)_8[Si_{12}Al_{12}O_{48}]\cdot \geq 20H_2O$, (Effenberger et al. 1998) is a Cu-bearing new zeolite structure type of cubic symmetry, space group F*m*3*m*, *a* = 31.62 Å, Z = 16. The structure (Fig. 20e) contains interconnections of double six-rings, double eight-rings, sodalite cages, truncated cubo-octahedra, and previously unknown 96-membered cages (tschörtnerite cage) composed of 24 four-rings, 8 six-rings, and 18 eight-rings. Cu has a square-like oxygen coordination forming $Cu_{12}(OH)_{24}$ clusters centered in the truncated cubo-octahedron. In spite of the Si/Al ratio of 1/1 and two symmetry-independent T sites, the T-O bond lengths do not indicate (Si,Al) ordering. Furthermore, the tetrahedral connection implies that Loewenstein's (1954) rule is violated.

Cowlesite (framework unknown), $Ca_6[Al_{12}Si_{18}O_{60}]\cdot 33H_2O$, is a Ca-dominate zeolite with minor K and Mg. The crystal structure is unknown, but the X-ray powder pattern of eight samples from different localities could be indexed with an orthorhombic unit cell *a* = 23.3, *b* = 30.6, *c* = 25 Å, Z = 8 - 9 (Vezzalini et al. 1992).

ACKNOWLEDGMENTS

We thank Dave Bish and Paul Ribbe for their excellent editorial assistance with our chapter; their comments and suggestions greatly improved our work. MEG thanks Kathy Zanetti and Brittany Brown for assisting in very tedious proof reading of the references and tables, Paul Ribbe for two decades of mentoring in crystal chemistry, and finanical support from British Nuclear Fuel Laboratories and National Science Foundation for grant CCLI-9952377.

APPENDIX — TABLE 1

(on the following six pages)

NOTE: Each mineral is indexed with the page number on which it is discussed in the text.

Table 1. Alphabetical list of zeolites and zeolite-like minerals covered in this chapter with their, chemical formulas, space group, cell parameters, channel description, and FD (T/1,000Å^3). (Channel descriptions from Meier et al. (1996); cell parameters and chemical formulas from Gottardi and Galli 1985; and new data taken from this chapter.)

Meier at al. (1996) use the following symbols for channel descriptions: bold numbers represent the number of tetrahedra defining the channel, the channel free diameter is given in Å, the number of stars represent the number of channels in a given direction, the connectivity of channels is given by "⇔" to represent connected channels or "|" to represent non-connected channels.

Amicite **p 23**
$Na_4K_4[Al_8Si_8O_{32}]\cdot 10H_2O$
*I*2
a = 10.226, *b* = 10.422, *c* = 9.884, β = 88.32
GIS: {[100] **8** 3.1×4.5 ⇔ [010] **8** 2.8×4.8}***
FD: 15.4 (14.7 expanded)

Ammonioleucite **p 17**
$(NH_4)_{16}[Al_{16}Si_{32}O_{96}]$
$P4_1ad$
a = 13.124, *c* = 13.173
ANA: [110] **8** distorted*
FD: 18.6

Analcime **p 15**
$Na_{16}[Al_{16}Si_{32}O_{96}]\cdot 16H_2O$
*Ia*3*d*
a = 13.73
ANA: [110] **8** distorted*
FD: 18.6

Barrerite **p 44**
$Na_8[Al_8Si_{27}O_{72}]\cdot 26H_2O$
Amma
a = 13.64, *b* = 18.20, *c* = 17.84
STI: [100] **10** 4.9×6.1* ⇔ [101] **8** 2.7×5.6*
FD: 16.9

Bellbergite **p 32**
$(K,Ba,Sr)_2Sr_2Ca_2(Ca,Na)_4[Al_{18}Si_{18}O_{72}]\cdot 30H_2O$
$P6_3/mmc$ or $P62c$ or $P6_3mc$
a = 13.244, *c* = 15.988
EAB: ⊥ [001] **8** 3.7×5.1**
FD: 15.4

Bikitaite **p 39**
$Li_2[Al_2Si_4O_{12}]\cdot 2H_2O$
$P2_1$
a = 8.61, *b* = 4.96, *c* = 7.60, β = 114.5
BIK: [001] **8** 2.8×3.7*
FD: 20.2

Boggsite **p 27**
$Ca_8Na_3[Al_{19}Si_{77}O_{192}]\cdot 70H_2O$
Imma
a = 20.236, *b* = 23.798, *c* = 12.798
BOG: [100] **12** 7.0×7.0* ⇔ [010] **10** 5.2×5.8*
FD: 15.6

Brewsterite **p 44**
$(Sr,Ba,Ca)_2[Al_4Si_{12}O_{32}]\cdot 10H_2O$
$P2_1/m$
a = 6.793, *b* = 17.57, *c* = 7.76, β = 94.54
BRE: [100] **8** 2.3×5.0* ⇔ [001] 2.8×4.1*
FD: 17.5

Chabazite **p 28**
$(Ca_{0.5},Na,K)_4[Al_4Si_8O_{24}]\cdot 12H_2O$
R-3*m* or *P*-1
a = 13.2, *c* = 15.1
CHA: ⊥ [001] **8** 3.8×3.8***
FD: 14.6

Chiavennite **p 47**
$CaMn[Be_2Si_5O_{13}(OH)_2]\cdot 2H_2O$
Pnab
a = 8.729, *b* = 31.33, *c* = 4.903
-CHI: [001] **9** 3.9×4.3*
FD: 20.9

Clinoptilolite **p 40**
$(Na,K)_6[Al_6Si_{30}O_{72}]\cdot 20H_2O$
*C*2/*m*
a = 17.7, *b* = 17.8, *c* = 7.4, β = 116.4
HEU: [100] **8** 2.6×4.7* ⇔ {[001] **10** 3.0×7.6* +
8 3.3×4.6*}
FD: 17.0

Cowlesite (structure unknown) **p 49**
$Ca_6[Al_{12}Si_{18}O_{60}]\cdot 33H_2O$
orthorhombic
a = 23.3, *b* = 30.6, *c* = 25.0

Dachiardite p 36
$(Na,K,Ca_{0.5})_4[Al_4Si_{20}O_{48}]\cdot 18H_2O$
Cm
a = 18.676, *b* = 7.518, *c* = 10.246, β = 107.87
DAC: [010] **10** 3.4×5.3* ⇔ [001] **8** 3.7×4.8*
FD: 17.3

Edingtonite p 15
$Ba_2[Al_4Si_6O_{20}]\cdot 8H_2O$
$P2_12_12_1$
a = 9.55, *b* = 9.67, *c* = 6.523
EDI: [110] **8** 2.8×3.8** ⇔ [001] **8** variable*
FD: 16.6 (14.5 expanded)

Epistilbite p 38
$Ca_3[Al_6Si_{18}O_{48}]\cdot 16H_2O$
*C*1
a = 9.08, *b* = 17.74, *c* = 10.15, α = 90, β = 124.6, γ = 90
EPI: [100] **10** 3.4×5.6* ⇔ [001] **8** 3.7 × 5.2*
FD: 18.0

Erionite p 32
$K_2(Na,Ca_{0.5})_8[Al_{10}Si_{26}O_{72}]\cdot 28H_2O$
$P6_3/mmc$
a = 13.26, *c* = 15.12
ERI: ⊥ [001] **8** 3.6×5.1***
FD: 15.6

Faujasite p 33
$Na_{20}Ca_{12}Mg_8[Al_{60}Si_{132}O_{384}]\cdot 235H_2O$
*Fd*3*m*
a = 24.60
FAU: <111> **12** 7.4***
FD: 12.7

Ferrierite p 39
$(Na,K)Mg_2Ca_{0.5}[Al_6Si_{30}O_{72}]\cdot 20H_2O$
Immm
a = 19.18, *b* = 14.14, *c* = 7.5
FER: [001] **10** 4.2×5.4* ⇔ [010] **8** 3.5×4.8*
FD: 17.7

Garronite p 23
$NaCa_{2.5}[Al_6Si_{10}O_{32}]\cdot 13H_2O$
I-4*m*2
a = 9.266, *c* = 10.3031
GIS: {[100] **8** 3.1×4.5 ⇔ [010] **8** 2.8×4.8}***
FD: 15.4 (14.7 expanded)

Gaultite p 46
$Na_4[Zn_2Si_7O_{18}]\cdot 5H_2O$
*F*2*dd*
a = 10.211, *b* = 39.88, *c* = 10.304
VSV: [011] **9** 3.3×4.5* ⇔ [101] **9** 3.3×4.5* ⇔
[101] **8** 3.7×3.7*
FD: 17.1

Gismondine p 23
$Ca_4[Al_8Si_8O_{32}]\cdot 16H_2O$
$P2_1/c$
a = 10.02, *b* = 10.62, *c* = 9.84, β = 92.5
GIS: {[100] **8** 3.1×4.5 ⇔ [010] **8** 2.8×4.8}***
FD: 15.4 (14.7 expanded)

Gmelinite p 28
$(Na,K,Ca_{0.5},Sr_{0.5})_8[Al_8Si_{16}O_{48}]\cdot 22H_2O$
$P6_3/mmc$
a = 13.75, *c* = 10.06GME: [001] **12** 7.0* ⇔ ⊥ [001] **8** 3.6×3.9**
FD: 14.6

Gobbinsite p 23
$Na_5[Al_5Si_{11}O_{32}]\cdot 11H_2O$
$Pmn2_1$
a = 10.108, *b* = 9.766, *c* = 10.171
GIS: {[100] **8** 3.1×4.5 ⇔ [010] **8** 2.8×4.8}***
FD: 15.4 (14.7 expanded)

Gonnardite p 13
$(Na, Ca)_{6\text{-}8}[(Al, Si)_{20}O_{40}]\cdot 12\ H_2O$
I-42*d*
a = 13.21, *c* = 6.62
NAT: <100> **8** 2.6×3.9** ⇔ [001] **8** variable*
FD: 17.8 (14.5 expanded)

Goosecreekite p 19
$Ca_2[Al_4Si_{12}O_{32}]\cdot 10H_2O$
$P2_1$
a = 7.401, b = 17.439, c = 7.293, β = 105.44
GOO: [100] **8** 2.8×4.0* ⇔ [010] **8** 2.7×4.1* ⇔ [001] **8** 2.9×4.7*
FD: 17.6

Gottardiite p 47
$Na_{2.5}K_{0.2}Mg_{3.1}Ca_{4.9}[Al_{18.8}Si_{117.2}O_{272}]\cdot 93H_2O$
Cmca
a = 13.698, b = 25.213, c = 22.660
NES: [100] **10** 4.7×6.0**
FD: 17.7

Harmotome p 25
$Ba_2(Ca_{0.5},Na)[Al_5Si_{11}O_{32}]\cdot 12H_2O$
$P2_1/m$
a = 9.865, b = 14.300, c = 8.668, β = 124.8
PHI: [100] **8** 3.6* ⇔ [010] **8** 3.0×4.3* ⇔ [001] **8** 3.2×3.3*
FD: 15.8

Heulandite p 40
$(Na,K)Ca_4[Al_9Si_{27}O_{72}]\cdot 24H_2O$
$C2/m$
a = 17.7, b = 17.8, c = 7.4, β = 116.4
HEU: [100] **8** 2.6×4.7* ⇔ {[001] **10** 3.0×7.6* + **8** 3.3×4.6*}
FD: 17.0

Hsianghualite p 18
$Li_{16}Ca_{24}F_{16}[Be_{24}Si_{24}O_{96}]$
$I2_13$
a = 12.864
ANA: [110] **8** distorted*
FD: 18.6

Kalborsite p 15
$K_6B(OH)_4Cl[Al_4Si_6O_{20}]$
$P\text{-}42_1c$
a = 13.45, c = 13.060
EDI: [110] **8** 2.8×3.8** ⇔ [001] **8** variable*
FD: 16.6 (14.5 expanded)

Laumontite p 18
$Ca_4[Al_8Si_{16}O_{48}]\cdot 18H_2O$
$C2/m$
a = 14.863, b = 13.169, c = 7.537, β = 110.18
LAU: [100] **10** 4.0×5.3*
FD: 17.7

Leucite p 17
$K_{16}[Al_{16}Si_{32}O_{96}]$
$Ia3d$
a = 13.0
ANA: [110] **8** distorted*
FD: 18.6

Levyne p 31
$(Ca_{0.5},Na,K)_6[Al_6Si_{12}O_{36}]\cdot 18H_2O$
$R\text{-}3m$
a = 13.338, c = 23.014
LEV: ⊥ [001] **8** 3.6×4.8**
FD: 15.2

Lovdarite p 46
$K_4Na_{12}[Be_8Si_{28}O_{72}]\cdot 18H_2O$
$Pma2$
a = 39.576, b = 6.9308, c = 7.1526
LOV: [010] **9** 3.2×4.4* ⇔ [001] **9** 3.2×3.7* ⇔ [100] **8** 3.6×3.7*
FD: 18.4

Maricopaite p 36
$Pb_7Ca_2[Al_{12}Si_{36}(O,OH)_{100}]\cdot n(H_2O,OH)$
$Cm2m$
a = 19.434, b = 19.702, c = 7.538
-MOR: [010] **12** 6.5×7.0* ⇔ [010] **8** 2.6×5.7*

Mazzite p 26
$K_{2.5}Mg_{2.1}Ca_{1.4}Na_{0.3}[Al_{10}Si_{26}O_{72}]\cdot 28H_2O$
$P6_3/mmc$
a = 18.392, c = 7.646
MAZ: [001] **12** 7.4* | **8** [001] 3.4×5.6*
FD: 16.1

Merlinoite p 25
$K_5Ca_2[Al_9Si_{23}O_{64}]\cdot 24H_2O$
Immm
a = 14.116, *b* = 14.229, *c* = 9.946
MER: [100] **8** 3.1×3.5* ⇔ [010] **8** 2.7×3.6* ⇔ [001] {**8** 3.4×5.1* + **8** 3.3×3.3*}
FD: 16.0

Mesolite p 11
$Na_{16}Ca_{16}[Al_{48}Si_{72}O_{240}]\cdot 64H_2O$
*Fdd*2
a = 18.405, *b* = 56.65, *c* = 6.554
NAT: <100> **8** 2.6×3.9** ⇔ [001] **8** variable*
FD: 17.8 (14.5 expanded)

Montesommaite p 20
$(K,Na)_9[Al_9Si_{23}O_{64}]\cdot 10H_2O$
*Fdd*2
a = 10.099, *b* = 10.099, *c* = 17.307
MON: [100] **8** 3.2×4.4* ⇔ [001] **8** 3.6×3.6*
FD: 18.1

Mordenite p 35
$(Na_2,K_2,Ca)_4[Al_8Si_{40}O_{96}]\cdot 28H_2O$
$Cmc2_1$
a = 18.11, *b* = 20.46, *c* = 7.52
MOR: [001] **12** 6.5×7.0* ⇔ [010] **8** 2.6×5.7*
FD: 17.2

Mutinaite p 49
$Na_{2.76}K_{0.11}Mg_{0.21}Ca_{3.78}[Al_{11.20}Si_{84.91}O_{192}]\cdot 60H_2O$
Pnma
a = 20.201, *b* = 19.991, *c* = 13.469
MFI: {[010] **10** 5.3×5.6 ⇔ **10** 5.1×5.3}***
FD: 17.9

Natrolite p 10
$Na_{16}[Al_{16}Si_{24}O_{80}]\cdot 16H_2O$
*Fdd*2
a = 18.29, *b* = 18.64, *c* = 6.59
NAT: <100> **8** 2.6×3.9** ⇔ [001] **8** variable*
FD: 17.8 (14.5 expanded)

Offretite p 32
$KCaMg[Al_5Si_{13}O_{36}]\cdot 15H_2O$
P-6*m*2
a = 13.29, *c* = 7.58
OFF: [001] **12** 6.7* ⇔ ⊥ [001] **8** 3.6 × 4.9**
FD: 15.5

Pahasapaite p 34
$(Ca_{5.5}Li_{3.6}K_{1.2}Na_{0.2})Li_8[Be_{24}P_{24}O_{96}]\cdot 38H_2O$
*I*23
a = 13.781
RHO: <100> **8** 3.6*** | <100> **8** 3.6***
FD: 14.3

Paranatrolite p 13
$Na_{16}[Al_{16}Si_{24}O_{80}]\cdot 24H_2O$
pseudo-orthorhombic
a = 19.07, *b* = 19.13, *c* = 6.58
NAT: <100> **8** 2.6×3.9** ⇔ [001] **8** variable*
FD: 17.8 (14.5 expanded)

Parthéite p 21
$Ca_2[Al_4Si_4O_{15}(OH)_2]\cdot 4H_2O$
*C*2/*c*
a = 21.555, *b* = 8.761, *c* = 9.304, β = 91.55
-PAR: [001] **10** 3.5×6.9*
FD: 18.2

Paulingite p 27
formula $Na_{14}K_{36}Ca_{59}Ba_2[Al_{173}Si_{499}O_{1344}]\cdot 550H_2O$
*Im*3*m*
a = 35.09
PAU: <100> **8** 3.8*** | <100> **8** 3.8***
FD: 15.5

Perlialite p 27
$K_9Na(Ca,Sr)[Al_{12}Si_{24}O_{72}]\cdot 15H_2O$
*P*6/*mmm*
a = 18.54, *c* = 7.53
LTL: [001] **12** 7.1*
FD: 16.4

Phillipsite p 25
$K_2(Ca_{0.5},Na)_4[Al_6Si_{10}O_{32}]\cdot 12H_2O$
*P*2$_1$/*m*
a = 9.869, *b* = 14.139, *c* = 8.693, β = 124.81
PHI: [100] **8** 3.6* ⇔ [010] **8** 3.0×4.3* ⇔ [001] **8** 3.2×3.3*
FD: 15.8

Pollucite p 17
$Cs_{16}[Al_{16}Si_{32}O_{96}]$
*Ia*3*d*
a = 13.69
ANA: [110] **8** distorted*
FD: 18.6

Roggianite p 21
$Ca_2[Be(OH)_2Al_2Si_4O_{13}]\cdot 2.5H_2O$
*I*4/*mcm*
a = 18.370, *c* = 9.187
-RON: [001] **12** 4.2*
FD: 15.6

Scolecite p 11
$Ca_8[Al_{16}Si_{24}O_{80}]\cdot 24H_2O$
*F*1*d*1
a = 18.51, *b* = 18.97, *c* = 6.53, β = 90.7
NAT: <100> **8** 2.6×3.9** ⇔ [001] **8** variable*
FD: 17.8 (14.5 expanded)

Stellerite p 44
$Ca_4[Al_8Si_{28}O_{72}]\cdot 28H_20$
F*mmm*
a = 13.55, *b* = 18.26, *c* = 17.80
STI: [100] **10** 4.9×6.1* ⇔ [101] **8** 2.7×5.6*
FD: 16.9

Stilbite p 42
$NaCa_4[Al_9Si_{27}O_{72}]\cdot 30H_2O$
*C*2/*m*
a = 13.64, *b* = 18.24, *c* = 11.27, β = 127.9
STI: [100] **10** 4.9×6.1* ⇔ [101] **8** 2.7×5.6*
FD: 16.9

Terranovaite p 48
$Na_{4.2}K_{0.2}Mg_{0.2}Ca_{3.7}[Al_{12.3}Si_{67.7}O_{160}]\cdot > 29H_2O$
Cmcm
a = 9.747, *b* = 23.880, *c* = 20.068
TER: [100] **10** 5.0×5.5* ⇔ [001] **10** 4.2×7.0*
FD: 17.1

Thomsonite p 13
$Na_4Ca_8[Al_{20}Si_{20}O_{80}]\cdot 24H_2O$
Pncn
a = 13.09, *b* = 13.05, *c* = 13.22
THO: [101] **8** 2.3×3.9* ⇔ [010] **8** 2.2×4.0* ⇔
[001] 8 variable*
FD: 17.7 (14.4 expanded)

Tschernichite p 47
$Ca[Al_2Si_6O_{16}]\cdot 8H_2O$
tetragonal
a = 12.88, *c* = 25.01
BEA: [001] **12** 5.5×5.5* ⇔ <100> **12** 7.6×6.4**
FD: 15.0

Tschörtnerite p 49
$Ca_4(K,Ca,Sr,Ba)_3Cu_3(OH)_8[Si_{12}Al_{12}O_{48}]\cdot \geq 20H_2O$
F*m*3*m*
a = 31.62
TSC: unknown
FD: 12.1

Tvedalite p 47
$(Ca,Mn)_4[Be_3Si_6O_{17}(OH)]\cdot 4.3H_2O$
orthorhombic
a = 8.7, *b* = 23.1, *c* = 4.9

Wairakite p 16
$Ca_8[Al_{16}Si_{32}O_{96}]\cdot 16H_2O$
*I*2/*a*
a = 13.699, *b* = 13.640, *c* = 13.546, β = 90.5
ANA: [110] **8** distorted*
FD: 18.6

Weinebeneite p 46
$Ca_4[Be_{12}P_8O_{32}(OH)_8]\cdot 16H_2O$
Cc
a = 11.987, *b* = 9.707, *c* = 9.633, β = 95.8
WEI: [001] **10** 3.1×5.4* ⇔ [100] **8** 3.3×5.1*
FD: 18.1

Willhendersonite p 31
$K_2Ca_2[Al_6Si_6O_{24}]\cdot 10H_2O$
P-1
a = 9.206, *b* = 9.216, *c* = 9.500, α = 92.34, β = 92.70, γ = 90.12
CHA: ⊥ [001] **8** 3.8×3.8***
FD: 14.6

Vugawaralite p 19
$Ca_2[Al_4Si_{12}O_{32}]\cdot 8H_2O$
*C*2/*m*
a = 6.72, *b* = 13.93, *c* = 10.04, β = 111.1
YUG: [100] **8** 2.8×3.6* ⇔ [001] **8** 3.1×5.0*
FD: 18.3

REFERENCES

Adiwidjaja G (1972) Strukturbeziehungen in der Natrolithgruppe und das Entwässerungsverhalten des Skolezits. Diss. Univ. Hamburg

Akizuki M (1981a) Origin of optical variation in analcime. Am Mineral 66:403-409

Akizuki M (1981b) Origin of optical variation in chabazite. Lithos 14:17-21

Akizuki M (1985) The origin of sector twinning in harmotome. Am Mineral 70:822-828

Akizuki M (1986) Al-Si ordering and twinning in edingtonite. Am Mineral 71:1510-1514

Akizuki M (1987a) An explanation of optical variation in yugawaralite. Mineral Mag 51:615-620

Akizuki M (1987b) Crystal symmetry and order-disorder structure of brewsterite. Am Mineral 72:645-648

Akizuki M, Harada, K (1988) Symmetry, twinning, and parallel growth of scolecite, mesolite, and natrolite. Am Mineral 73:613-618

Akizuki M, Konno H (1985) Order-disorder structure and the internal texture of stilbite. Am Mineral 70:814-821

Akizuki M, Nishido H (1988) Epistilbite: Symmetry and twinning. Am Mineral 73:1434-1439

Akizuki M, Kudoh Y, Satoh Y (1993) Crystal structure of the orthorhombic {001} growth sector of stilbite. Eur J Mineral 5:839-843

Akizuki M, Kudoh Y, Kuribayashi T (1996) Crystal structures of the {011}, {610}, and {010} growth sectors in brewsterite. Am Mineral 81:1501-1506

Akizuki M, Kudoh Y, Nakamura S (1999) Growth texture and symmetry of heulandite-Ca from Poona, India. Can Mineral 37:1307-1312

Alberti A (1972) On the crystal structure of the zeolite heulandite. Tschermaks mineral petrogr Mitt 18:129-146

Alberti A (1973) The structure type of heulandite B (heat-collapsed phase). Tschermaks mineral petrogr Mitt 19:173-184

Alberti A (1975a) Sodium-rich dachiardite from Alpe di Siusi, Italy. Contrib Mineral Petrol 49:63-66

Alberti A (1975b) The crystal structures of two clinoptilolites. Tschermaks mineral petrogr Mitt 22:25-37

Alberti A (1979) Possible 4-connected frameworks with 4-4-1 unit found in heulandite, stilbite, brewsterite, and scapolite. Am Mineral 64:1188-1198

Alberti A (1986) The absence of T-O-T angles of 180° in zeolites. *In* New Developments in Zeolite Science Technology. Proc 7th Int'l Zeolite Conf. Murakami Y, Iijima A, Ward JW (eds) p 437-441

Alberti A (1991) Crystal chemistry of Si-Al distribution in natural zeolites. *In* Chemistry of Microporous Crystals. Proc Int'l Symp on Chemistry of Microporous Crystals, Tokyo; Kodansha Ltd, p 107-122

Alberti A (1995) Crystal structure and chemistry of newly discovered zeolites and dehydration of known zeolites: A review. *In* Natural Zeolites '93 Occurrence, Properties, Use. D.W. Ming FA. Mumpton (eds) Int'l Comm on Natural Zeolites; Brockport, NY, p 159-171

Alberti A (1997) Location of Brønsted sites in mordenite. Zeolites 19:411-415

Alberti A, Gottardi G (1975) Possible structures in fibrous zeolites. N Jahrb Mineral Mh 1975:396-411

Alberti A, Sabelli C (1987) Statistical and true symmetry of ferrierite: Possible absence of straight T-O-T bridging bonds. Z Kristallogr 178:249-256

Alberti A, Vezzalini G (1978) Crystal structures of heat-collapsed phases of barrerite. *In* Natural Zeolites, Occurrence, Properties, Use. Sand LB, Mumpton FA (eds) Pergamon Press, Oxford, p 85-98

Alberti A, Vezzalini G (1979) The crystal structure of amicite, a zeolite. Acta Crystallogr B35:2866-2869

Alberti A, Vezzalini G (1981a) A partially disordered natrolite: Relationships between cell parameters and Si-Al distribution. Acta Crystallogr B37:781-788

Alberti A, Vezzalini G (1981b) Crystal energies and coordination of ions in partly occupied sites: Dehydrated mazzite. Bull Minéral 104:5-9

Alberti A, Vezzalini G (1983) The thermal behaviour of heulandites: A structural study of the dehydration of Nadap heulandite. Tschermaks mineral petrogr Mitt 31:259-270

Alberti, A, Vezzalini G, Tazzoli V (1981) Thomsonite: a detailed refinement with cross checking crystal energy calculations. Zeolites 1:91-97

Alberti A, Galli E, Vezzalini G, Passaglia E, Zanazzi PF (1982) Positions of cations and water molecules in hydrated chabazite. Natural and Na-, Ca-, Sr-, and K-exchanged chabazite. Zeolites 2:303-309

Alberti A, Galli E, Vezzalini G (1985) Epistilbite: An acentric zeolite with domain structure. Z Kristallogr 173:257-265

Alberti A, Davoli P, Vezzalini G (1986) The crystal structure refinement of natural mordenite. Z Kristallogr 175:249-256

Alberti A, Gottardi G, Lai T (1990) The determination of (Si,Al) distribution in zeolites. *In* Guidelines for Mastering the Properties of Molecular Sieves. D. Barthomeuf (ed) Plenum, New York, p 145-155

Alberti A, Quartieri S, Vezzalini G (1994) Structural modifications induced by dehydration in yugawaralite. *In* Zeolites and Related Microporous Materials. State of the Art 1994. Weitkamp J, Karge HG, Pfeifer H, Höldrich W (eds) Studies in Surface Science and Catalysis 84:637-644

Alberti A, Cruciani G, Dauru I (1995) Order-disorder in natrolite-group minerals. Eur J Mineral 7:501-508

Alberti A, Cruciani G, Galli E, Vezzalini G (1996a) A reexamination of the crystal structure of the zeolite offretite. Zeolites 17:457-461

Alberti A, Vezzalini G, Galli E, Quartieri S (1996b) The crystal structure of gottardiite, a natural zeolite. Eur J Mineral 8:69-75

Alberti A, Martucci A, Galli E, Vezzalini G (1997) A reexamination of the crystal structure of erionite. Zeolites 19:349-352

Alberti A, Sacerdoti M, Quartieri, S, Vezzalini G (1999) Heating-induced phase transformation in zeolite brewsterite: new 4- and 5-coordinated (Si,Al) sites. Phys Chem Minerals 26:181-186

Andersson S, Fälth L (1983) An alternative description of the paulingite structure. J Solid State Chem 46:265-268

Aoki M, Minato H (1980) Lattice constants of wairakite as a function of chemical composition. Am Mineral 65:1212-1216

Armbruster T (1993) Dehydration mechanism of clinoptilolite and heulandite: Single crystal X-ray study of Na-poor, Ca-, K-, Mg-rich clinoptilolite at 100 K. Am Mineral 78:260-264

Armbruster T, Gunter ME (1991) Stepwise dehydration of a heulandite-clinoptilolite from Succor Creek, Oregon, U.S.A.: A single crystal X-ray study at 100 K. Am Mineral 76:1872-1883

Armbruster T, Kohler T (1992) Re- and dehydration of laumontite: a single crystal X-ray study at 100 K. N Jahrb Mineral Mh 1992:385-397

Armbruster T, Yang P, Liebich BW (1996) Mechanism of the SiO_4 for CO_3 substitution in defernite, $Ca_6(CO_3)_{1.58}(Si_2O_7)_{0.21}(OH)_7[Cl_{0.5}(OH)_{0.08}(H_2O)_{0.42}]$: A single-crystal X-ray study at 100 K. Am Mineral 81:625-631

Artioli G (1992) The crystal structure of garronite. Am Mineral 77:189-196

Artioli G, Foy H (1994) Gobbinsite from Magheramorne Quarry, Northern Ireland. Mineral Mag 58: 615-620

Artioli G, Galli E (1999) Gonnardite: Re-examination of holotype material and discreditation of tetranatrolite. Am Mineral 84:1445-1450

Artioli G, Kvick, Å (1990) Synchrotron X-ray Rietveld study of perlialite, the natural counterpart of synthetic zeolite-L. Eur J Mineral 2:749-759

Artioli G, Ståhl K (1993) Fully hydrated laumontite: A structure study by flat-plate and capillary powder diffraction techniques. Zeolites 13:249-255

Artioli G, Torres Salvador MR (1991) Characterization of the natural zeolite gonnardite. Structure analysis of natural and cation exchanged species by the Rietveld method. Mater Sci Forum 79-81:845-850

Artioli G, Smith JV, Kvick, Å (1984) Neutron diffraction study of natrolite, $Na_2Al_2Si_3O_{10}{\cdot}2H_2O$, at 20 K. Acta Crystallogr C40:1658-1662

Artioli G, Smith JV, Kvick, Å (1985) Multiple hydrogen positions in the zeolite brewsterite, $Sr_{0.95}Ba_{0.5}Al_2Si_6O_{16}{\cdot}5H_2O$. Acta Crystallogr C41:492-497

Artioli G, Smith JV, Pluth JJ (1986a) X-ray structure refinement of mesolite. Acta Crystallogr C42:937-942

Artioli G, Rinaldi R, Kvick, Å, Smith JV (1986b) Neutron diffraction structure refinement of the zeolite gismondine at 15 K. Zeolites 6:361-366

Artioli G, Smith JV, Kvick, Å (1989) Single crystal neutron diffraction study of partially dehydrated laumontite at 15 K. Zeolites 9:377-391

Bakakin VV, Alexeev VI, Seryotkin, YuV, Belitsky IA, Fursenko BA, Balko VP (1994) Crystal chemical surprises of sodium in dehydrated analcime. Abstracts 16th Genl Meeting Int'l Mineral Assoc; Pisa, Italy, p 24-25

Barrer RM, Villiger H (1969) The crystal structure of synthetic zeolite-L. Z Kristallogr 128:352-370

Baturin SV, Malinovskii, YuA, Runova IB (1985) Kristallicheskaya struktura nizkokremnezemistogo merlinoita s Kol'skogo poluostrova (translated title: Crystalline structure of the low-silica merlinoite from the Kola Peninsula). Mineralog Zhur 7;6:67-74

Bauer T, Baur WH (1998) Structural changes in the natural zeolite gismondine (GIS) induced by cation exchange with Ag, Cs, Ba, Li, Na, K and Rb. Eur J Mineral 10:133-147

Baur WH (1964) On the cation and water positions in faujasite. Am Mineral 49:697-704

Baur WH, Joswig W (1996) The phases of natrolite occurring during dehydration and rehydration studied by single crystal X-ray diffraction methods between room temperature and 923 K. N Jahrb Mineral Mh 1996:171-187

Baur WH, Kassner D, Kim CH, Sieber NHW (1990) Flexibility and distortion of the framework of natrolite: Crystal structures of ion-exchanged natrolites. Eur J Mineral 2:761-769

Baur WH, Joswig W, Fursenko BA, Belitsky IA (1997) Symmetry reduction of the aluminosilicate framework of LAU topology by ordering of exchangeable cations: The crystal structure of primary leonhardite with a primitive Bravais lattice. Eur J Mineral 9:1173-1182

Barrer RM, Villiger H (1969) The crystal structure of synthetic zeolite-L. Z Kristallogr 128:352-370

Bazhan IS, Kholdeev OV, Fursenko BA (1999) Phase transformations in scolecite at high hydrostatic pressures. Dokl Akad Nauk 364:97-100

Beger RM (1969) The crystal structure and chemical composition of pollucite. Z Kristallogr 129:280-302

Belitsky IA, Gabuda SP, Joswig W, Fuess H (1986) Study of the structure and dynamics of water in zeolite edingtonite at low temperature by neutron diffraction and NMR-spectroscopy. N Jahrb Mineral Mh 1986:541-551

Belitsky IA, Fursenko BA, Gabuda SP, Kholdeev OV, Seryotkin, YuV (1992) Structural transformations in natrolite and edingtonite. Phys Chem Minerals 18:497-505

Belokoneva EL, Maksimov BA, Verin IA, Sirota MI, Voloshin AV, Pakhomovskii, Ya. A (1985) Crystal structure of iron chabazite at 293 and 570 K and comparison with structures of other natural chabazites. Sov Phys Crystallogr 30:507-510

Bergerhoff G, Baur WH, Nowacki W (1958) Über die Kristallstrukturen des Faujasits. N Jahrb Mineral Mh 1958:193-200

Bieniok A (1997) The dehydration of the zeolite paulingite. N Jahrb Mineral Mh 1997:498-504

Bieniok A, Joswig W, Baur WH (1996) A study of paulingites: Pore filling by cations and water molecules. N Jahrb Mineral Abh 171:119-134

Bish DL (1988) Effects of composition on the dehydration behavior of clinoptilolite and heulandite. *In* Occurrence, Properties and Utilization of Natural Zeolites. D. Kallo HS. Sherry (eds) Akademiai Kiado, Budapest, p 565-576

Bissert G, Liebau F (1986) The crystal structure of a triclinic bikitaite, $Li(AlSi_2O_6)\cdot H_2O$, with ordered Al/Si distribution. N Jahrb Mineral Mh 1986:241-252

Blum JR (1843) Leonhardit, ein N Mineral. Poggendorff Annalen der Physik Chemie 59:336-339

Boggs RC, Howard DG, Smith JV, Klein GL (1993) Tschernichite, a new zeolite from Goble, Columbia County, Oregon. Am Mineral 78:822-826

Bondi M, Griffin WL, Mattioli V, Mottana A (1983) Chiavennite, $CaMnBe_2Si_5O_{13}(OH)_2\cdot 2H_2O$, a new mineral from Chiavenna (Italy). Am Mineral 68:623-627

Breck DW (1974) Zeolite Molecular Sieves. John Wiley and Sons, New York, 771 p

Bresciani-Pahor N, Calligaris M, Nardin G, Randaccio L, Russo E, Comin-Chiaramonti P (1980) Crystal structure of a natural and a partially silver-exchanged heulandite. J Chem Soc Dalton Trans 1980:1511-1514

Brown ID (1992) Chemical and steric constraints in inorganic solids. Acta Crystallogr B48:553-572

Butikova IK, Shepelev, YuF, Smolin, YuI (1993) Structure of hydrated and dehydrated (250°C) forms of Ca-chabazite. Crystallogr Rep 38:461-463

Cabella R, Lucchetti G, Palenzona A, Quartieri S, Vezzalini G, (1993) First occurrence of a Ba-dominant brewsterite: Structural features. Eur J Mineral 15:353-360

Cappelletti P, Langella A, Cruciani G (1999) Crystal-chemistry and synchrotron Rietveld refinement of two different clinoptilolites from volcanoclastics of North-Western Sardiania. Eur J Mineral 11:1051-1060

Chao GY (1980) Paranatrolite, a new zeolite from Mount St-Hilaire, Québec. Can Mineral 18:85-88

Chen TT, Chao GY (1980) Tetranatrolite from Mount St-Hilaire, Québec. Can Mineral 18:77-84

Coombs DS (1952) Cell size, optical properties and chemical composition of laumontite and leonhardite. Am Mineral 37:812-830

Coombs DS (1955) X-ray observations of wairakite and non-cubic analcime. Mineral Mag 30:699-708

Coombs DS, Alberti A, Armbruster T, Artioli G, Colella C, Galli E, Grice JD, Liebau F, Mandarino JA, Minato H, Nickel EH, Passaglia E, Peacor DR, Quartieri S, Rinaldi R, Ross M, Sheppard RA, Tillmanns E, Vezzalini G (1998) Recommended nomenclature for zeolite minerals: Report of the subcommittee on zeolites of the International Mineralogical Association, Commission on New Minerals and Mineral Names. Am Mineral Special Feature, 28 p (a corresponding PDF file may be downloaded from the internet: http://www.minsocam.org/ MSA/AmMin/AmMineral.html)

Corbin DR, Abrams L, Jones GA, Harlow RL, Dunn PJ (1991) Flexibility of the zeolite rho framework: Effect of dehydration on the crystal structure of the beryllophosphate mineral, pahasapaite. Zeolites 11:364-367

Cruciani G, Gualtieri A (1999) Dehydration dynamics of analcime by *in situ* synchrotron powder diffraction. Am Mineral 84:112-119

Cruciani G, Artioli G, Gualtieri A, Ståhl K, Hanson JC (1997) Dehydration dynamics of stilbite using synchrotron X-ray powder diffraction. Am Mineral 82:729-739

Delffs W (1843) Analyse des Leonhardits. Poggendorff Annalen Phys Chem 59:339-342

Di Renzo F, Gabelica Z (1995) New data on the structure and composition of the silicoaluminophosphate viséite and discreditation of its status as a zeolite. *In* Natural Zeolites '93 Occurrence, Properties, Use; DW Ming, FA Mumpton (eds) Int'l Comm on Natural Zeolites, Brockport, NY, p 173-185

Dove MT, Cool T, Palmer DC, Putnis A, Salje EK.H, Winkler B (1993) On the role of Al-Si ordering in the cubic-tetragonal phase transition of leucite. Am Mineral 78:486-492

Eberlein GD, Erd RC, Weber F, Beatty LB (1971) New occurrence of yugawaralite from the Chena hot springs area, Alaska. Am Mineral 56:1699-1717

Effenberger H, Giester G, Krause W, Bernhardt H-J (1998) Tschörtnerite, a copper-bearing zeolite from the Bellberg volcano, Eifel, Germany. Am Mineral 83:607-617

Elsen J, King GSD, Mortier WJ (1987) Influence of temperature on the cation distribution in calcium mordenite. J Phys Chem 91:5800-5805

Engel N, Yvon K (1984) The crystal structure of parthéite. Z Kristallogr 169:165-175

Engelhardt G, Michel D (1987) High-Resolution Solid-State NMR of Silicates and Zeolites. John Wiley & Sons, Chichester, UK, 485 p

Ercit TS, Velthuizen J van (1994) Gaultite, a new zeolite-like mineral species from Mont Saint-Hilaire, Québec, and its crystal structure. Can Mineral 32:855-863

Evans HT, Jr (1973) The crystal structures of cavansite and pentagonite. Am Mineral 58:412-424

Ferraris G, Jones DW, Yerkess J (1972) A neutron-diffraction study of the crystal structure of analcime, $NaAlSi_2O_6 \cdot H_2O$. Z Kristallogr 135:240-252

Fersman AE (1909) Etudes sur les zeolites de la Russie. I. Leonhardite et laumontite dans les environs de Simferopolis (Crimee). Trav Musée Géol Pierre le Grand Acad Imp Sci St Pétersbourg 2:103-150 [Extended abstract (in German) N Jahrb Mineral Geol Paläontol (1912) 1:405-408]

Fischer K (1966) Untersuchung der Kristallstruktur von Gmelinit. N Jahrb Mineral Mh 1966:1-13

Fischer KF, Schramm V (1971) Crystal structure of gismondite, a detailed refinement. Adv Chem Ser 101:250-258

Foster MF (1965) Compositional relations among thomsonites, gonnardites, and natrolites. U S Geol Surv Prof Paper 504-D:E1-E10

Gabuda SP, Kozlova SG (1995) Guest-guest interaction and phase transitions in the natural zeolite laumontite. J Inclusion Phenom Mol Recogn Chem 22:1-13

Gabuda SP, Kozlova SG (1997) Anomalous mobility of molecules, structure of the guest sublattice, and transformation of tetra- to paranatrolite. J Struct Chem—Engl tr 38:562-569

Galli E (1971) Refinement of the crystal structure of stilbite. Acta Crystallogr B27:833-841

Galli E (1975) Crystal structure refinement of mazzite. Rendiconti Soc Ital Mineral Petrol 31:599-612

Galli E (1976) Crystal structure refinement of edingtonite. Acta Crystallogr B32:1623-1627

Galli E, Alberti A (1975a) The crystal structure of stellerite. Bull Soc fr Minéral Cristallogr 98:11-18

Galli E, Alberti A (1975b) The crystal structure of barrerite. Bull Soc fr Minéral Cristallogr 98:331-342

Galli E, Gottardi G (1966) The crystal structure of stilbite. Mineralog Petrogr Acta (Bologna) 12:1-10

Galli E, Gottardi G, Pongiluppi D (1979) The crystal structure of the zeolite merlinoite. N Jahrb Mineral Mh 1979:1-9

Galli E, Passaglia E, Zanazzi PF (1982) Gmelinite: Structural refinements of sodium-rich and calcium-rich natural crystals. N Jahrb Mineral Mh 1982:145-155

Galli E, Quartieri S, Vezzalini G, Alberti A (1995) Boggsite and tschernichite-type zeolites from Mt. Adamson, Northern Victoria Land (Antarctica). Eur J Mineral 7:1029-1032

Galli E, Quartieri S, Vezzalini G, Alberti A (1996) Gottardiite, a new high-silica zeolite from Antarctica: the natural counterpart of synthetic NU-87. Eur J Mineral 8:687-693

Galli E, Quartieri S, Vezzalini G, Alberti A, Franzini M (1997a) Terranovaite from Antarctica: A new 'pentasil' zeolite. Am Mineral 82:423-429

Galli E, Vezzalini G, Quartieri S, Alberti A, Franzini M (1997b) Mutinaite, a new zeolite from Antartica: The natural counterpart of ZSM-5. Zeolites 19:318-322

Gard JA, Tait JM (1972) The crystal structure of the zeolite offretite, $K_{1.1}Ca_{1.1}Mg_{0.7}[Si_{12.8}Al_{5.2}O_{36}]\cdot 15.2H_2O$. Acta Crystallogr B28:825-834

Gellens LR, Price GD, Smith JV (1982) The structural relation between svetlozarite and dachiardite. Mineral Mag 45:157-161

Gibbs GV (1982) Molecules as models for bonding in silicates. Am Mineral 67:421-450

Gies H (1985) Clathrate mit SiO_2 Wirtstrukturen: Clathrasile. Nachr Chem Techn Lab 33:387-392

Giuseppetti G, Mazzi F, Tadini C, Galli E (1991) The revised crystal structure of roggianite: $Ca_2[Be(OH)_2Al_2Si_4O_{13}]\cdot<2.5H_2O$. N Jahrb Mineral Mh 1991:307-314

Gordon EK, Samson S, Kamb WB (1966) Crystal structure of the zeolite paulingite. Science 154: 1004-1007

Gottardi G, Galli E (1985) Natural Zeolites. Springer-Verlag, Berlin, 409 p

Gottardi G, Meier WM (1963) The crystal structure of dachiardite. Z Kristallogr 119:53-64

Gramlich-Meier R (1981) Strukturparameter in Zeolithen der Mordenitfamilie. Diss Nr 6760, Eidgen Techn Hochschule Zürich

Gramlich-Meier R, Meier WM, Smith BK (1984) On faults in the framework structure of the zeolite ferrierite. Z Kristallogr 169:201-210

Gramlich-Meier R, Gramlich V, Meier WM (1985) The crystal structure of the monoclinic variety of ferrierite. Am Mineral 70:619-623

Grögel T, Boysen H, Frey F (1984) Phase transition and ordering in leucite. Collected Abstracts, 13th Int'l Conf of Crystallography, Acta Crystallogr A40 Suppl:C256-C257

Gualtieri A, Artioli G, Passaglia E, Bigi S, Viani A, Hanson JC (1998) Crystal structure – crystal chemistry relationships in the zeolites erionite and offretite. Am Mineral 83:590-606

Gualtieri AF, Passaglia E, Galli E, Viani A (1999a) Rietveld structure refinement of Sr-exchanged phillipsite. Microporous Mesoporous Mater 31:33-43

Gualtieri AF, Caputo D, Colella C (1999b) Ion exchange selectivity of phillipsite for Cs^+: A structural investigation using the Rietveld method. Microporous Mesoporous Mater 32:319-322

Gunter ME, Armbruster T, Kohler T, Knowles CR (1994) Crystal structure and optical properties of Na- and Pb-exchanged heulandite-group zeolites. Am Mineral 79:675-682

Hakanson U, Fälth L, Hansen S (1990) Structure of a high-silica variety of zeolite Na-P2. Acta Crystallogr C46:1363-1364

Hambley TW, Taylor JC (1984) Neutron diffraction studies on natural heulandite and partially dehydrated heulandite. J Solid State Chem 54:1-9

Hazen RM, Finger LW (1979) Polyhedral tilting:A common type of pure displacive phase transition and its relationship to analcite at high pressure. Phase Transitions 1:1-22

Hey M (1930) Studies on zeolites: Part I. General review. Mineral Mag 22:422-437

Hori H, Nagashima K, Yamada M, Miyawaki R, Marubashi T (1986) Ammonioleucite, a new mineral from Tatarazawa, Fujioka, Japan. Am Mineral 71:1022-1027

Howard DG (1994) Crystal habit and twinning of garronite from Fara Vicentina, Vicenza (Italy). N Jahrb Mineral Mh 1994:91-96

Joswig W, Baur WH (1995) The extreme collapse of a framework of NAT topology: the crystal structure of metanatrolite (dehydrated natrolite) at 548 K. N Jahrb Mineral Mh 1995:26-38

Joswig W, Bartl H, Fuess H (1984) Structure refinement of scolecite by neutron diffraction. Z Kristallogr 166:219-223

Kato M, Hattori T (1998) Ordered distribution of aluminum atoms in analcime. Phys Chem Minerals 25:556-565

Kawahara A, Curien H (1969) La structure cristalline de l'érionite. Bull Soc fr Minéral Cristallogr 92:250-256

Kerr IS (1964) Structure of epistilbite. Nature 202:589

Kerr IS, Williams DJ (1967) The crystal structure of yugawaralite. Z Kristallogr 125:220-225

Kerr IS, Williams DJ (1969) The crystal structure of yugawaralite. Acta Crystallogr B25:1183-1190

Khomyakov AP, Semenov EI, Bykova AV, Voronkov AA, Smol'yaninova NN (1975) New data on lovdarite. Dokl Akad Nauk SSSR 221:154-157

Kirkpatrick RJ (1988) MAS NMR spectroscopy of minerals and glasses. Rev Mineral 18:341-403

Kocman V, Gait RI, Rucklidge J (1974) The crystal structure of bikitaite, $Li[AlSi_2O_6]\cdot H_2O$. Am Mineral 59:71-78

Kokotailo GT, Lawton SL, Olson DH, Meier WM (1978) Structure of synthetic zeolite ZSM-5. Nature 272:437-438

Koningsveld, van H (1992) Structural relationships and building units in the family of 5-ring zeolites. Zeolites 12:114-120

Korekawa M (1969) Über die Verzwillingung des Leucits. Z Kristallogr 129:343-350

Koyama K, Takéuchi Y (1977) Clinoptilolite: The distribution of potassium atoms and its role in thermal stability. Z Kristallogr 145:216-239

Krogh Andersen E, Krogh Andersen IG, Ploug-Sorensen G (1990) Disorder in natrolites: structure determinations of three disordered natrolites and one lithium-exchanged disordered natrolite. Eur J Mineral 2:799-807

Kuntzinger S, Ghermani NE, Dusausoy Y, Lecomte C (1998) Distribution and topology of the electron density in an aluminosilicate compound from high-resolution X-ray diffraction data: The case of scolecite. Acta Crystallogr B54:819-833

Kunz M, Armbruster T (1990) Difference displacement parameters in alkali feldspars: Effects of (Si,Al) order-disorder. Am Mineral 75:141-149

Kvick, Å, Smith JV (1983) Neutron diffraction study of the zeolite edingtonite. J Chem Phys 79:2356-2362

Kvick, Å, Ståhl K, Smith JV (1985) A neutron diffraction study of the bonding of zeolitic water in scolecite at 20 K. Z Kristallogr 171:141-154

Kvick, Å, Artioli G, Smith JV (1986) Neutron diffraction study of the zeolite yugawaralite at 13 K. Z Kristallogr 174:265-281

Larsen AO, Åsheim A, Raade G, Taftø J (1992) Tvedalite, $(Ca,Mn)_4Be_3Si_6O_{17}(OH)_4 \cdot 3H_2O$, a new mineral from syenite pegmatite in the Oslo Region, Norway. Am Mineral 77:438-443

Leimer HW, Slaughter M (1969) The determination and refinement of the crystal structure of yugawaralite. Z Kristallogr 130:88-111

Lengauer CL, Giester G, Tillmanns E (1997) Mineralogical characterization of paulingite from Vinarická Hora, Czech Republic. Mineral Mag 61:591-606

Liou JG (1970) Synthesis and stability relations of wairakite, $CaAl_2Si_4O_{12} \cdot 2H_2O$. Contrib Mineral Petrol 27:259-282

Loewenstein W (1954) The distribution of aluminum in the tetrahedra of silicates and aluminates. Am Mineral 39:92-96

Maleev MN (1976) Svetlozarite, a new high-silica zeolite (in Russian). Zap Vse Miner Obshchest 105:449-453

Malinovskii, YuA (1984) The crystal structure of K-gmelinite. Sov Phys Crystallogr 29:256-258

Malinovskii, YuA, Belov NV (1980) Crystal structure of kalborsite. Dokl Akad Nauk SSSR 252:611-615

Malinovskii, YuA, Burzlaff H, Rothammel W (1998) Method of quantitative crystallochemical comparison of structures. Comparative studies of fibrous zeolites of the natrolite group. Crystallogr Rep 43: 241-255

Marchi M, Artioli G, Gualtieri A, Hanson JC (1998) The dehydration process in garronite: an *in situ* synchrotron XRPD study. Proc IV Convegno Nazionale Scienza e Tecnologia delle Zeoliti, Cernobbio (Como), Italy, p 143-148

Mazzi F, Galli E (1978) Is each analcime different? Am Mineral 63:448-460

Mazzi F, Galli E (1983) The tetrahedral framework of chabazite. N Jahrb Mineral Mh 1983:461-480

Mazzi F, Galli E, Gottardi G (1976) The crystal structure of tetragonal leucite. Am Mineral 61:108-115

Mazzi F, Galli E, Gottardi G (1984) Crystal structure refinement of two tetragonal edingtonites. N Jahrb Mineral Mh 1984:372-382

Mazzi F, Larsen AO, Gottardi G, Galli E (1986) Gonnardite has the tetrahedral framework of natrolite: Experimental proof with a sample from Norway. N Jahrb Mineral Mh 1986:219-228

McCusker LB, Baerlocher C, Nawaz R (1985) Rietveld refinement of the crystal structure of the new zeolite mineral gobbinsite. Z Kristallogr 171:281-289

Meier R, Ha TK (1980) A theoretical study of the electronic structure of disiloxane $[(SiH_3)_2O]$ and its relation to silicates. Phys Chem Minerals 6:37-46

Meier WM (1961) The crystal structure of mordenite (ptilolite). Z Kristallogr 115:439-450

Meier WM (1978) Constituent sheets in the zeolite frameworks of the mordenite group. *In* Natural Zeolites, Occurrence, Properties, Use. Sand LB, Mumpton FA (eds) Pergamon Press, Oxford, p 99-103

Meier WM, Groner M (1981) Zeolite structure type EAB: Crystal structure and mechanism for the topotactic transformation of the Na, TMA form. J Solid State Chem 37:204-218

Meier R, Ha TK (1980) A theoretical study of the electronic structure of disiloxane $[(SiH_3)_2O]$ and its relation to silicates. Phys Chem Minerals 6:37-46

Meier WM, Meier R, Gramlich V (1978) Mordenite: Interpretation of a superimposed structure. Z Kriatallogr 147:329

Meier WM, Olson DH, Baerlocher C (1996) Atlas of Zeolite Structure Types. 4th revised edn. Zeolites 17:1-230 (http://www.iza.ethz.ch/IZA-SC/Atlas/AtlasHome.html)

Meneghinello E, Martucci A, Alberti A, Di Renzo F (1999) Structural refinement of a K-rich natrolite: evidence of a new extraframework cation site. Microporous Mesoporous Mater 30:89-94

Men'schikov, YuP, Denisov AP, Uspenskaya YI, Lipatova EA (1973) Lovdarite, a new hydrous alkali-beryllium silicate. Dokl Akad Nauk SSSR 213:130-133

Merkle AB, Slaughter M (1968) Determination and refinement of the structure of heulandite. Am Mineral 53:1120-1138

Merlino S (1965) Struttura dell' epistilbite. Atti Soc Toscana Sci Nat A72:480-483

Merlino S (1990) Lovdarite, $K_4Na_{12}(Be_8Si_{28}O_{72})\cdot 18H_2O$, a zeolite-like mineral: Structural features and OD character. Eur J Mineral 2:809-817

Merlino S, Galli E, Alberti A (1975) The crystal structure of levyne. Tschermaks mineral petrogr Mitt 22:117-129

Mikheeva MG, Pushcharovskii DY, Khomyakov AP, Yamnova NA (1986) Crystal structure of tetranatrolite. Sov Phys Crystallogr 31:254-257

Milazzo E, Artioli G, Gualtieri A, Hanson JC (1998) The dehydration process in gismondine: An *in situ* synchrotron XRPD study. Proc IV Convegno Nazionale Scienza e Tecnologia delle Zeoliti, Cernobbio (Como), Italy, p 160-165

Miller SA, Taylor JC (1985) Neutron single-crystal diffraction study of an Australian stellerite. Zeolites 5:7-10

Millward GR, Thomas JM, Terasaki O, Watanabe D (1986) Direct imaging and characterization of intergrowth-defects in erionite. Zeolites 6:91-95

Moroz NK, Seryotkin YV, Afanasiev IS, Belitzky I.A (1998) Arrangement of extraframework cations in NH_4-analcime. J Struct Chem—Engl tr 39:281-283

Mortier WJ, Pluth JJ, Smith JV (1976a) The crystal structure of dehydrated natural offretite with stacking faults of erionite type. Z Kristallogr 143:319-332

Mortier WJ, Pluth JJ, Smith JV (1976b) Crystal structure of natural zeolite offretite after carbon monoxide adsorption. Z Kristallogr 144:32-41

Mortier WJ, Pluth JJ, Smith. J.V (1978) Positions of cations and molecules in zeolites with the mordenite type framework. IV. De-hydrated and re-hydrated K-exchanged "ptilolite." *In* Natural Zeolites, Occurrence, Properties, Use. Sand LB, Mumpton FA (eds) Pergamon Press, Oxford, p 53-63

Nawaz R (1983) New data on gobbinsite and garronite. Mineral Mag 47:567-568

Nawaz R, Malone JF (1982) Gobbinsite, a new zeolite mineral from Co. Antrim N Ireland. Mineral Mag 46:365-369

Palmer DC, Putnis A, Salje EKH (1988) Twinning in tetragonal leucite. Phys Chem Minerals 16:298-303

Palmer DC, Salje EKH, Schmahl WW (1989) Phase transitions in leucite: X-ray diffraction studies. Phys Chem Minerals 16:714-719

Parise JB, Corbin DR, Abrams L, Northrup P, Rakovan J, Nenoff TM, Stucky GD (1994) Structural relationships among some BePO-, BeAsO, and AlSiO-rho frameworks. Zeolites 14:25-34

Passaglia E, Sacerdoti M (1982) Crystal structure of Na-exchanged stellerite. Bull Minéral 105:338-342

Passaglia E, Tagliavini A (1994) Chabazite-offretite epitaxial overgrowths in cornubianite from Passo Forcel Rosso, Adamello, Italy. Eur J Mineral 6:397-405

Passaglia E, Vezzalini G (1988) Roggianite: Revised chemical formula and zeolitic properties. Mineral Mag 52:201-206

Passaglia E, Artioli G, Gualtieri A, Carnevali R (1995). Diagenetic mordenite from Ponza, Italy. Eur J Mineral 7:429-438

Pauling L (1930) The structure of some sodium and calcium aluminosilicates. Proc Nat Acad Sci USA 16:453-459

Pauling L (1939) The Nature of the Chemical Bond and the Structure of Molecules and Crystals. Cornell University Press, Ithaca, New York, 420 p

Peacor DR (1968) A high temperature single crystal diffractometer study of leucite $(K,Na)AlSi_2O_6$. Z Kristallogr 127:213-224

Peacor DR (1973) High-temperature, single-crystal X-ray study of natrolite. Am Mineral 58:676-680

Peacor DR, Rouse RC (1988) Holdawayite, $Mn_6(CO_3)_2(OH)_7(Cl,OH)$, a structure containing anions in zeolite-like channels. Am Mineral 73:637-642

Peacor DR, Dunn PJ, Simmons WB, Tillmanns E, Fischer RX (1984) Willhendersonite, a new zeolite isostructural with chabazite. Am Mineral 69:186-189

Peacor DR, Dunn PJ, Simmons WB, Wicks FJ, Raudsepp M (1988) Maricopaite, a new hydrated Ca-Pb zeolite-like silicate from Arizona. Can Mineral 26:309-313

Perrotta AJ (1967) The crystal structure of epistilbite. Mineral Mag 36:480-490

Perrotta AJ, Smith JV (1964) The crystal of brewsterite, $(Sr,Ba,Ca)(Al_2Si_6O_{16})\cdot 5H_2O$. Acta Crystallogr 17:857-862

Phillips BL, Kirkpatrick RJ (1994) Short-range Si-Al order in leucite and analcime: Determination of the configurational entropy from ^{27}Al and variable-temperature ^{29}Si NMR spectroscopy of leucite, its Cs- and Rb-exchanged derivatives and analcime. Am Mineral 79:1025-1031

Pipping F (1966) The dehydration and chemical composition of laumontite. Mineralogical Soc India, Int'l Mineral Assoc Volume, p 159-166

Pluth JJ, Smith JV (1990) Crystal structure of boggsite, a new high-silica zeolite with the first three-dimensional channel system bounded by both 12- and 10-rings. Am Mineral 75:501-507

Quartieri S, Vezzalini G, (1987) Crystal chemistry of stilbites: Structure refinements of one normal and four chemically anomalous samples. Zeolites 7:163-170

Quartieri S, Vezzalini G, Alberti A (1990) Dachiardite from Hokiya-dake: Evidence of a new topology. Eur J Mineral 2:187-193

Quartieri S, Sani A, Vezzalini G, Galli E, Fois E, Gamba A, Tabacchi G (1999) One-dimensional ice in bikitaite: Single-crystal X-ray diffraction, infra-red spectroscopy and ab-initio molecular dynamics studies. Microporous Mesoporous Mater 30:77-87

Raade G, Åmli R, Mladeck MH, Din VK, Larsen AO, Åsheim A (1983) Chiavennite from syenite pegmatites in the Oslo Region, Norway. Am Mineral 68:628-633

Rastsvetaeva RK, Rekhlova OYu, Andrianov VI, Malinovskii, YuA (1991) Crystal structure of hsyanghualite (in Russian). Dokl Akad Nauk SSSR 316:624-628

Reeuwijk LP. van (1971) The dehydration of gismondite. Am Mineral 56:1655-1659

Rinaldi R (1976) Crystal chemistry and structural epitaxy of offretite-erionite from Sasbach, Kaiserstuhl. N Jahrb Mineral Mh 1976:145-156

Rinaldi R, Vezzalini G (1985) Gismondine: Detailed X-ray structure refinement of two natural samples. *In* Zeolites. Drzaj, Hocevar, Pejovnik (eds) Elsevier, Amsterdam, p 481-491

Rinaldi R, Pluth JJ, Smith JV (1974) Zeolites of the phillipsite family. Refinement of the crystal structures of phillipsite and harmotome. Acta Crystallogr B30:2426-2433

Rinaldi R, Pluth JJ, Smith JV (1975a) Crystal structure of cavansite dehydrated at 220°C. Acta Crystallogr B31:1598-1602

Rinaldi R, Pluth JJ, Smith JV (1975b) Crystal structure of mazzite dehydrated at 600°C. Acta Crystallogr B31:1603-1608

Ross M, Flohr MJ.K, Ross DR (1992) Crystalline solution series and order-disorder within the natrolite mineral group. Am Mineral 77:685-703

Rouse RC, Peacor DR (1986) Crystal structure of the zeolite mineral goosecreekite, $CaAl_2Si_6O_{16}\cdot 5H_2O$. Am Mineral 71:1494-1501

Rouse RC, Peacor DR (1994) Maricopaite, an unusual lead calcium zeolite with an interrupted mordenite-like framework and intrachannel Pb_4 tetrahedral clusters. Am Mineral 79:175-184

Rouse RC, Peacor DR, Dunn PJ, Campbell TJ, Roberts WL, Wicks FJ, Newbury D (1987) Pahasapaite, a beryllophosphate zeolite related to synthetic zeolite rho, from the Tip Top Pegmatite of South Dakota. N Jahrb Mineral Mh 1987:433-440

Rouse RC, Peacor DR, Merlino S (1989) Crystal structure of pahasapaite, a beryllophosphate mineral with a distorted zeolite rho framework. Am Mineral 74:1195-1202

Rouse RC, Dunn PJ, Grice JD, Schlenker JL, Higgins JB (1990) Montesommaite, $(K,Na)_9(Al_9Si_{23}O_{64})\cdot 10H_2O$, a new zeolite related to merlinoite and the gismondine group. Am Mineral 75:1415-1420

Rüdinger B, Tillmanns E, Hentschel G (1993) Bellbergite—a new mineral with the zeolite structure type EAB. Mineral Petrol 48:147-152

Sacerdoti M (1996) New refinements of the crystal structure of levyne using twinned crystals. N Jahrb Mineral Mh 1996:114-124

Sacerdoti M, Gomedi I (1984) Crystal structural refinement of Ca-exchanged barrerite. Bull Minéral 107:799-804

Sacerdoti M, Passaglia E, Carnevali R (1995) Structural refinements of Na-, K-, and Ca-exchanged gmelinites. Zeolites 15:276-281

Sacerdoti M, Sani A, Vezzalini G (1999) Structural refinement of two barrerites from Alaska. Microporous Mesoporous Mater 30:103-109

Sadanaga R, Marumo F, Takéuchi Y (1961) The crystal structure of harmotome. Acta Crystallogr 14:1153-1163

Sani A, Vezzalini G, Delmotte L, Gabelica Z, Marichal C (1998) ^{29}Si and ^{27}Al MAS NMR study of the natural zeolite barrerite and its dehydrated phases. Proc IV Convegno Nazionale Scienza e Tecnologia delle Zeoliti, Cernobbio (Como), Italy, p 206-207

Sani A, Vezzalini G, Ciambelli P, Rapacciuolo MT (1999) Crystal structure of hydrated and partially NH_4-exchanged heulandite. Microporous Mesoporous Mater 31:263-270

Sato M (1979) Derivation of possible framework structures formed from parallel four- and eight-membered rings. Acta Crystallogr 35A:547-552

Sato M, Gottardi G (1982) The slipping scheme of the double crankshaft structures in tectosilicates and its mineralogical implication. Z Kristallogr 161:187-193

Schlenker JL, Pluth JJ, Smith JV (1977a) Dehydrated natural erionite with stacking faults of the offretite type. Acta Crystallogr B33:3265-3268

Schlenker JL, Pluth JJ, Smith JV (1977b) Refinement of the crystal of brewsterite, $Ba_{0.5}Sr_{1.5}Al_4Si_{12}O_{32}\cdot 10H_2O$. Acta Crystallogr B33:2907-2910

Schlenker JL, Pluth JJ, Smith JV (1978) Positions of cations and molecules in zeolites with the mordenite type framework. VI. De-hydrated barium mordenite. Mater Res Bull 13:169-174

Schröpfer L, Joswig W (1997) Structure analyses of a partially dehydrated synthetic Ca-garronite single crystal under different T, p(H_2O) conditions. Eur J Mineral 9:53-66

Shannon MD, Casci JL, Cox PA, Andrews SJ (1991) Structure of the two-dimensional medium-pore high silica zeolite NU-87. Nature 353:417-420

Shiokawa K, Ito M, Itabashi K (1989) Crystal structure of synthetic mordenites. Zeolites 9:170-176

Slaughter M (1970) Crystal structure of stilbite. Am Mineral 55:387-397

Slaughter M, Kane WT (1969) The crystal structure of a disordered epistilbite. Z Kristallogr 130:68-87

Smith BK (1986) Variations in the framework structure of the zeolite ferrierite. Am Mineral 71:989-998

Smith JV (1978) Enumeration of 4-connected 3-dimensional nets and classification of framework silicates. II. Perpendicular and near-perpendicular linkages from 4.8^2, 3.12^2 and $4.6.^{12}$ nets. Am Mineral 63:960-969

Smith JV (1983) Enumeration of 4-connected 3-dimensional nets and classification of framework silicates: Combination of 4-1 chain and 2D nets. Z Kristallogr 165:191-198

Smith JV (1988) Topochemistry of zeolites and related materials. 1. Topology and geometry. Chem Rev 88:149-182

Smith JV, Bennett JM (1981) Enumeration of 4-connected 3-dimensional nets and classification of framework silicates: the infinite set of ABC-6 nets; the Archimedean and σ–related nets. Am Mineral 66:777-788

Smith JV, Pluth JJ, Boggs RC, Howard DG (1991) Tschernichite, the mineral analogue of zeolite beta. J Chem Soc Chem Commun 1991:363-364

Smyth JR, Spaid AT, Bish DL (1990) Crystal structures of a natural and a Cs-exchanged clinoptilolite. Am Mineral 75:522-528

Solov'eva LP, Borisov SV, Bakakin VV (1972) New skeletal structure in the crystal structure of barium chloroaluminosilicate $BaAlSiO_2(Cl,OH) \Rightarrow Ba_2[X]BaCl_2[(Si,Al)_8O_{16}]$. Sov Phys Crystallogr 16: 1035-1038

Song SG (1999) Crystal defects of mordenite structures. J Mater Res 14:2616-2620

Ståhl K, Artioli G (1993) A neutron powder diffraction study of fully deuterated laumontite. Eur J Mineral 5:851-856

Ståhl K, Hanson JC (1998) An *in situ* study of the edingtonite dehydration process from X-ray synchrotron powder diffraction. Eur J Mineral 10:221-228

Ståhl K, Hanson JC (1999) Multiple cation sites in dehydrated brewsterite. An *in situ* X-ray synchrotron powder diffraction study. Microporous Mesoporous Mater 32:147-158

Ståhl K, Thomasson R (1994) The dehydration and rehydration processes in the natural zeolite mesolite studied by conventional and synchrotron X-ray powder diffraction. Zeolites 14:12-17

Ståhl K, Kvick, Å, Ghose S (1989) One-dimensional water chain in the zeolite bikitaite: Neutron diffraction study at 13 and 295 K. Zeolites 9:303-311

Ståhl K, Kvick, Å, Smith JV (1990) Thomsonite, a neutron diffraction study at 13 K. Acta Crystallogr C46:1370-1373

Ståhl K, Artioli G, Hanson JC (1996) The dehydration process in the zeolite laumontite: A real-time synchrotron X-ray powder diffraction study. Phys Chem Minerals 23:328-336

Stamires DN (1973) Properties of the zeolite, faujasite, substitutional series: A review with new data. Clays & Clay Miner 21:379-389

Stolz J, Armbruster T (1997) X-ray single-crystal structure refinement of Na,K-rich laumontite, originally designated 'primary leonhardite'. N Jahrb Mineral Mh 1997:131-144

Stolz J, Yang P, Armbruster T (2000a) Cd-exchanged heulandite: Symmetry lowering and site preference. Microporous Mesoporous Mater 37:233-242

Stolz J, Armbruster T, Hennessey B (2000b) Site preference of exchanged alkylammonium ions in heulandite: Single-crystal X-ray structure refinements. Z Kristallogr 215:278-287

Stuckenschmidt E, Fuess H, Kvick, Å (1990) Investigation of the structure of harmotome by X-ray (293 K, 100 K) and neutron diffraction (15 K). Eur J Mineral 2:861-874

Stuckenschmidt E, Kassner D, Joswig W, Baur WH (1992) Flexibility and distortion of the collapsible framework of NAT topology: The crystal structure of NH_4-exchanged natrolite. Eur J Mineral 4:1229-1240

Stuckenschmidt E, Joswig W, Baur WH (1996) Flexibility and distortion of the collapsible framework of NAT topology: the crystal structure of H_3O-natrolite. Eur J Mineral 8:85-92

Stuckenschmidt E, Joswig W, Baur WH, Hofmeister W (1997) Scolecite, Part 1: Refinement of high-order data, separation of internal and external vibrational amplitudes from displacement parameters. Phys Chem Minerals 24:403-410

Sugiyama K, Takéuchi Y (1986) Distribution of cations and water molecules in the heulandite-type framework. Stud Surf Sci Catal 28:449-456

Takaishi T (1998) Ordered distribution of Al atoms in the framework of analcimes. J Chem Soc Faraday Trans 94:1507-1518

Takéuchi Y, Mazzi F, Haga N, Galli E (1979) The crystal structure of wairakite. Am Mineral 64:993-1001

Taylor WH, Jackson WW (1933) The structure of edingtonite. Z Kristallogr 86:53-54

Taylor WH, Meek CA, Jackson WW (1933) The structure of fibrous zeolites. Z Kristallogr 84:373-398

Tazzoli V, Domeneghetti MC, Mazzi F, Cannillo E (1995) The crystal structure of chiavennite. Eur J Mineral 7:1339-1344

Teertstra DK, Cerny P (1992) First natural occurrence of end-member pollucite: A product of low-temperature re-equilibration. Eur J Mineral 17:1137-1148

Teertstra DK, Cerny P Chapman R (1992) Compositional heterogeneity of pollucite from high grade dyke, Maskwa Lake, Southeastern Manitoba. Can Mineral 30:687-697

Teertstra DK, Dyer A (1994) The informal discreditation of "doranite" as the magnesium analog of analcime. Zeolites 14:411-413

Teertstra DK, Cerny P, Sherriff BL, Hawthorne FC (1994a) The crystal chemistry, structure and evolution of pollucite. Abstr 16th General Meeting Int'l Mineral Assoc, Pisa, Italy, p 406

Teertstra DK, Sherriff BL, Xu Z, Cerny P (1994b) MAS and DOR NMR study of Al-Si order in the analcime-pollucite series. Can Mineral 32:69-80

Teertstra DK, Cerny P (1995) First natural occurrences of end-member pollucite: A product of low-temperature reequilibration. Eur J Mineral 7:1137-1148

Tillmanns E, Fischer RX, Baur WH (1984) Chabazite-type framework in the new zeolite willhendersonite, $KCaAl_3Si_3O_{12}{\cdot}5H_2O$. N Jahrb Mineral Mh 1984:547-558

Torres-Martinez LM, Gard JA, Howie RA, West AR (1984) Synthesis of $Cs_2BeSi_5O_{12}$ with a pollucite structure. J Solid State Chem 51:100-103

Tschernich RW (1992) Zeolites of the World. Geoscience Press, Phoenix, AZ, 563 p

Vaughan PA (1966) The crystal structure of the zeolite ferrierite. Acta Crystallogr 21:983-990

Vezzalini G (1984) A refinement of Elba dachiardite: Opposite acentric domains simulating a centric structure. Z Kristallogr 166:63-71

Vezzalini G, Quartieri S, Passaglia E (1990) Crystal structure of K-rich natural gmelinite and comparison with the other refined gmelinite samples. N Jahrb Mineral Mh 1990:504-516

Vezzalini G, Artioli G, Quartieri S, Foy H (1992) The crystal chemistry of cowlesite. Mineral Mag 56: 575-579

Vezzalini G, Quartieri S, Alberti A (1993) Structural modifications induced by dehydration in the zeolite gismondine. Zeolites 13:34-42

Vezzalini G, Quartieri S, Galli E (1997a) Occurrence and crystal structure of a Ca-pure willhender-sonite. Zeolites 19:75-79

Vezzalini G, Quartieri S, Galli E, Alberti A, Cruciani G, Kvick, Å (1997b) Crystal structure of the zeolite mutinaite, the natural analog of ZSM-5. Zeolites 19:323-325

Vezzalini G, Alberti A, Sani A, Triscari M (1999) The dehydration process in amicite. Microporous Mesoporous Mater 31:253-262

Vigdorchik AG, Malinovskii YA (1986) Crystal structure of Ba-substituted gmelinite $Ba_4[Al_8Si_{16}O_{48}]\cdot n H_2O$. Sov Phys Crystallogr 31:519-521

Voloshin AV, Pakhomovskii, YaA, Rogachev DL, Tyusheva FN, Shishkin NM (1986) Ginzburgite—A new calcium-beryllium silicate from desilicated pegmatites. Mineralog Zhur 8;4:85-90 (in Russian). Abstracted in Am Mineral (1988) 73:439-440

Walter F (1992) Weinebeneite, $CaBe_3(PO_4)_2(OH)_2\cdot 4H_2O$, a new mineral species: Mineral data and crystal structure. Eur J Mineral 4:1275-1283

White JS, Erd RC (1992) Kehoeite is not a valid species. Mineral Mag 50:256-258

Wuest T, Armbruster T (1997) Type locality leonhardite: A single crystal X-ray study at 100K. *In* Program and Abstracts of Zeolite '97, 5th Int'l Conf on the Occurrence, Properties, and Utilization of Natural Zeolites; Ischia, Naples, Italy, p 327-328

Yakubovich OV, Massa W, Pekov IV, Kucherinenko, Ya.V (1999) Crystal structure of a Na,K-variety of merlinoite. Crystallogr Rep 44:776-782

Yang P, Armbruster T (1996a) Na, K, Rb, and Cs exchange in heulandite single-crystals: X-ray structure refinements at 100 K. J Solid State Chem 123:140-149

Yang P, Armbruster T (1996b) (010) disorder, partial Si,Al ordering, and Ca distribution in triclinic (*C*1) epistilbite. Eur J Mineral 8:263-271

Yokomori Y, Idaka S (1998) The crystal structure of analcime. Microporous Mesoporous Mater 21:365-370

Zemann J (1991) Nichtsilikatische Zeolithe. Mitt Österr Mineral Ges 136:21-34